Supporting information

Perenosins: a new class of anion transporter with anti-cancer activity

Wim Van Rossom, Daniel J. Asby, Ali Tavassoli, Philip A. Gale*

Chemistry, University of Southampton, Southampton, SO17 1BJ, UK; Tel +44 (023) 8059 3332; E-mail:philip.gale@soton.ac.uk

Table of Contents

1. Synthetic and characterization data

^{1}H NMR spectra were recorded using Bruker Avance AVII400 and AVIIIHD400 FT-NMR spectrometers at a frequency of 400 MHz, and are reported as parts per million (ppm) with DMSO-d_6 (δ_H 2.50 ppm) or $CDCl_3$ (δ_H 7.26 ppm) as internal references. The data are reported as chemical shift (δ), multiplicity (br = broad, s = singlet, d = doublet, m = multiplet), coupling constant (J, Hz) and relative integral. ^{13}C NMR spectra were recorded using Bruker Avance AVII400 and AVIIIHD400 FT-NMR spectrometers at a frequency of 100 MHz and are reported as parts per million (ppm) with DMSO-d_6 (δ_H 39.51 ppm) or $CDCl_3$ (δ_H 77.00 ppm) as internal references.

For low resolution mass spectrometry, samples were analysed using a Waters (Manchester, UK) TQD mass spectrometer equipped with a triple quadrupole analyser. Samples were introduced to the mass spectrometer via an Acquity H-Class quaternary solvent manager (with TUV detector at 254 nm, sample and column manager). Ultra-performance liquid chromatography was undertaken via a Waters BEH C18 column (50 mm x 2.1 mm 1.7 µm). Gradient 20% acetonitrile (0.2% formic acid) to 100% acetonitrile (0.2% formic acid) in five minutes at a flow rate of 0.6 mL/min. Low resolution mass spectra were recorded using positive/negative ion electrospray ionisation.

For high resolution mass spectrometry, samples were analysed using a MaXis (Bruker Daltonics, Bremen, Germany) mass spectrometer equipped with a Time of Flight (TOF) analyser. Samples were introduced to the mass spectrometer via a Dionex Ultimate 3000 autosampler and uHPLC pump. Ultra performance liquid chromatography was undertaken via a Waters UPLC BEH C18 (50 mm x 2.1 mm 1.7 µm) column. Gradient 20% acetonitrile (0.2% formic acid) to 100% acetonitrile (0.2% formic acid) in five minutes at a flow rate of 0.6 mL/min. High resolution mass spectra were recorded using positive/negative ion electrospray ionisation.

Melting points were collected on a Griffin Melting Point Apparatus.

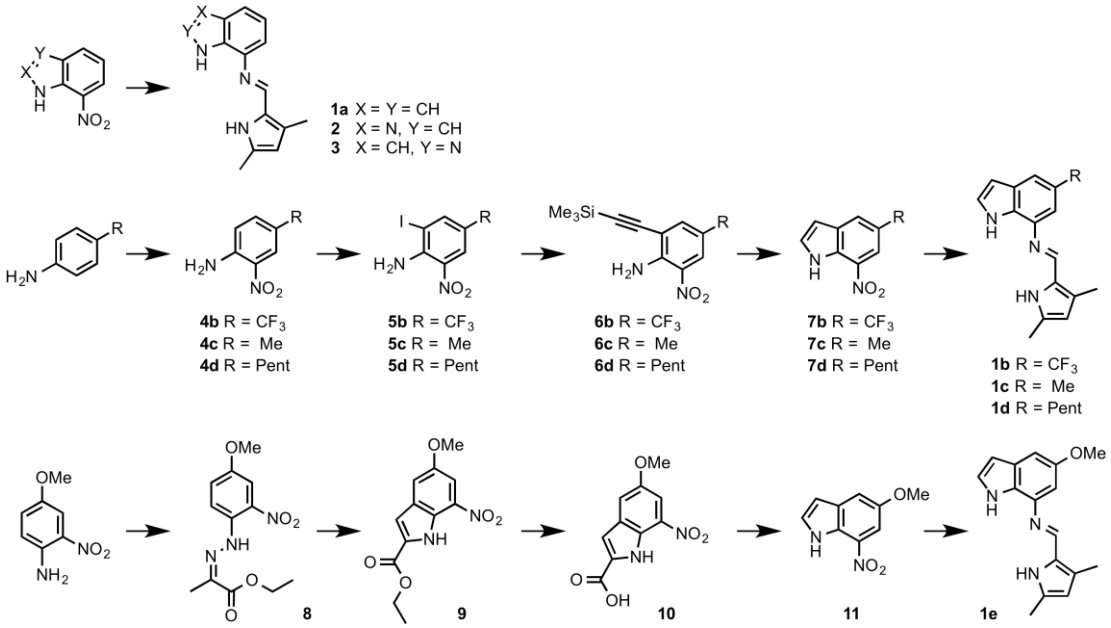

(*E*)-1-(3,5-dimethyl-1*H*-pyrrol-2-yl)-*N*-(1*H*-indol-7-yl)methanimine (1a). General procedure 1: A 100 mL round-bottom flask was charged with 7-nitro-1*H*-indole (500 mg, 3.0 mmol), Pd/C 10% (200 mg) and EtOH (10 mL). The flask was evacuated, the mixture placed under a hydrogen atmosphere and stirred vigorously at room temperature during 5h in the dark. The mixture was filtered over a glass fibre filter to remove the catalyst. To the filtrate were added $MgSO_4$ (250 mg, 2.1 mmol) and 3,5-dimethylpyrrole-2-carbaldehyde (380 mg, 3.0 mmol) and the mixture was stirred overnight at room temperature shielded from light. The reaction mixture was filtered and run through a SCX-2 column (eluent: MeOH; wash out NH_3 1N in MeOH) and the solvent was evaporated. Purification by column chromatography (silica, eluent hexane–ethyl acetate–Et_3N, 80–20–3) and recrystallization from hexane gave **1a** as a yellow solid (95 mg, 13%). **mp** 97-98 °C; **^{1}H NMR** (400 MHz, $CDCl_3$): δ 8.81 (s, 1H; NH), 8.51 (s, 1H; CH), 7.47 (d, J = 8.0 Hz, 1H; Ar-H), 7.19 (s, 1H; NH), 7.12 (t, J = 8.0 Hz, 1H; Ar-H), 6.98 (d, J = 7.2 Hz, 1H; Ar-H), 6.56 (s, 1H; Ar-H), 5.84 (s, 1H; Ar-H), 2.27 (s, 3H; CH_3), 2.25 (s, 3H; CH_3); **^{13}C NMR** (100 MHz, $CDCl_3$): δ 146.8, 137.2, 133.8, 131.7, 128.6, 128.3, 126.7, 123.9, 120.3, 117.6, 110.9, 108.6, 102.6, 13.1, 10.7; **HRMS** (ESI+) calcd. for $C_{15}H_{16}N_3$ $[M+H]^+$: 238.1339, found *m/z* 238.1218.

(*E*)-1-(3,5-dimethyl-1*H*-pyrrol-2-yl)-*N*-(5-(trifluoromethyl)-1*H*-indol-7-yl)methanimine (1b). Synthesis according to general procedure 1: 7-nitro-5-(trifluoromethyl)-1*H*-indole (300 mg, 1.3 mmol), Pd/C 10% (200 mg), EtOH (8 mL); $MgSO_4$ (250 mg, 2.1 mmol), 3,5-dimethylpyrrole-2-carbaldehyde (161 mg, 1.3 mmol). Eluent: hexane–ethyl acetate–Et_3N, 80–20–3. The compound **1b** was obtained as a yellow solid (123 mg, 31%). **mp** 143-144 °C; **^{1}H NMR** (400 MHz, DMSO-d_6): δ 11.35 (s, 1H; NH), 11.06 (s, 1H; NH), 8.57 (s, 1H; CH), 7.69 (s, 1H; Ar-H), 7.50 (t, J = 2.8 Hz, 1H; Ar-H), 7.20 (d, J = Hz, 1H; Ar-H), 6.60 (t, J = Hz, 1H; Ar-H), 5.81 (s, 1H; Ar-H), 2.27 (s, 3H; CH_3), 2.24 (s, 3H; CH_3); **^{13}C NMR** (100 MHz, DMSO-d_6): δ 148.1, 137.8, 134.1, 133.0, 127.4 (q), 120.7, 120.4, 113.6 (q), 110.6, 104.3, 102.5, 12.9, 10.8; **HRMS** (ESI+) calcd. for $C_{16}H_{14}N_3F_3$ $[M+H]^+$: 306.1213, found *m/z* 306.1218.

(*E*)-1-(3,5-dimethyl-1*H*-pyrrol-2-yl)-*N*-(5-methyl-1*H*-indol-7-yl)methanimine (1c). Synthesis according to general procedure 1: 5-methyl-7-nitro-1*H*-indole (300 mg, 1.7 mmol), Pd/C 10% (100 mg), EtOH (10 mL); $MgSO_4$ (250 mg, 2.1 mmol), 3,5-dimethylpyrrole-2-carbaldehyde (210 mg, 1.7 mmol). Eluent: hexane–ethyl acetate–Et_3N, 60–40–3. The compound **1c** was obtained as a yellow solid (168 mg, 39%). **mp** 171-172 °C; **^{1}H NMR** (400 MHz, DMSO-d_6): δ 10.97 (s, 1H; NH), 10.74 (s, 1H; NH), 8.46 (s, 1H; CH), 7.25 (t, J = 2.4 Hz, 1H; Ar-H), 7.09 (s, 1H; Ar-H), 6.74 (s, 1H; Ar-H), 6.32 (t, J = 2.4 Hz, 1H; Ar-H), 5.78 (s, 1H; Ar-H), 2.38 (s, 3H; CH_3), 2.25 (s, 3H; CH_3), 2.22 (s, 3H; CH_3); **^{13}C NMR** (100 MHz, DMSO-d_6): δ 146.3, 136.9, 133.1, 129.9, 128.6, 127.9, 126.8, 126.1, 124.8, 116.1, 110.2, 109.6, 100.6, 21.3, 12.8, 10.7; **HRMS** (ESI+) calcd. for $C_{16}H_{18}N_3$ $[M+H]^+$: 252.1495, found *m/z* 252.1497.

(*E*)-1-(3,5-dimethyl-1*H*-pyrrol-2-yl)-*N*-(5-pentyl-1*H*-indol-7-yl)methanimine (1d). Synthesis according to general procedure 3: 7-nitro-5-pentyl-1*H*-indole (360 mg, 1.5 mmol), Pd/C 10% (140 mg), EtOH (10 mL); $MgSO_4$ (250 mg, 2.1 mmol), 3,5-dimethylpyrrole-2-carbaldehyde (190 mg, 1.5 mmol). Eluent: hexane–ethyl acetate–Et_3N, 75–25–3. The compound **1d** was obtained as a yellow solid (296 mg, 62%). **mp** 119-120 °C; **^{1}H NMR** (400 MHz, DMSO-d_6): δ 10.96 (s, 1H; NH), 10.75 (s, 1H; NH), 8.48 (s, 1H; CH), 7.26 (t, J = 2.8 Hz, 1H; Ar-H), 7.09 (s, 1H; Ar-H), 6.76 (d, J = 0.8 Hz, 1H; Ar-H), 6.33 (dd, J = 2.8 Hz, J = 2.4 Hz, 1H; Ar-H), 5.78 (s, 1H; Ar-H), 2.63 (t, J = 7.2 Hz, 2H; CH_2), 2.26 (s, 3H; CH_3), 2.22 (s, 3H; CH_3), 1.67–1.59 (m, 2H; CH_2), 1.38–1.26 (m, 4H; CH_2), 0.87 (t, J = 6.8 Hz, 3H; CH_3); **^{13}C NMR** (100 MHz, DMSO-d_6): δ 146.2, 136.8, 133.3, 133.1, 130.1, 128.5, 126.8, 126.1, 124.8, 115.6, 110.2, 109.0, 100.8, 22.0, 13.9, 12.8, 10.8; **HRMS** (ESI+) calcd. for $C_{20}H_{26}N_3$ $[M+H]^+$: 308.2121, found *m/z* 308.2123.

(*E*)-1-(3,5-dimethyl-1*H*-pyrrol-2-yl)-*N*-(5-methoxy-1*H*-indol-7-yl)methanimine (1e). Synthesis according to general procedure 1: 5-methoxy-7-nitro-1*H*-indole (305 mg, 1.6 mmol), Pd/C 10% (105 mg), EtOH (10 mL); $MgSO_4$ (200 mg, 1.7 mmol), 3,5-dimethylpyrrole-2-carbaldehyde (192 mg, 1.6 mmol). Eluent: hexane–ethyl acetate–Et_3N, 50–50–3. The compound **1e** was obtained as a yellow solid (180 mg, 42%). **mp** 165-166 °C; **^{1}H NMR** (400 MHz, DMSO-d_6): δ 11.00 (s, 1H; NH), 10.73 (s, 1H; NH), 8.46 (s, 1H; CH), 7.26 (t, J = 2.8 Hz, 1H; Ar-H), 6.82 (s, 1H; Ar-H), 6.58 (s, 1H; Ar-H), 6.34 (q, J = 2.8 Hz, J = 2.4 Hz, 1H; Ar-H), 5.79 (s, 1H; Ar-H), 3.76 (s, 3H; CH_3), 2.25 (s, 3H; CH_3), 2.22 (s, 3H; CH_3); **^{13}C NMR** (100 MHz, DMSO-d_6): δ 154.0, 147.0, 137.6, 133.5, 128.3, 126.9, 126.7, 125.3, 110.3, 101.0, 98.5, 98.3, 55.3, 12.8, 10.8; **HRMS** (ESI+) calcd. for $C_{16}H_{18}N_3O$ $[M+H]^+$: 268.1444, found *m/z* 268.1446.

(*E*)-1-(3,5-dimethyl-1*H*-pyrrol-2-yl)-*N*-(1*H*-benzimidazole-7-yl)methanimine (2). Synthesis according to general procedure 1: 7-nitro-1*H*-benzimidazole (300 mg, 1.8 mmol), Pd/C 10% (90 mg), EtOH (10 mL); $MgSO_4$ (250 mg, 2.1 mmol), 3,5-dimethylpyrrole-2-carbaldehyde (226 mg, 1.8 mmol). The reaction mixture was filtered and run through a SCX-2 column (eluent: MeOH; wash out NH_3 1N in MeOH) and the solvent was evaporated. The residue was dissolved in a minimal amount of isopropanol to which were added a few drops of HCl 6N isopropanol solution and Et_2O. The precipitate was collected, dissolved in H_2O and neutralized with saturated $NaHCO_3$ solution. Extraction with ethyl acetate (3x), evaporation of the solvent, and recrystallization from ethyl acetate–hexane gave **2** as a yellow solid (184 mg, 42%). **mp** 115-116 °C; **^{1}H NMR** (400 MHz, DMSO-d_6): δ 12.47 (s, 0.6H; NH), 12.41 (s, 0.4H; NH), 11.16 (s, 0.6H; NH), 11.06 (s, 0.4H; NH), 9.22 (s, 0.6H; Ar-H), 8.42 (s, 0.4H; Ar-H), 8.18 (s, 0.6H; CH), 8.14 (s, 0.4H; CH), 7.40 (d, 0.4H; Ar-H), 7.25 (d, J = Hz, 0.6H; Ar-H), 7.19–7.11 (m, 1H; Ar-H), 6.94 (m, 1H; Ar-H), 5.79 (s, 04H; Ar-H), 5.77 (s, 0.6H; Ar-H), 2.25-2.19 (m, 6H; CH_3); **^{13}C NMR** (100 MHz, DMSO-d_6): δ 150.9, 148.0, 144.0, 142.9, 144.6, 141.1, 138.5, 135.8, 134.7, 133.8, 133.7, 127.1, 126.7, 126.4, 122.7, 121.7, 115.9, 115.0, 110.6, 110.4, 110.1, 107.5, 12.7, 10.8; **HRMS** (ESI+) calcd. for $C_{14}H_{15}N_4$ $[M+H]^+$: 239.1291, found *m/z* 239.1290.

(*E*)-1-(3,5-dimethyl-1*H*-pyrrol-2-yl)-*N*-(1*H*-indazol-7-yl)methanimine (3). Synthesis according to general procedure 1: 7-nitro-1*H*-indazole (400 mg, 2.5 mmol), Pd/C 10% (150 mg), EtOH (10 mL); $MgSO_4$ (250 mg, 2.1 mmol), 3,5-dimethylpyrrole-2-carbaldehyde (302 mg, 2.5 mmol). Eluent gradient: hexane–ethyl acetate–Et_3N, 70–30–3 to 50–50–3. The compound **3** was obtained as a yellow solid (28 mg, 5%). **mp** 107-108 °C; **^{1}H NMR** (400 MHz, DMSO-d_6): δ 13.04 (s, 1H; NH), 11.03 (s, 1H; NH), 8.49 (s, 1H; CH), 8.05 (s, 1H; Ar-H), 7.51–7.46 (m, 1H; Ar-H), 7.10–7.06 (m, 2H; Ar-H), 5.08 (s, 1H; Ar-H), 2.25 (s, 3H; CH_3), 2.23 (s, 3H; CH_3); **^{13}C NMR** (100 MHz, DMSO-d_6): δ 147.8, 137.0, 136.1, 134.0, 133.5, 127.3, 126.6, 123.9, 121.1, 112.1, 116.1, 112.6, 110.5, 12.8, 10.8; **HRMS** (ESI+) calcd. for $C_{14}H_{15}N_4$ $[M+H]^+$: 239.1291, found *m/z* 239.1287.

2-Nitro-4-pentylaniline (4d). A mixture of 4-pentylaniline (2.2 mL, 12 mmol) and acetic anhydride 3.51 (7.0 mL, 72 mmol) was stirred at room temperature for 1h. The precipitate was filtered, dissolved in acetic acid (10 mL), the solution was cooled to –10°C and HNO_3 (70%; 2.2mL, 36 mmol) was added dropwise. The mixture was stirred at room temperature during 3h, poured in ice-water and the precipitate was collected. To a solution of EtOH (20 mL) and KOH (40% aqueous solution; 5 mL) was added the precipitate and the mixture was refluxed during 1h. The reaction mixture was left to cool to room temperature, poured into water, neutralized with NH_4Cl and extracted with ethyl acetate (3x). The organic phases were combined, dried (Na_2SO_4) and the solvent evaporated under vacuo. The crude product was purified by column chromatography (silica, eluent hexane–ethyl acetate, 4–1) to give **4d** as a red oil (overall 72%). **^{1}H NMR** (400 MHz, DMSO-d_6): δ 7.73 (d, J = 2.0 Hz, 1H; Ar-H), 7.28 (s, 2H; NH_2), 7.25 (q, J = 8.4 Hz, J = 1.6 Hz, 1H; Ar-H), 6.94 (d, J = 8.8 Hz, 1H; Ar-H), 2.45 (t, J = 7.2, 2H; CH_2), 1.54–1.46 (m, 2H; CH_2), 1.31–1.18 (m, 4H; CH_2), 0.84 (t, J = 6.8 Hz, 3H; CH_3); **^{13}C NMR** (100 MHz, DMSO-d_6): δ 144.5, 136.5, 129.8, 129.4, 123.4, 119.2, 33.5,

30.6, 30.2, 21.8, 13.8; **HRMS** (ESI+) calcd. for $C_{11}H_{17}N_2O_2$ $[M+H]^+$: 209.1285, found *m/z* 209.1283.

2-Iodo-6-nitro-4-(trifluoromethyl)aniline (5b). This compound has been prepared according to the procedure reported by Koradin *et al*.[1] Material identity was confirmed by MS, ^1H and ^{13}C NMR.

2-Iodo-4-methyl-6-nitroaniline (5c). To a solution of 4-methyl-2-nitroaniline (3.00 g, 20 mmol), $Ag_2(I)SO_4$ (8.50 g, 28 mmol) in ethanol (150 mL) was added iodine (7 g, 28 mmol). The reaction mixture, shielded from light, was stirred at room temperature during 36h, filtered and the solvent evaporated. The residue was diluted with CH_2Cl_2, washed with aqueous $Na_2S_2O_3$ solution and dried (Na_2SO_4). After evaporation of the solvent **5c** was obtained as an orange solid (5.48 g, quant.). **mp** 79-80 °C; **^{1}H NMR** (400 MHz, DMSO-*d*$_6$): δ 7.93 (s, 1H; Ar-H), 7.87 (s, 1H; Ar-H), 6.87 (s, 2H; NH_2), 2.19 (s, 3H; CH_3); **^{13}C NMR** (100 MHz, DMSO-*d*$_6$): δ 147.1, 142.5, 130.5, 126.8, 125.6, 88.0, 18.8; **HRMS** (ESI+) calcd. for $C_7H_8N_2O_2I$ $[M+H]^+$: 278.9625, found *m/z* 278.9625.

2-Iodo-6-nitro-4-pentylaniline (5d). To a solution of 2-nitro-4-pentylaniline (1.79 g, 8.7 mmol), $Ag_2(I)SO_4$ (3.79 g, 12 mmol), ethanol (75 mL) was added iodine (3.07 g, 12 mmol). The reaction mixture, shielded from light, was stirred at room temperature during 36h, filtered and the solvent evaporated. The residue was diluted with CH_2Cl_2, washed with aqueous $Na_2S_2O_3$ solution and dried (Na_2SO_4). Purification by column chromatography (silica, eluent hexane–ethyl acetate, 9–1) gave **5d** as a dark red solid (2.76 g, 95%). **mp** 45-46 °C; **^{1}H NMR** (400 MHz, $CDCl_3$): δ 7.96 (d, *J* = 2.0 Hz;, 1H; Ar-H), 7.78 (d, *J* = 1.6 Hz;, 1H; Ar-H), 6.51 (s, 2H; NH_2), 2.50 (t, *J* = 7.6 Hz;, 2H; CH_2), 1.57 (m, 2H; CH_2), 1.34–1.29 (m, 4H; CH_2), 0.90 (t, *J* = 6.8 Hz, 3H; CH_3); **^{13}C NMR** (100 MHz, $CDCl_3$): δ 146.2, 142.1, 132.8, 131.6, 125.9, 87.3, 34.1, 31.1, 30.7, 22.4, 13.9; **HRMS** (ESI+) calcd. for $C_{11}H_{16}N_2O_2I$ $[M+H]^+$: 335.0251, found *m/z* 335.0243.

2-Nitro-4-(trifluoromethyl)-6-((trimethylsilyl)ethynyl)aniline (6b). General procedure 2: To a stirred mixture of 2-iodo-6-nitro-4-(trifluoromethyl)aniline (2.038 g, 6.25 mmol), $Pd(PPh_3)_2Cl_2$ (430 mg, 10 mol%), CuI (233 mg, 20 mol%) and ethynyl trimethylsilane (1.31 mL, 9.18 mmol) in toluene (5 mL) at 0 °C under argon was added dropwise piperidine (1.81 mL, 19 mmol). The reaction mixture was stirred at room temperature during 4h, saturated NH_4Cl solution was added, extracted by CH_2Cl_2 (3x) and dried (Na_2SO_4). Purification by column chromatography (silica, eluent CH_2Cl_2–hexane, 7–3) gave **6b** as a yellow solid (1.34g, 74%). **mp** 139-140 °C; **^{1}H NMR** (400 MHz, $CDCl_3$): δ 8.41 (d, *J* = 1.2 Hz, 1H; Ar-H), 7.41 (d, *J* = 1.6 Hz, 1H; Ar-H), 1.55 (s, 2H; NH_2), 0.31 (s, 9H; CH_3); **^{13}C NMR** (100 MHz, $CDCl_3$): δ 146.8, 134.5 (q), 131.1, 124.3 (q), 117.9, 113.1, 105.3, 97.4, -0.23; **HRMS** (ESI+) calcd. for $C_{12}H_{14}N_2O_2F_3Si$ $[M+H]^+$: 303.0771, found *m/z* 303.0765.

4-Methyl-2-nitro-6-((trimethylsilyl)ethynyl)aniline (6c). Synthesis according to general procedure 2: 2-iodo-4-methyl-6-nitroaniline (2.00 g, 7.19 mmol), $Pd(PPh_3)_2Cl_2$ (505 mg, 10 mol%), CuI (274 mg, 20 mol%), ethynyl trimethylsilane (1.53 mL, 9.18 mmol), toluene (5 mL), piperidine (2.13 mL, 22 mmol). Purification by column chromatography (silica, eluent CH_2Cl_2–hexane, 4–2) gave **6c** as a yellow solid (1.23 g, 69%). **mp** 71-72 °C; **^{1}H NMR** (400 MHz, $CDCl_3$): δ 7.93 (s, 1H; Ar-H), 7.41 (s, 1H; Ar-H), 6.59 (s, 2H; NH_2), 2.25 (s, 3H; CH_3), 0.29 (s, 9H; CH_3); **^{13}C NMR** (100 MHz, $CDCl_3$): δ 143.6, 139.8, 131.8, 126.4, 125.2, 111.9, 102.8, 99.1, 19.9, -0.09; **HRMS** (ESI+) calcd. for $C_{12}H_{17}N_2O_2Si$ $[M+H]^+$: 249.1054, found *m/z* 249.1050; calcd. for $C_{12}H_{17}N_2O_2SiNa$ $[M+Na]^+$: 271.0873, found *m/z* 271.0869.

2-Nitro-4-pentyl-6-((trimethylsilyl)ethynyl)aniline (6d). Synthesis according to general procedure 2: 2-iodo-6-nitro-4-pentylaniline (2.60 g, 11 mmol), $Pd(PPh_3)_2Cl_2$ (546 mg, 10

[1] Koradin, C.; Dohle, W.; Rodriguez, A. L.; Schmid, B.; Kochel, P. *Tetrahedron* **2003**, *59*, 1571–1587.

mol%), CuI (296 mg, 20 mol%), ethynyl trimethylsilane (1.66 mL, 16 mmol), toluene (10 mL), piperidine (2.30 mL, 33 mmol). Purification by column chromatography (silica, eluent CH_2Cl_2–hexane, 1–1) gave **6d** as a yellow solid (1.94 g, 81%). **mp** 45-46 °C; **^{1}H NMR** (400 MHz, DMSO-d_6): δ 7.85 (d, J = 1.2 Hz, 1H; Ar-H), 7.50 (d, J = 1.2 Hz, 1H; Ar-H), 6.90 (s, 2H; NH_2), 2.46 (t, J = 7.6 Hz, 2H; CH_2), 1.54–1.46 (m, 2H; CH_2), 1.30–1.20 (m, 4H; CH_2), 0.84 (t, J = 6.8 Hz, 3H; CH_3), 0.26 (s, 9H; CH_3); **^{13}C NMR** (100 MHz, DMSO-d_6): δ 143.7, 139.4, 130.9, 129.6, 125.5, 111.1, 102.1, 99.3, 33.1, 30.5, 30.1, 21.8, 13.8, -0.23; **HRMS** (ESI+) calcd. for $C_{16}H_{24}N_2O_2SiNa$ $[M+Na]^+$: 327.1499, found *m/z* 327.1506.

7-Nitro-5-(trifluoromethyl)-1*H*-indole (7b). General procedure 3: A mixture of 2-nitro-4-(trifluoromethyl)-6-((trimethylsilyl)ethynyl)aniline (1.327 g, 4.3 mmol), *t*-BuOK (1.489 g, 12.9 mmol) and NMP (50 mL) was stirred at room temperature during 4h. The reaction mixture as neutralized with saturated NH_4Cl solution, extracted with ethyl actate (3x), and dried over Na_2SO_4. Purification by column chromatography (silica, eluent hexane–ethyl acetate, 4–1) gave **7b** as a yellow solid (645 mg, 64%). **mp** 151-152 °C; **^{1}H NMR** (400 MHz, $CDCl_3$): δ 10.10 (s, 1H; NH), 8.44 (s, 1H; Ar-H), 8.26 (s, 1H; Ar-H), 7.54 (t, J = 2.8 Hz, 1H; Ar-H), 6.85 (t, J = 2.4 Hz, 1H; Ar-H); **^{13}C NMR** (100 MHz, $CDCl_3$): δ 131.7, 130.2, 128.4, 125.4 (q), 125.2, 122.4, 122.1, 116.2 (q), 105.1; **HRMS** (ESI–) calcd. for $C_9H_4N_2O_2F_3$ $[M–H]^–$: 229.0230, found *m/z* 229.0233.

5-Methyl-7-nitro-1*H*-indole (7c). Synthesis according to general procedure 3: 4-methyl-2-nitro-6-((trimethylsilyl)ethynyl)aniline (1.20 g, 4.8 mmol), *t*-BuOK (1.63 g, 14.4 mmol), NMP (50 mL). Purification by column chromatography (silica, eluent hexane–ethyl acetate, 5–1) gave **7c** as a yellow solid (668 mg, 81%). **mp** 111-112 °C; **^{1}H NMR** (400 MHz, $CDCl_3$): δ 9.80 (s, 1H; NH), 8.01 (s, 1H; Ar-H), 7.79 (s, 1H; Ar-H), 7.37 (t, J = 2.0 Hz, 1H; Ar-H), 6.63 (t, J = 2.0 Hz, 1H; Ar-H), 2.53 (s, 3H; CH_3); **^{13}C NMR** (100 MHz, $CDCl_3$): δ 132.5, 131.8, 129.1, 127.8, 126.6, 123.0, 120.0, 103.4, 21.0; **HRMS** (ESI+) calcd. for $C_9H_8N_2O_2$ $[M]^+$: 176.0586, found *m/z* 176.0579.

7-Nitro-5-pentyl-1*H*-indole (7d). Synthesis according to general procedure 3: 2-nitro-4-pentyl-6-((trimethylsilyl)ethynyl)aniline (1.80 g, 5.9 mmol), *t*-BuOK (1.99 g, 17.7 mmol), NMP (60 mL). Purification by column chromatography (silica, eluent hexane–ethyl acetate, 6–1) gave **7d** as an orange-brown solid (827 mg, 60%). **mp** 64-65 °C; **^{1}H NMR** (400 MHz, $CDCl_3$): δ 9.83 (s, 1H; NH), 8.01 (s, 1H; Ar-H), 7.79 (s, 1H; Ar-H), 7.37 (t, J = 2.4 Hz, 1H; Ar-H), 6.64 (t, J = 2.4 Hz, 1H; Ar-H), 2.77 (t, J = 7.6, 2H; CH_2), 1.74–1.66 (m, 2H; CH_2), 1.38–1.33 (m, 4H; CH_2), 0.91 (t, J = 6.8 Hz, 3H; CH_3); **^{13}C NMR** (100 MHz, $CDCl_3$): δ 134.4, 132.6, 131.7, 128.6, 127.9, 126.5, 119.5, 103.5, 35.4, 31.5, 31.3, 22.4, 14.0; **HRMS** (ESI+) calcd. for $C_{13}H_{17}N_2O_2$ $[M+H]^+$: 233.1285, found *m/z* 233.1286.

Ethyl 2-(2-(4-methoxy-2-nitrophenyl)hydrazono)propanoate (8). To a solution of ethyl-2-methylacetoacetate (8.6 g, 59 mmol) in EtOH (72 mL) at 0 °C were added ice (84 g), a solution of KOH (18 g, 321 mmol) in H_2O (20 mL) and a cold solution of 4-methoxy-2-nitroaniline (10.0 g, 59 mmol), $NaNO_2$ (4.2 g, 59 mmol) and HCl 12M (30 mL) in H_2O (48 mL) was added slowly. The reaction mixture was stirred during 1h and the precipitate was collected. Purification by recrystallization from wet MeOH gave **8** as a red solid (16.3 g, 97%). **mp** 100-101 °C; **^{1}H NMR** (400 MHz, DMSO-d_6): δ 10.49 (s, 1H; NH), 7.79 (d, J = 9.2 Hz, 1H; Ar-H), 7.57 (d, J = 2.8 Hz, 1H; Ar-H), 7.45 (dd, J = 9.6 Hz, J = 2.8 Hz, 1H; Ar-H), 4.27–4.21 (m, 2H; CH_2), 3.81 (s, 3H; CH_3), 2.13 (s, 3H; CH_3), 1.29 (t, J = 7.2 Hz, 3H; CH_3); **^{13}C NMR** (100 MHz, DMSO-d_6): δ 164.0, 152.7, 138.1, 134.7, 132.4, 125.9, 117.6, 106.9, 60.8, 55.7, 14.1, 11.3; **HRMS** (ESI+) calcd. for $C_{12}H_{15}N_3O_5Na$ $[M+Na]^+$: 304.0904, found *m/z* 304.0906.

Ethyl 5-methoxy-7-nitro-1*H*-indole-2-carboxylate (9). To a solution of ethyl 2-(2-(4-methoxy-2-nitrophenyl)hydrazono)propanoate (7.42 g, 26 mmol) in xylene (20 mL) was added polyphosphoric acid (12.5 g) and the mixture was stirred at 180 °C during 4h. The

reaction mixture was cooled to room temperature, H_2O was added (50 mL) and the phosphoric acid layer was extracted with toluene (10x, decanted). The organic phases were combined, washed with H_2O, dried (Na_2SO_4) and the solvent evaporated under vacuo. Purification by recrystallization from EtOH gave **9** as a yellow solid (3.03 g, 43%). **mp** 91-92 °C; **^{1}H NMR** (400 MHz, DMSO-d_6): δ 11.23 (s, 1H; NH), 7.84 (d, J = 2.4 Hz, 1H; Ar-H), 7.79 (d, J = 2.4 Hz, 1H; Ar-H), 7.34 (d, J = 1.6 Hz, 1H; Ar-H), 4.37 (m, 2H; CH_2), 3.88 (s, 3H; CH_3), 1.35 (t, J = 7.2, 3H; CH_3); **^{13}C NMR** (100 MHz, DMSO-d_6): δ160.2, 152.8, 133.1, 131.0, 130.9, 124.8, 113.5, 110.6, 108.8, 61.0, 56.2, 14.1; **HRMS** (ESI+) calcd. for $C_{12}H_{13}N_2O_5$ $[M+H]^+$: 265.0819, found *m/z* 265.0817; calcd. for $C_{12}H_{12}N_2O_5Na$ $[M+Na]^+$: 287.0638, found *m/z* 287.0636.

5-Methoxy-7-nitro-1*H*-indole-2-carboxylic acid (10). To a solution of ethyl 5-methoxy-7-nitro-1*H*-indole-2-carboxylate (2.45 g, 9.3 mmol) in THF (25 mL) was added NaOH 1N (25 mL) and the mixture was stirred at 80 °C during 2h. The reaction mixture was cooled to room temperature, neutralized with HCl 1N and the precipitate was filtered and dried under vacuo to give **10** as a dark yellow solid (1.55 g, 70%). **mp** decomposes; **^{1}H NMR** (400 MHz, DMSO-d_6): δ 10.96 (s, 1H; NH), 7.81 (d, J = 2.4 Hz, 1H; Ar-H), 7.79 (d, J = 2.4 Hz, 1H; Ar-H), 7.28 (s, 1H; Ar-H), 3.87 (s, 3H; CH_3); **^{13}C NMR** (100 MHz, DMSO-d_6): δ161.7, 152.8, 132.9, 132.1, 131.2, 124.7, 113.5, 110.2, 108.4, 56.2; **HRMS** (ESI–) calcd. for $C_{10}H_7N_2O_5$ $[M]^-$: 235.0360, found *m/z* 235.0365.

5-Methoxy-7-nitro-1*H*-indole (11). A solution of 5-methoxy-7-nitro-1*H*-indole-2-carboxylic acid (1.50 g, 6.3 mmol), $CuCO_3.Cu(H_2O)_2.H_2O$ (296 mg, mmol) in DMI (1,3-dimethyl-2-imidazolidinone; 10 mL) was stirred at 180 °C during 2h. The reaction mixture was cooled to room temperature, Et_2O added, filtered and the filtrate washed with HCl 2N and brine. Purification by column chromatography (silica, eluent hexane–ethyl acetate, 9–1) gave **11** as an orange solid (800 mg, 63%). **mp** 109-110 °C; **^{1}H NMR** (400 MHz, DMSO-d_6): δ 11072 (s, 1H; NH), 7.69 (d, J = 2.0 Hz, 1H; Ar-H), 7.65 (d, J = 2.4 Hz, 1H; Ar-H), 7.50 (t, J = 2.8 Hz, 1H; Ar-H), 6.63 (q, J = 2.8 Hz, J = 2.0 Hz, 1H; Ar-H), 3.86 (s, 3H; CH_3); **^{13}C NMR** (100 MHz, DMSO-d_6): δ 152.0, 132.5, 132.0, 129.6, 123.9, 113.2, 105.5, 102.5, 56.1; **HRMS** (ESI+) calcd. for $C_9H_9N_2O_3$ $[M+H]^+$: 193.0608, found *m/z* 193.0608; calcd. for $C_9H_8N_2O_3Na$ $[M+Na]^+$: 215.0427, found *m/z* 215.0427.

2. ^{1}H and ^{13}C NMR spectra

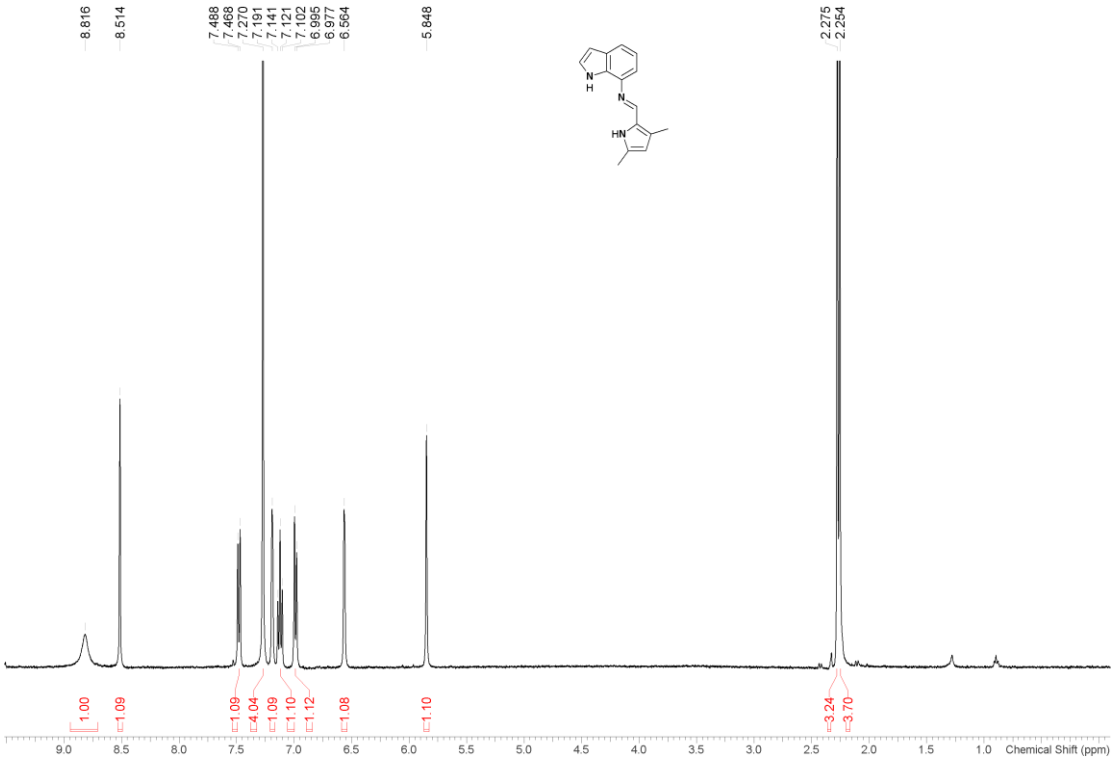

Figure S1. ^{1}H NMR (400 MHz) spectrum of compound **1a** in $CDCl_3$ at 298 K.

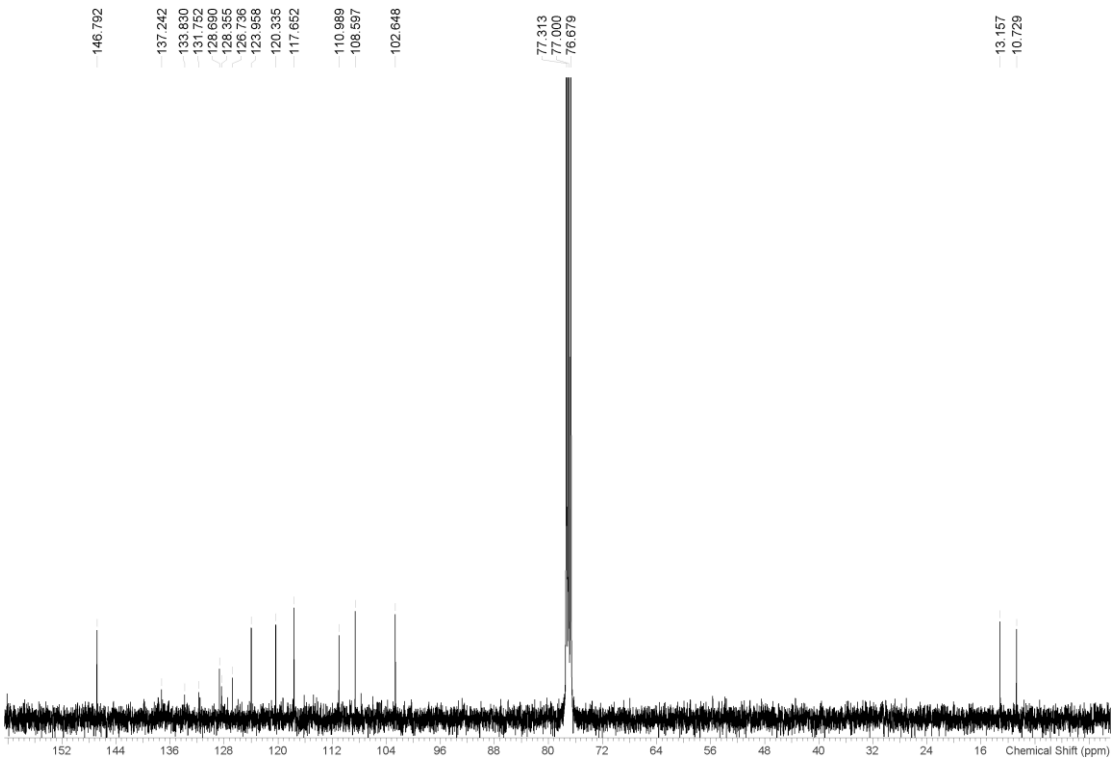

Figure S2. ^{13}C NMR (100 MHz) spectrum of compound **1a** in $CDCl_3$ at 298 K.

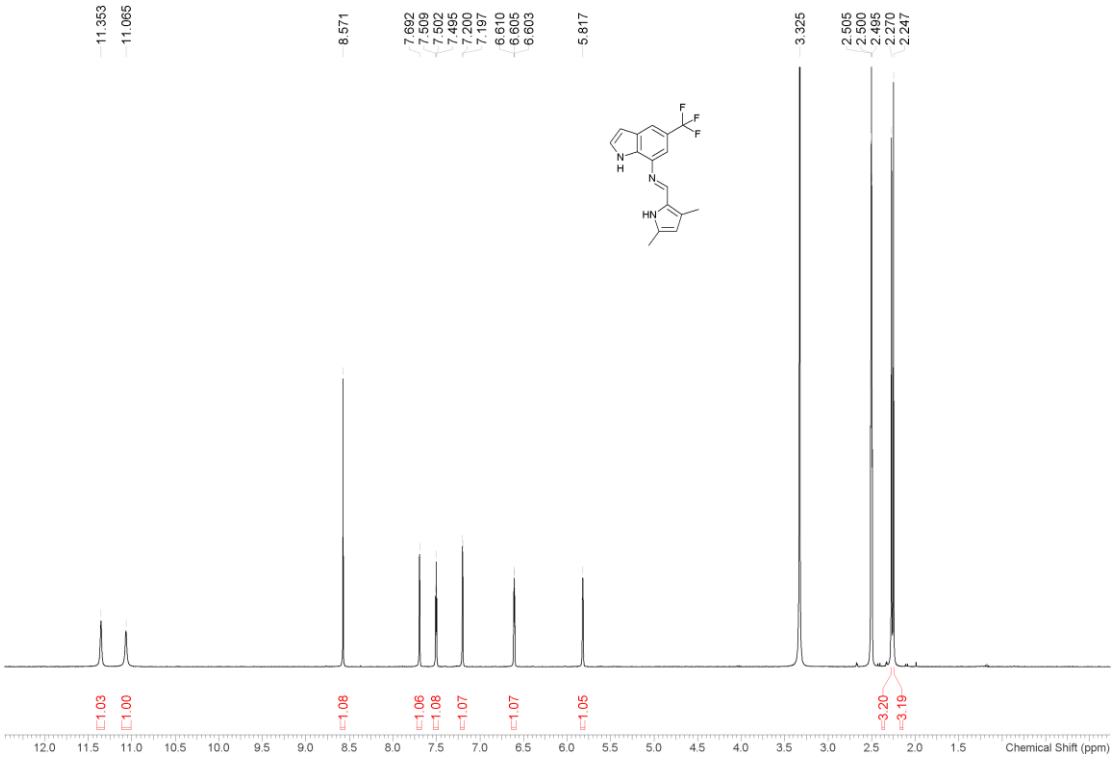

Figure S3. ^{1}H NMR (400 MHz) spectrum of compound **1b** in DMSO-d_6 at 298 K.

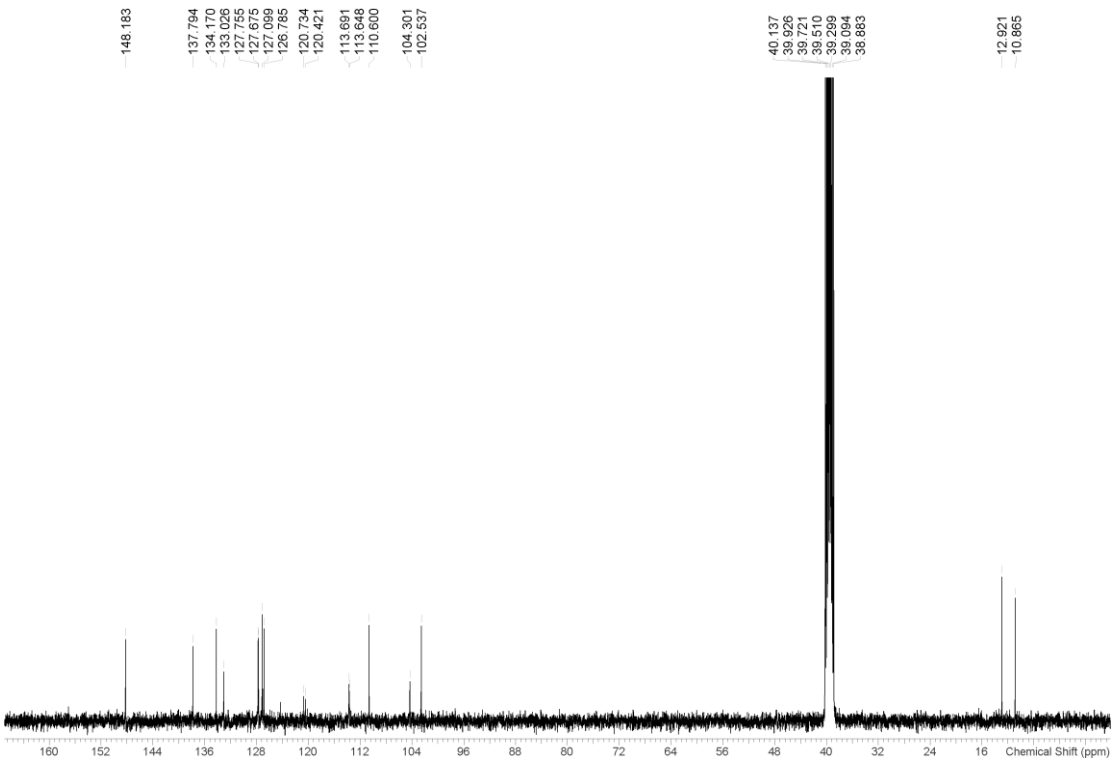

Figure S4. ^{13}C NMR (100 MHz) spectrum of compound **1b** in DMSO-d_6 at 298 K.

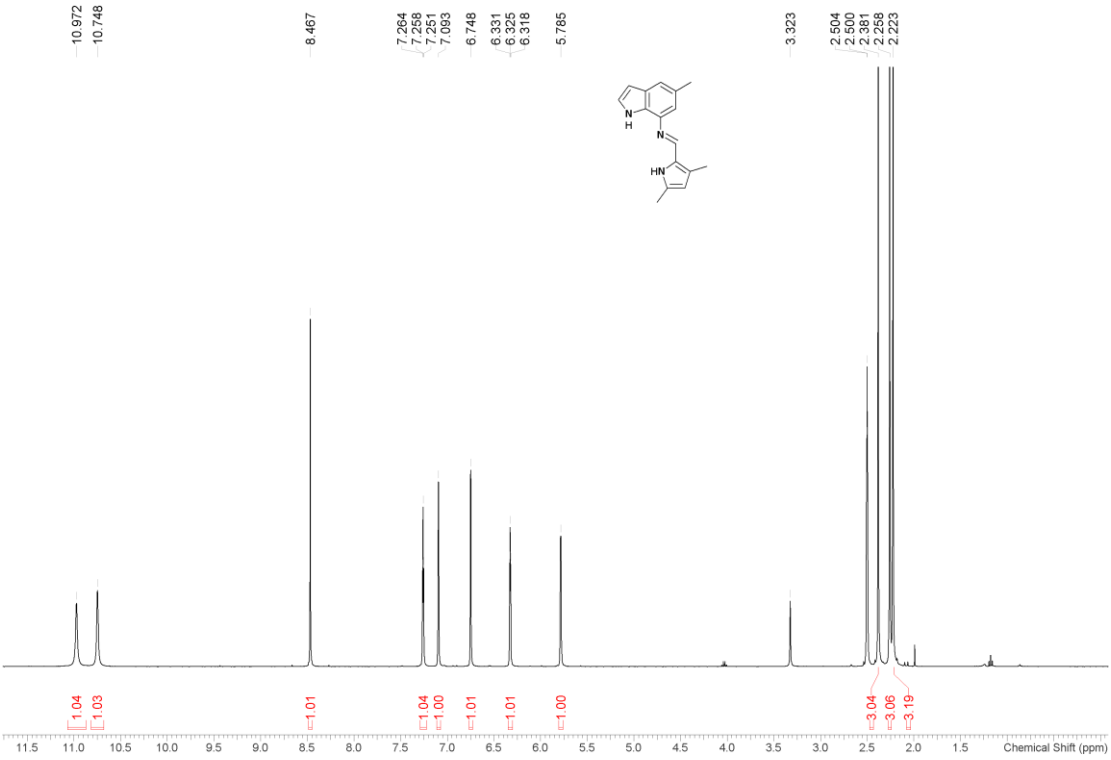

Figure S5. ^{1}H NMR (400 MHz) spectrum of compound **1c** in DMSO-d_6 at 298 K.

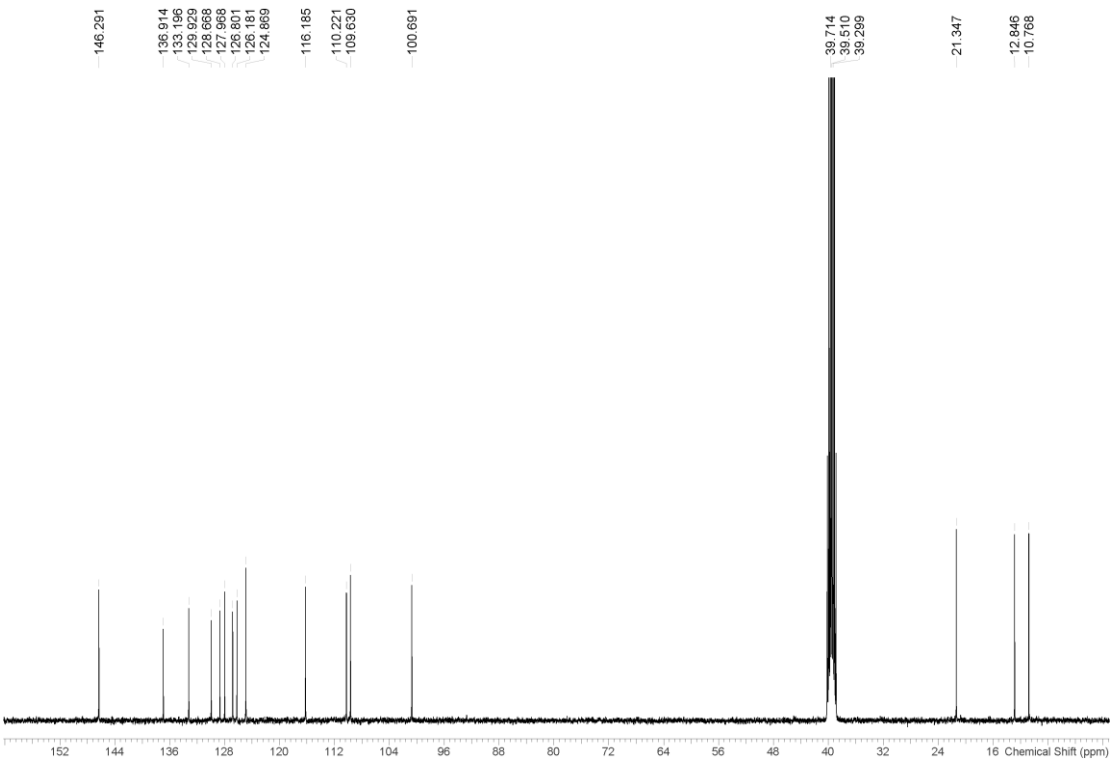

Figure S6. ^{13}C NMR (100 MHz) spectrum of compound **1c** in DMSO-d_6 at 298 K.

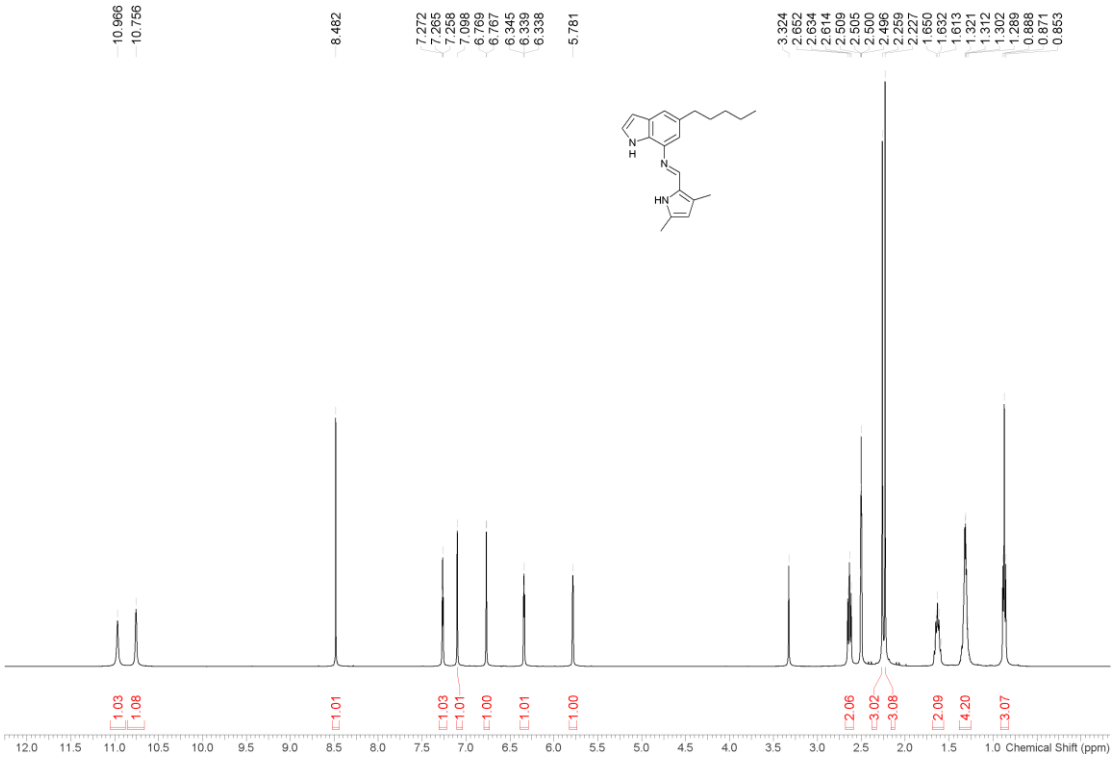

Figure S7. ^{1}H NMR (400 MHz) spectrum of compound **1d** in DMSO-d_6 at 298 K.

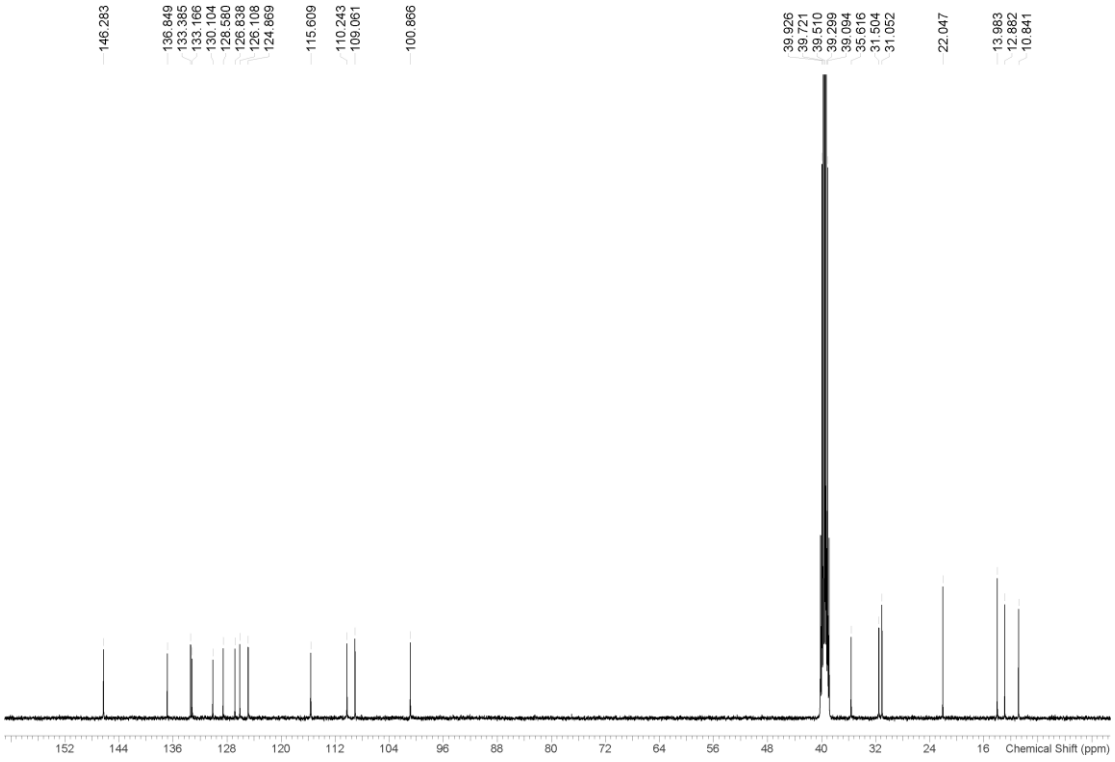

Figure S8. ^{13}C NMR (100 MHz) spectrum of compound **1d** in DMSO-d_6 at 298 K.

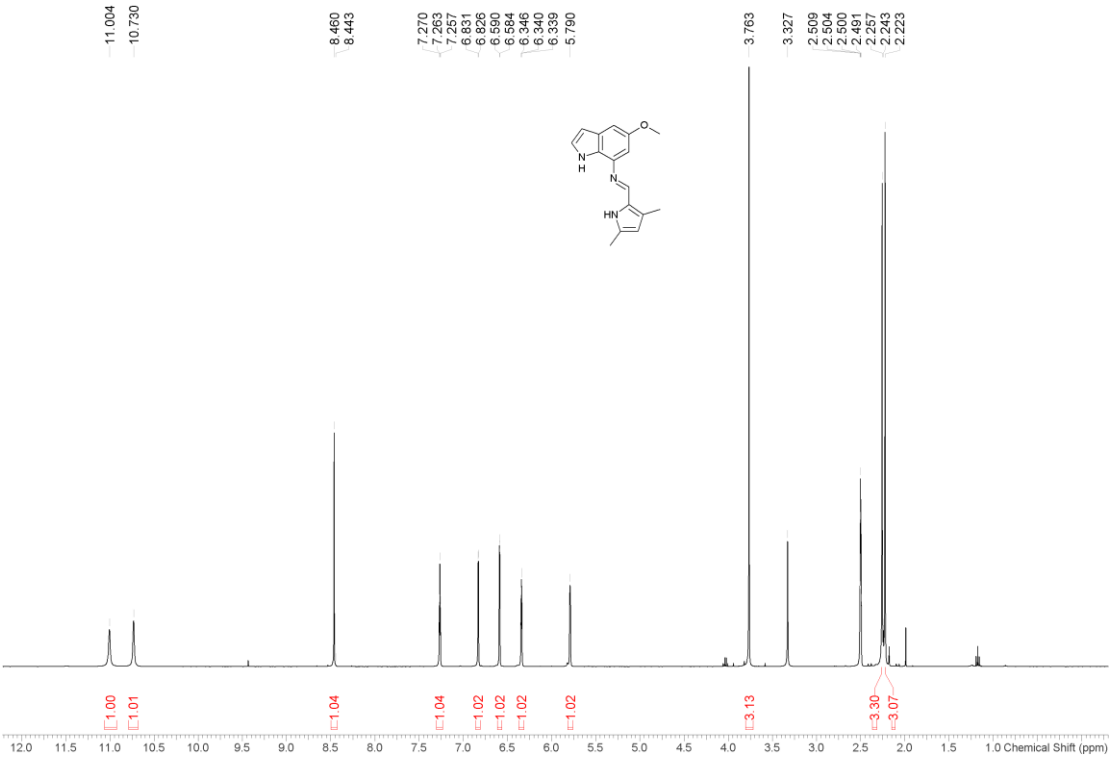

Figure S9. ^{1}H NMR (400 MHz) spectrum of compound **1e** in DMSO-d_6 at 298 K.

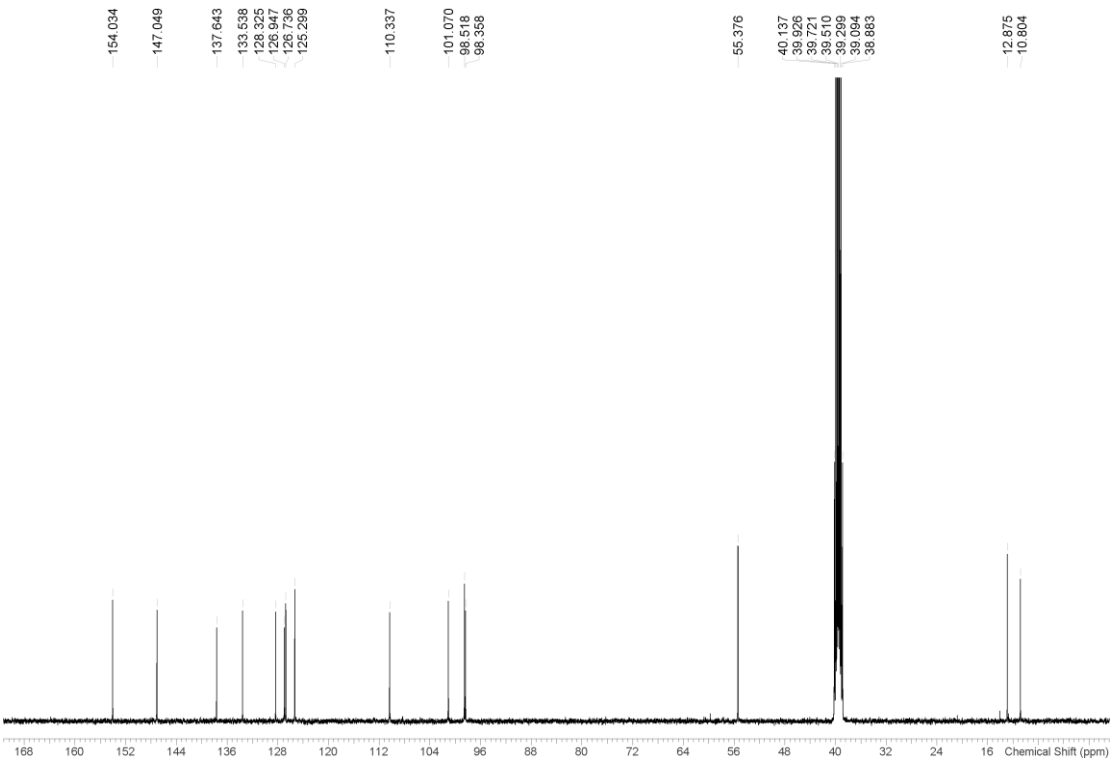

Figure S10. ^{13}C NMR (100 MHz) spectrum of compound **1e** in DMSO-d_6 at 298 K.

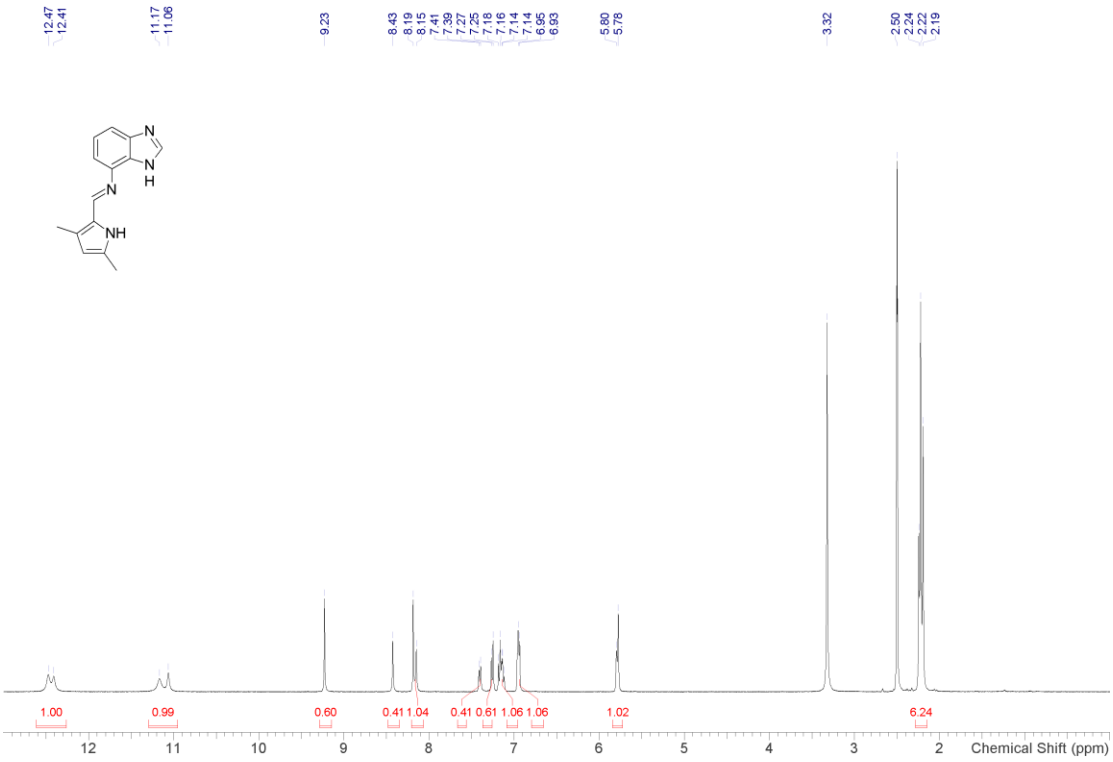

Figure S11. ^{1}H NMR (400 MHz) spectrum of compound **2** in DMSO-d_6 at 298 K.

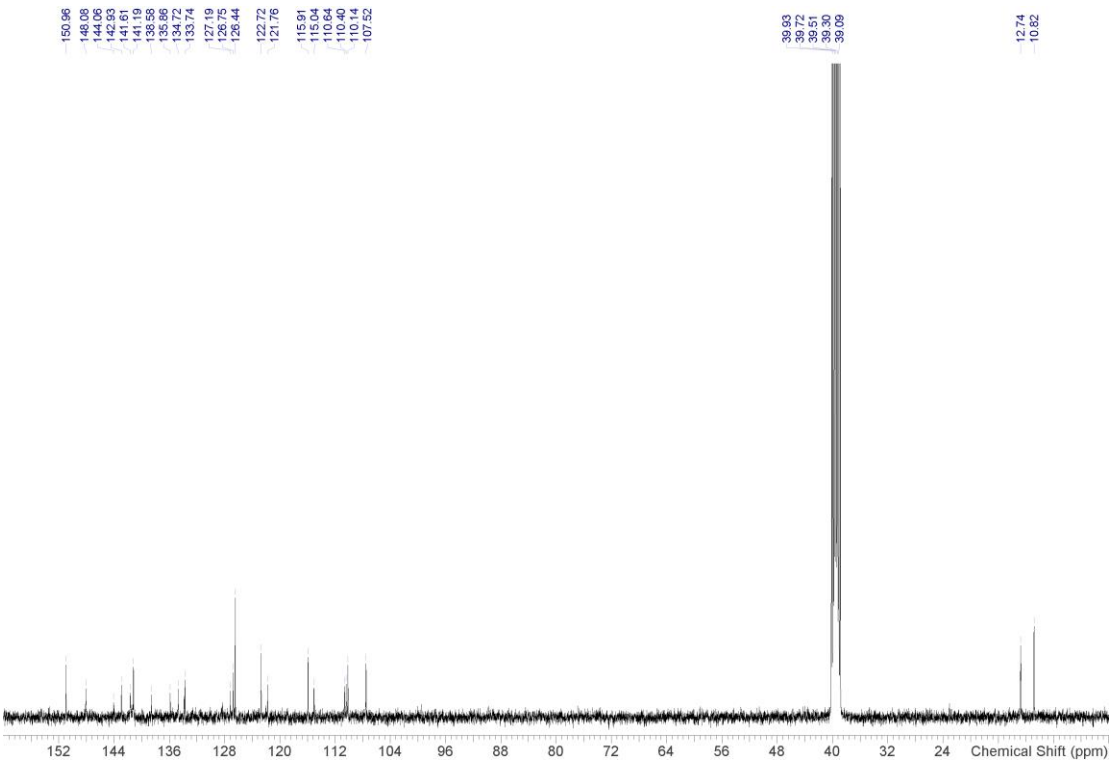

Figure S12. ^{13}C NMR (100 MHz) spectrum of compound **2** in DMSO-d_6 at 298 K.

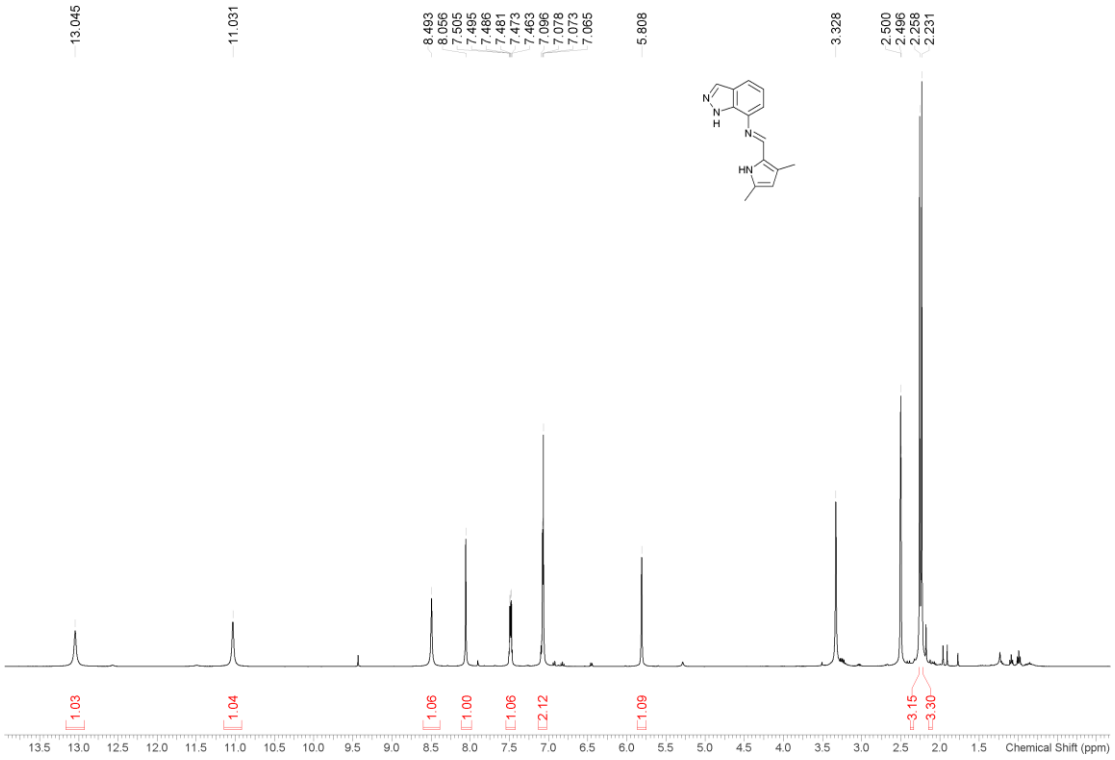

Figure S13. ^{1}H NMR (400 MHz) spectrum of compound **3** in DMSO-d_6 at 298 K.

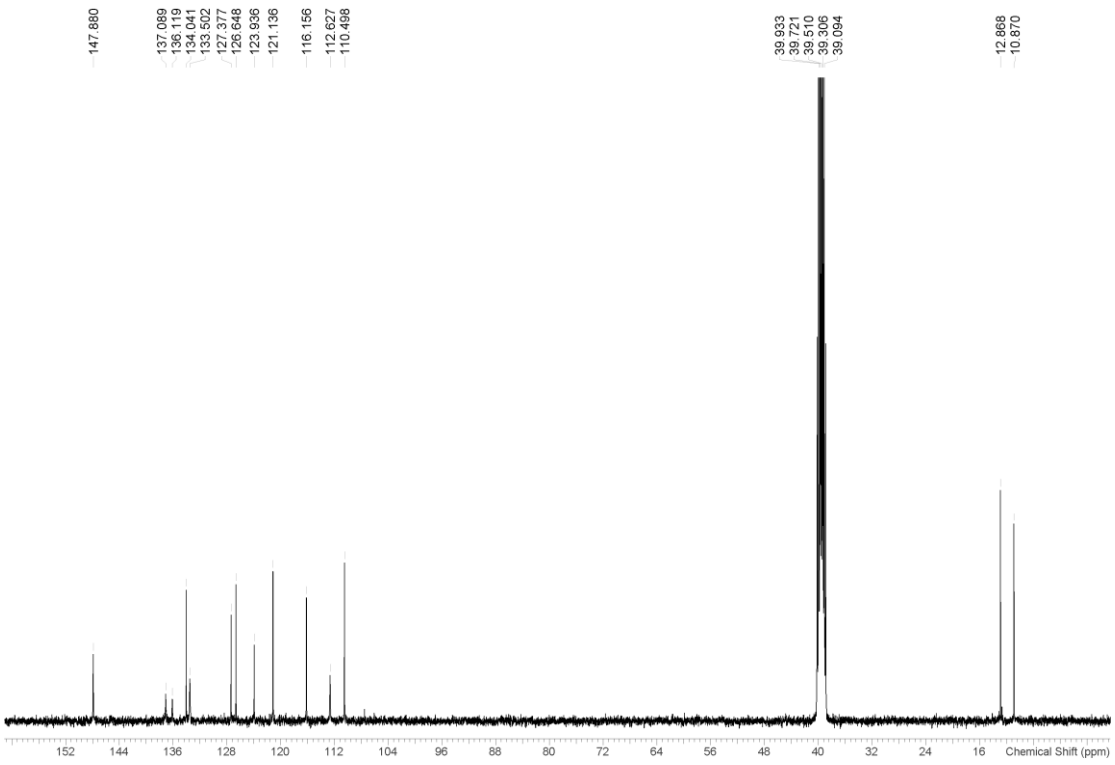

Figure S14. ^{13}C NMR (100 MHz) spectrum of compound **3** in DMSO-d_6 at 298 K.

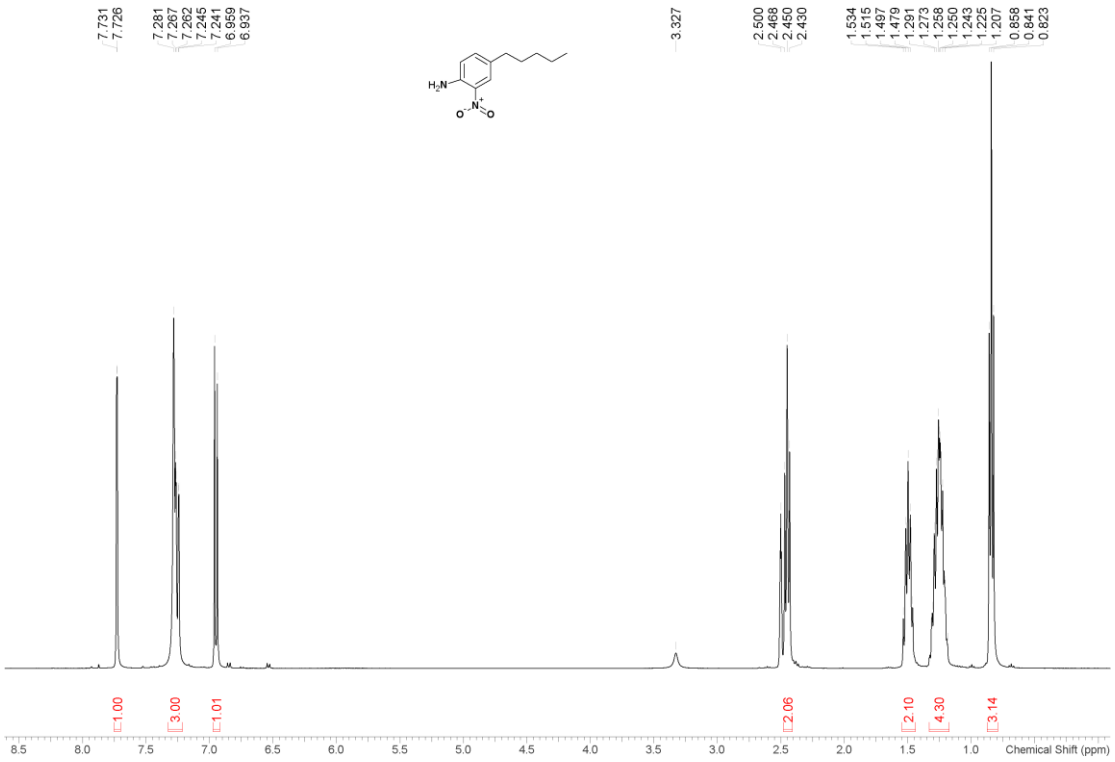

Figure S15. ^{1}H NMR (400 MHz) spectrum of compound **4d** in DMSO-d_6 at 298 K.

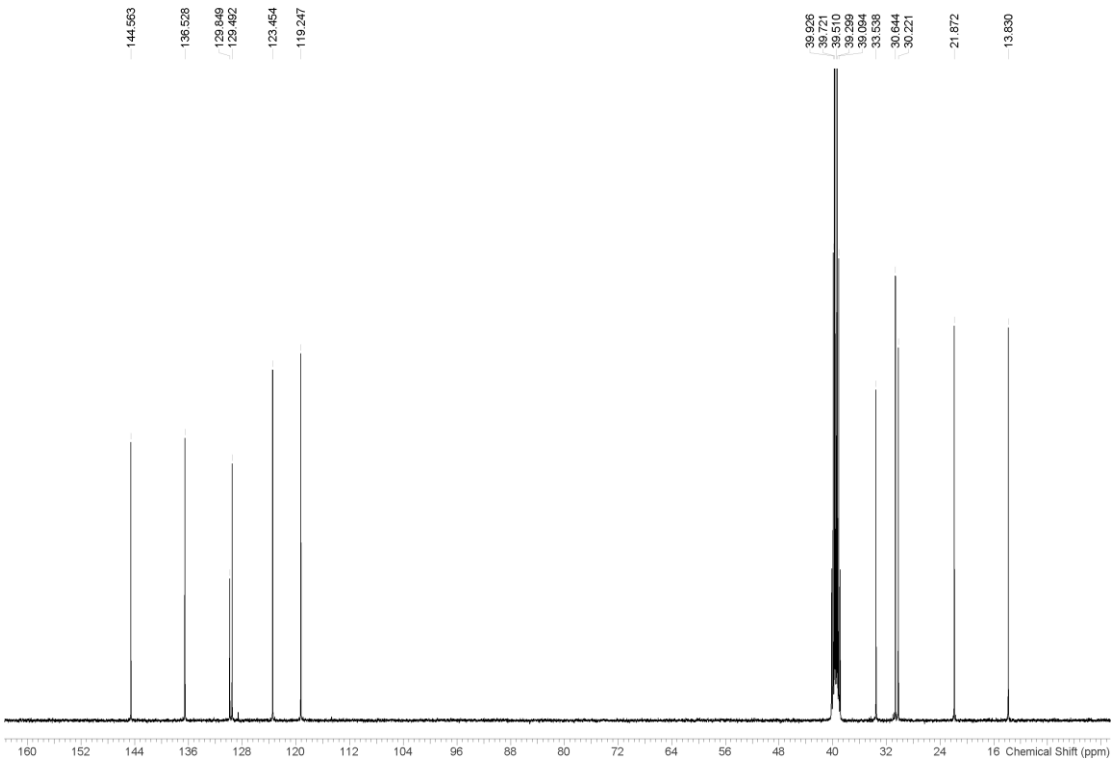

Figure S16. ^{13}C NMR (100 MHz) spectrum of compound **4d** in DMSO-d_6 at 298 K.

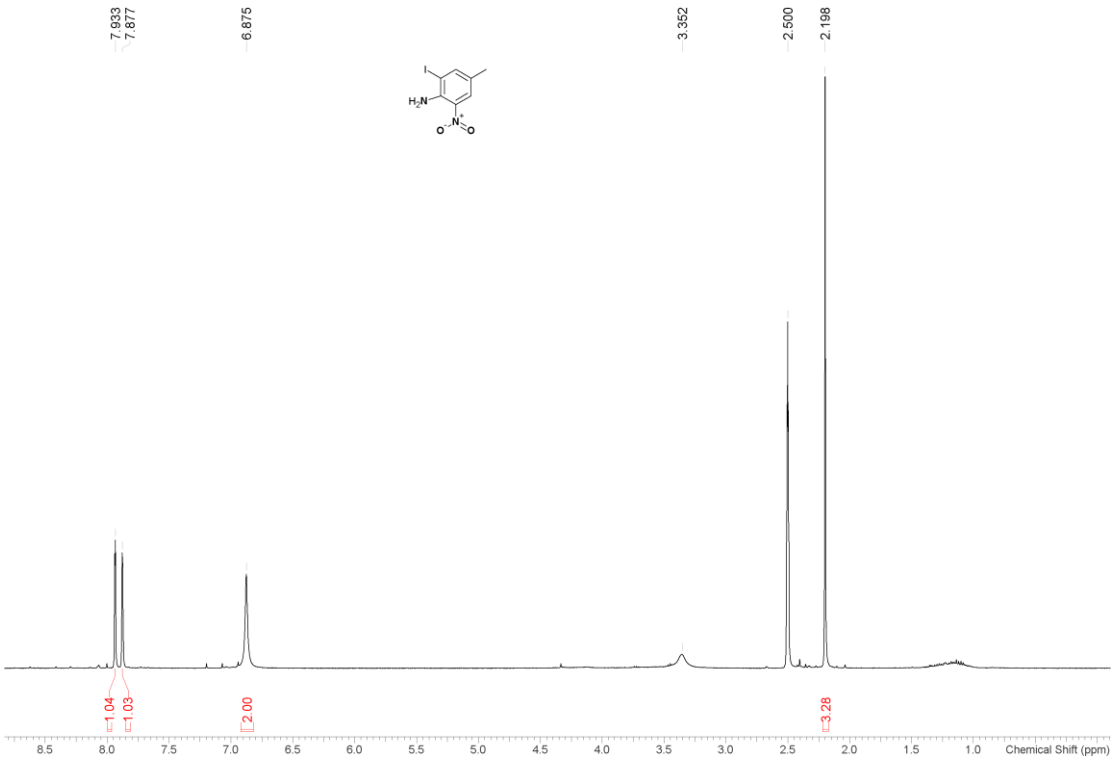

Figure S17. ^{1}H NMR (400 MHz) spectrum of compound **5c** in DMSO-d_6 at 298 K.

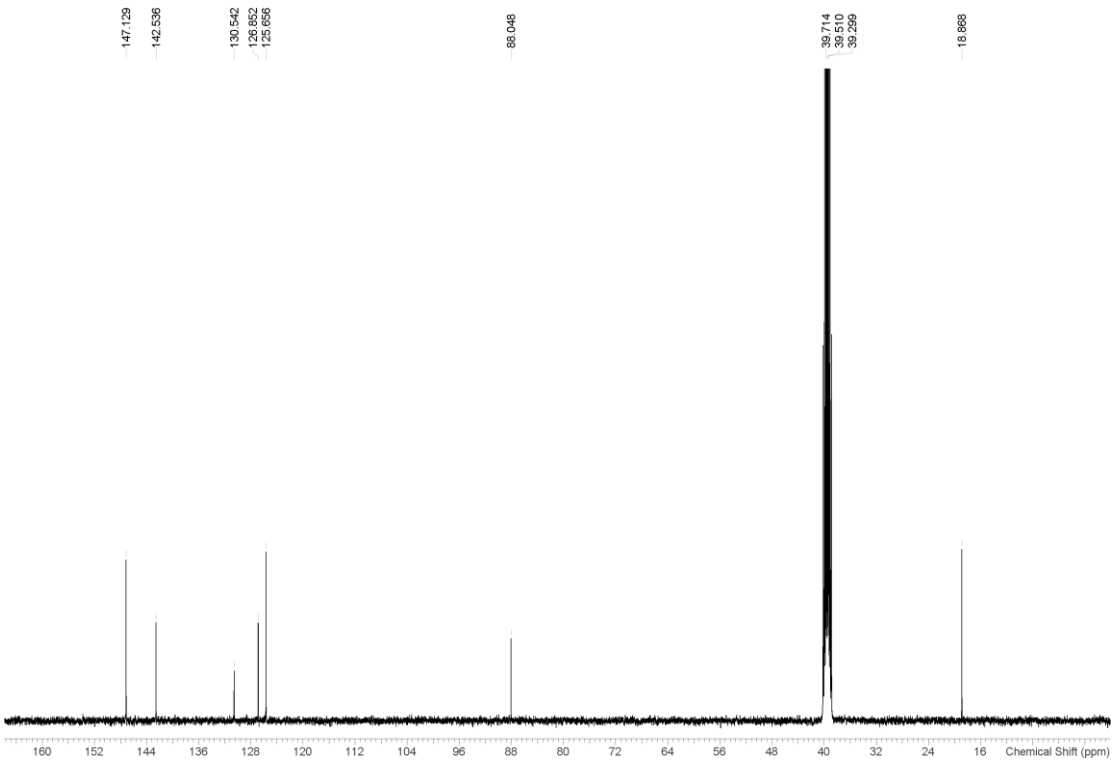

Figure S18. ^{13}C NMR (100 MHz) spectrum of compound **5c** in DMSO-d_6 at 298 K.

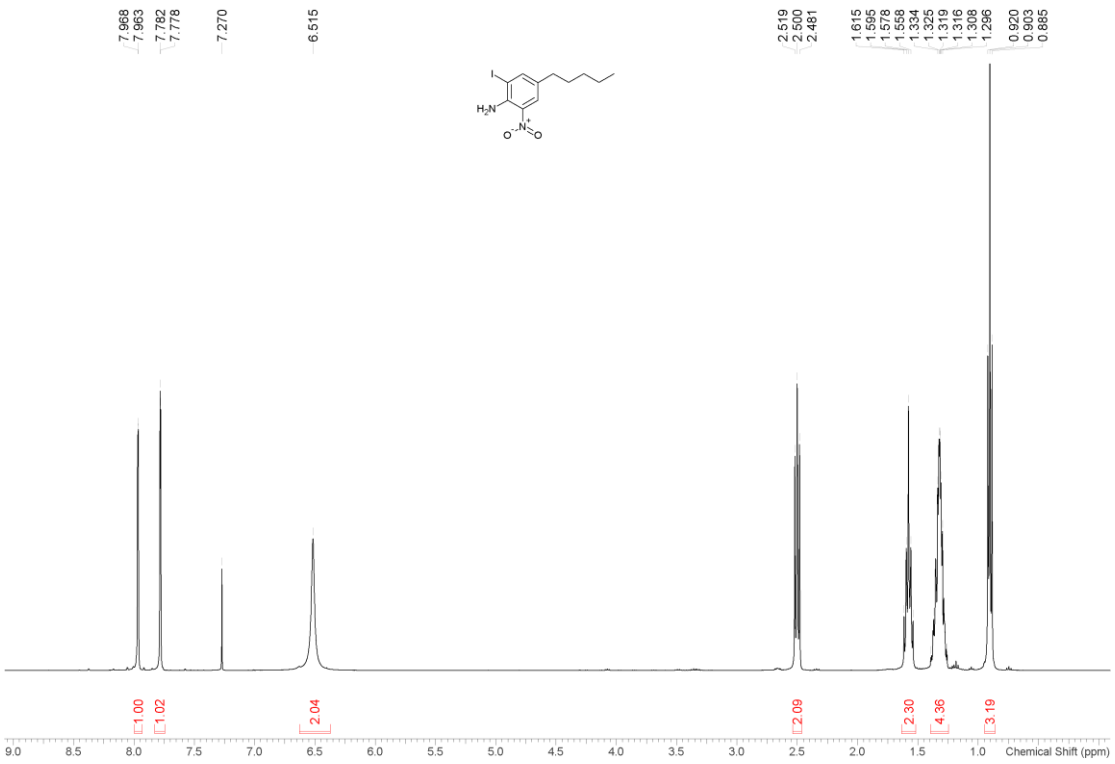

Figure S19. ^{1}H NMR (400 MHz) spectrum of compound **5d** in $CDCl_3$ at 298 K.

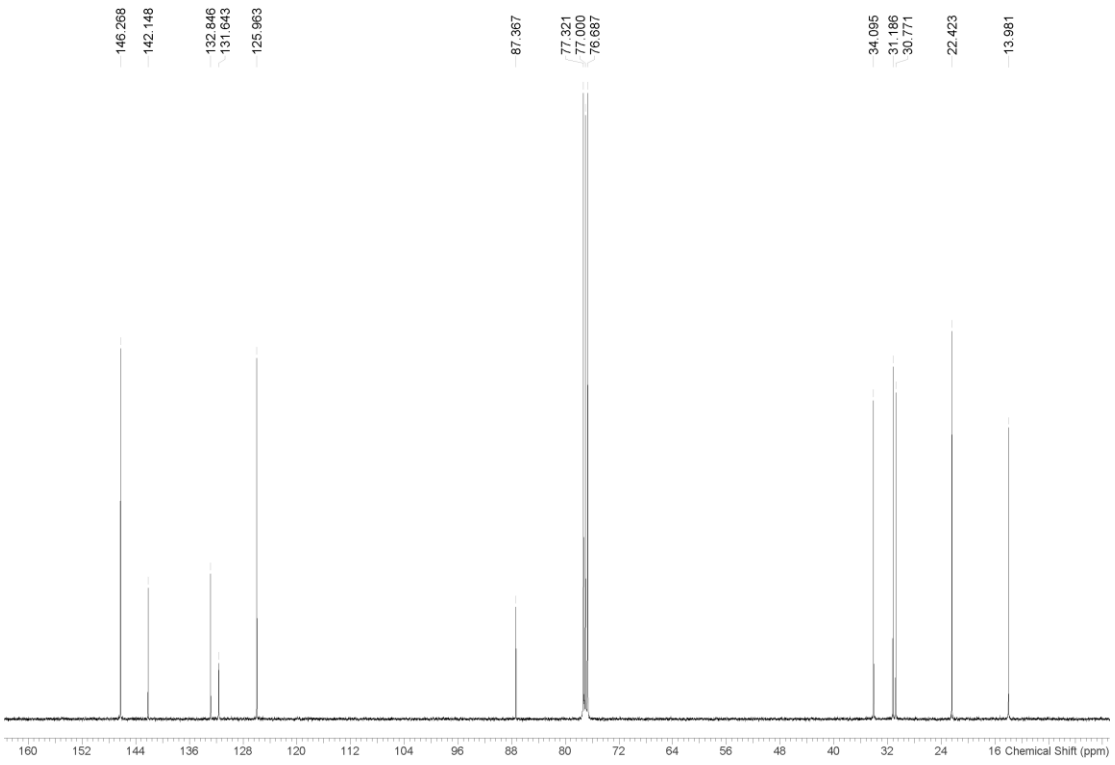

Figure S20. ^{13}C NMR (100 MHz) spectrum of compound **5d** in $CDCl_3$ at 298 K.

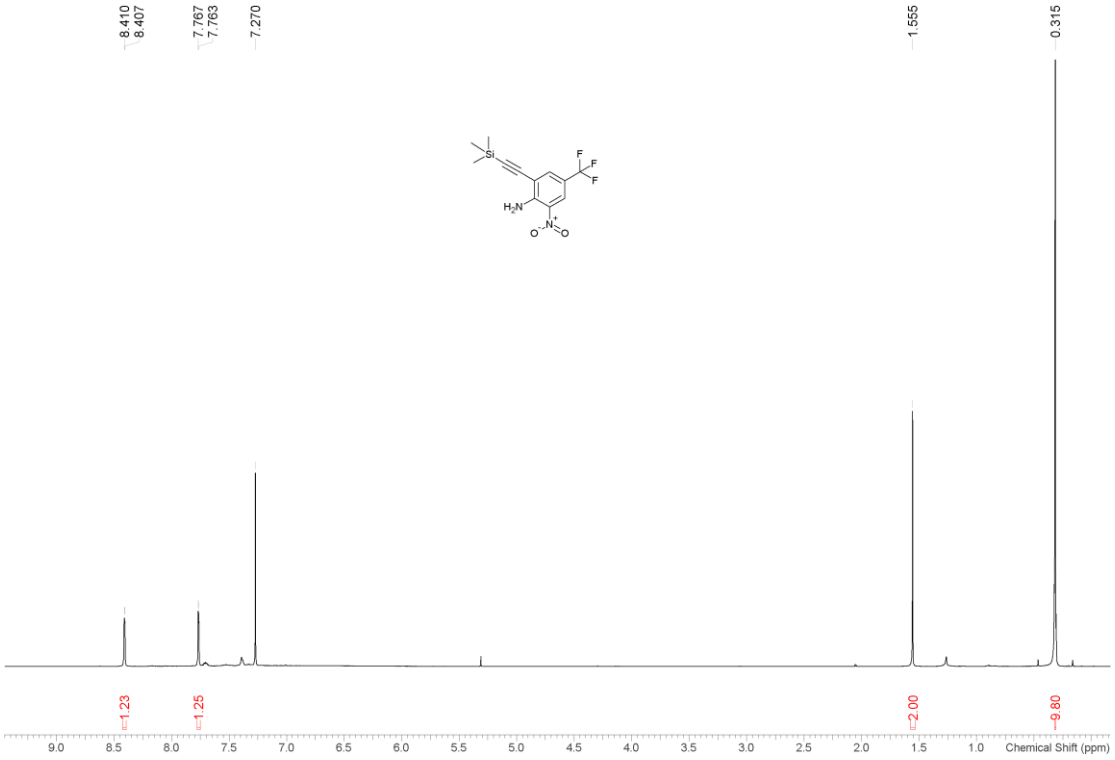

Figure S21. ^{1}H NMR (400 MHz) spectrum of compound **6b** in $CDCl_3$ at 298 K.

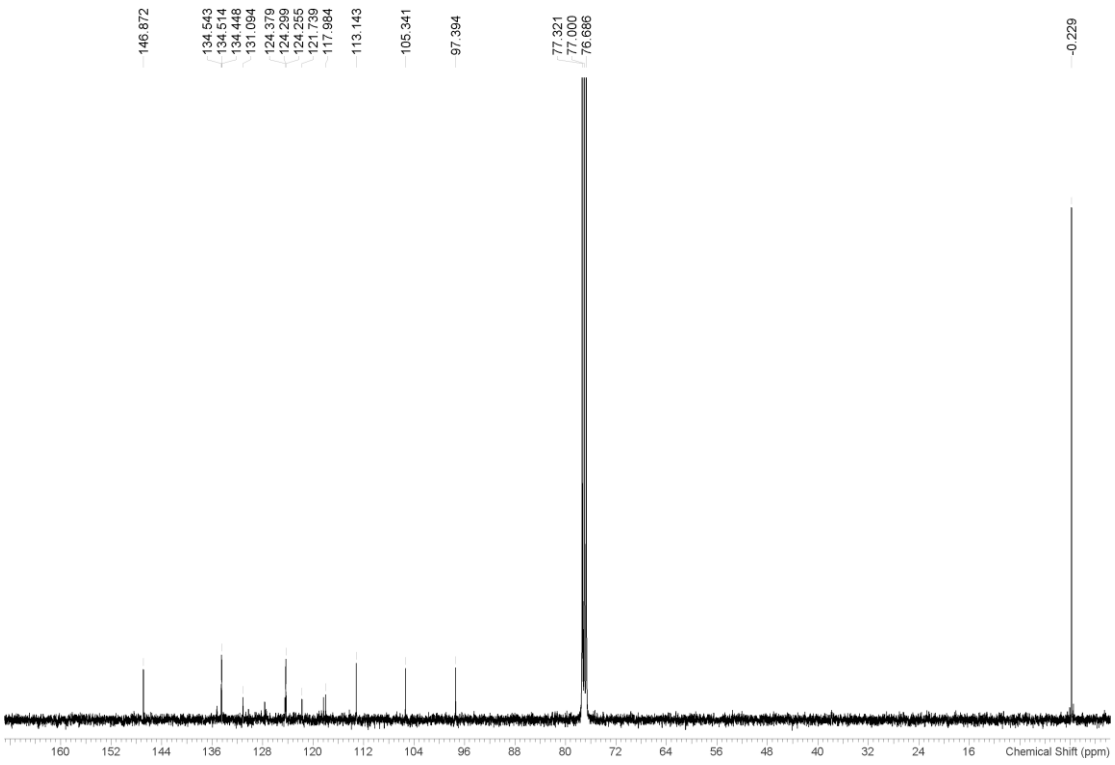

Figure S22. ^{13}C NMR (100 MHz) spectrum of compound **6b** in $CDCl_3$ at 298 K.

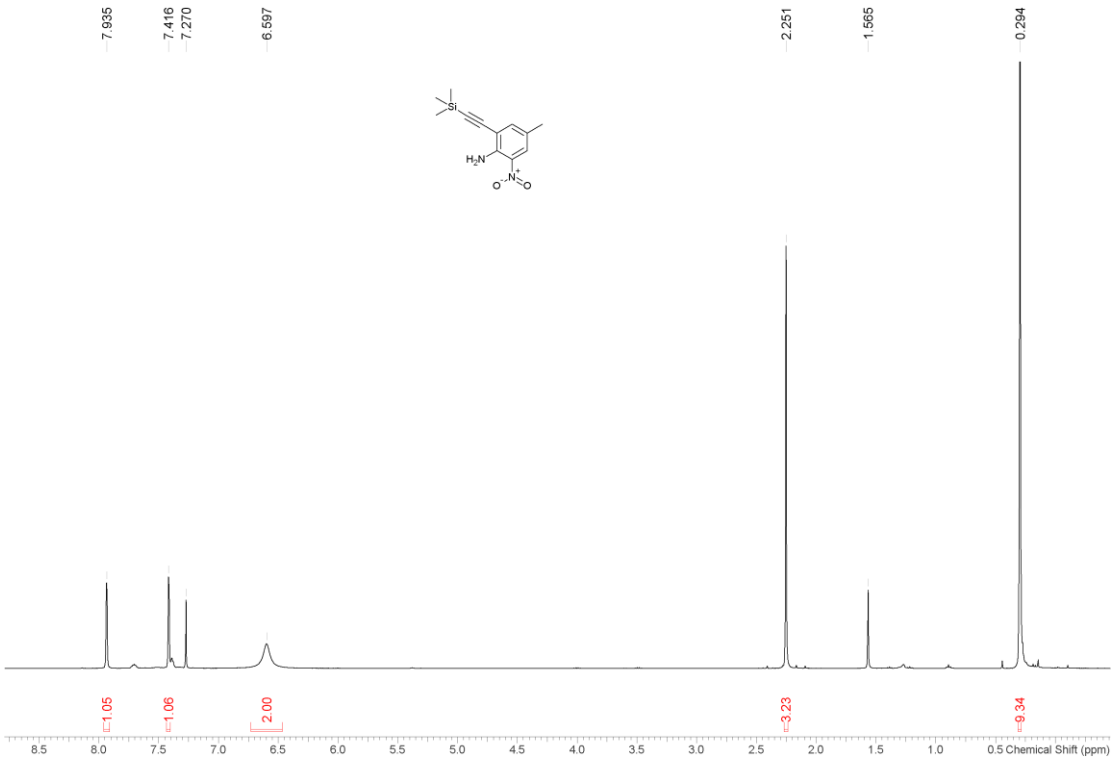

Figure S23. ^{1}H NMR (400 MHz) spectrum of compound **6c** in $CDCl_3$ at 298 K.

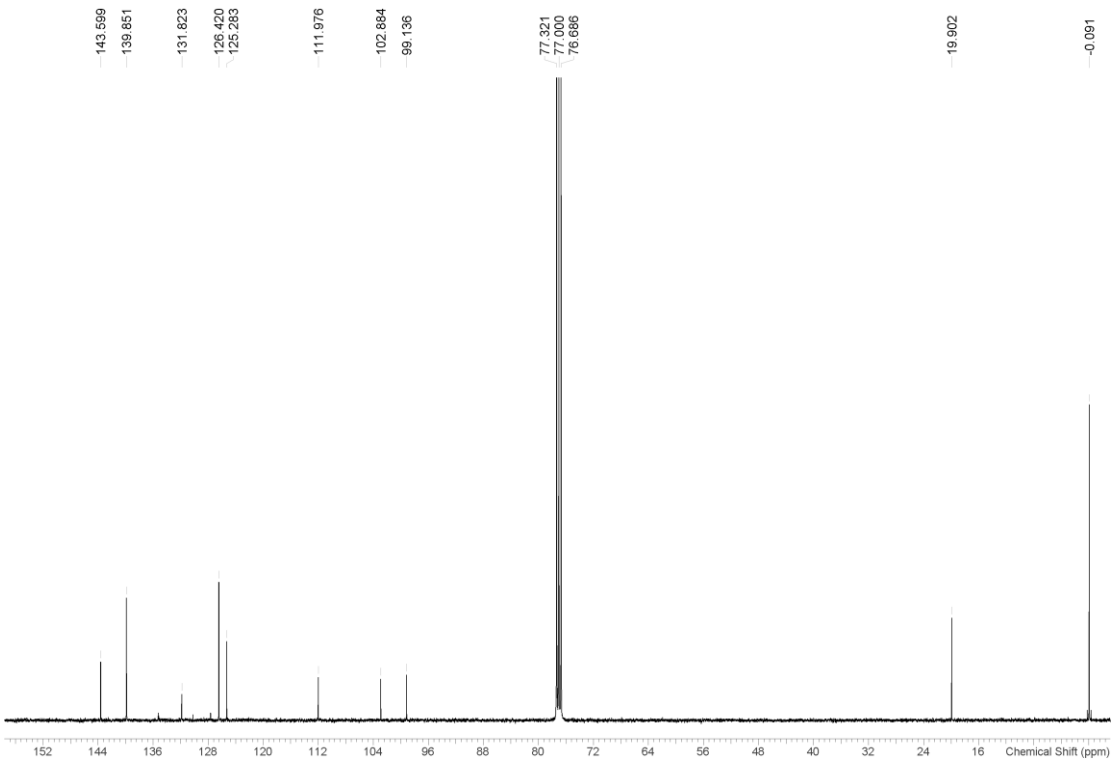

Figure S24. ^{13}C NMR (100 MHz) spectrum of compound **6c** in $CDCl_3$ at 298 K.

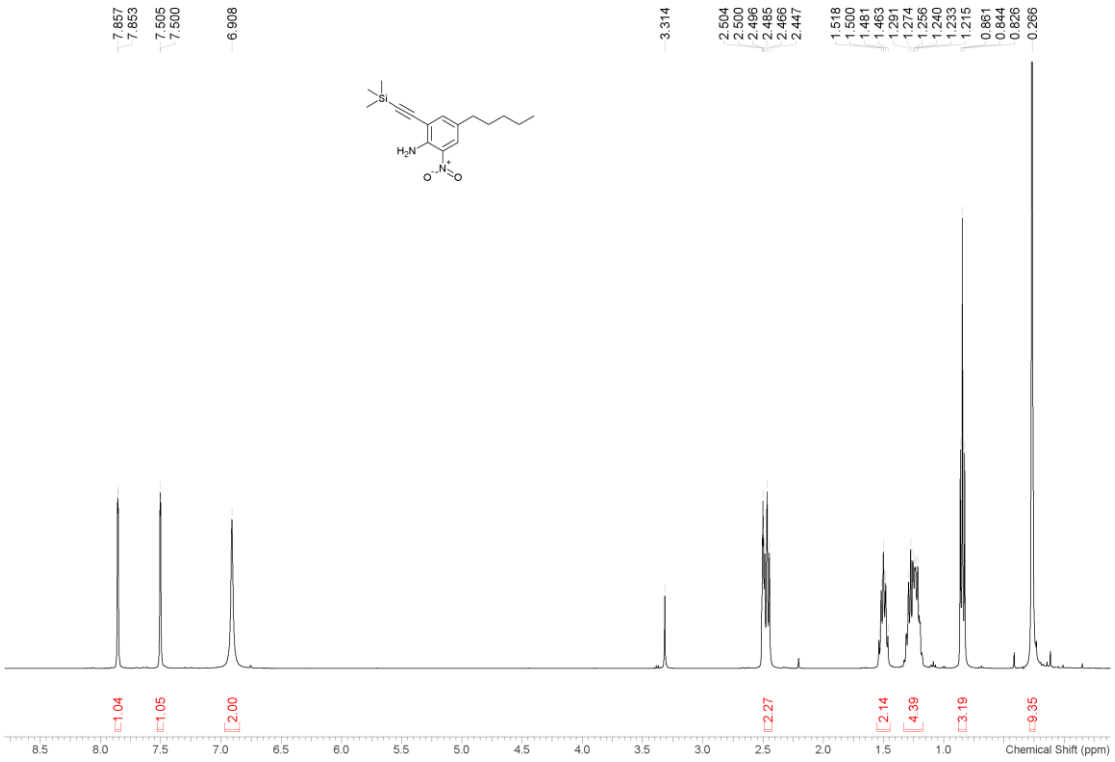

Figure S25. ^{1}H NMR (400 MHz) spectrum of compound **6d** in DMSO-d_6 at 298 K.

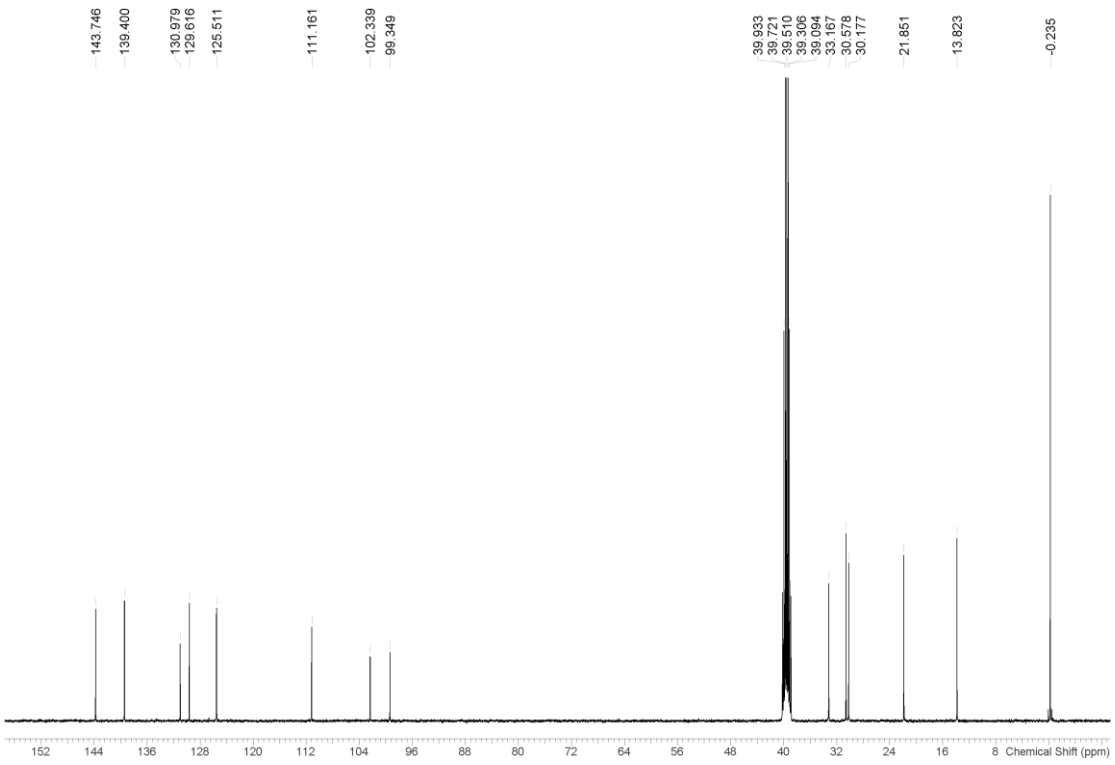

Figure S26. ^{13}C NMR (100 MHz) spectrum of compound **6d** in DMSO-d_6 at 298 K.

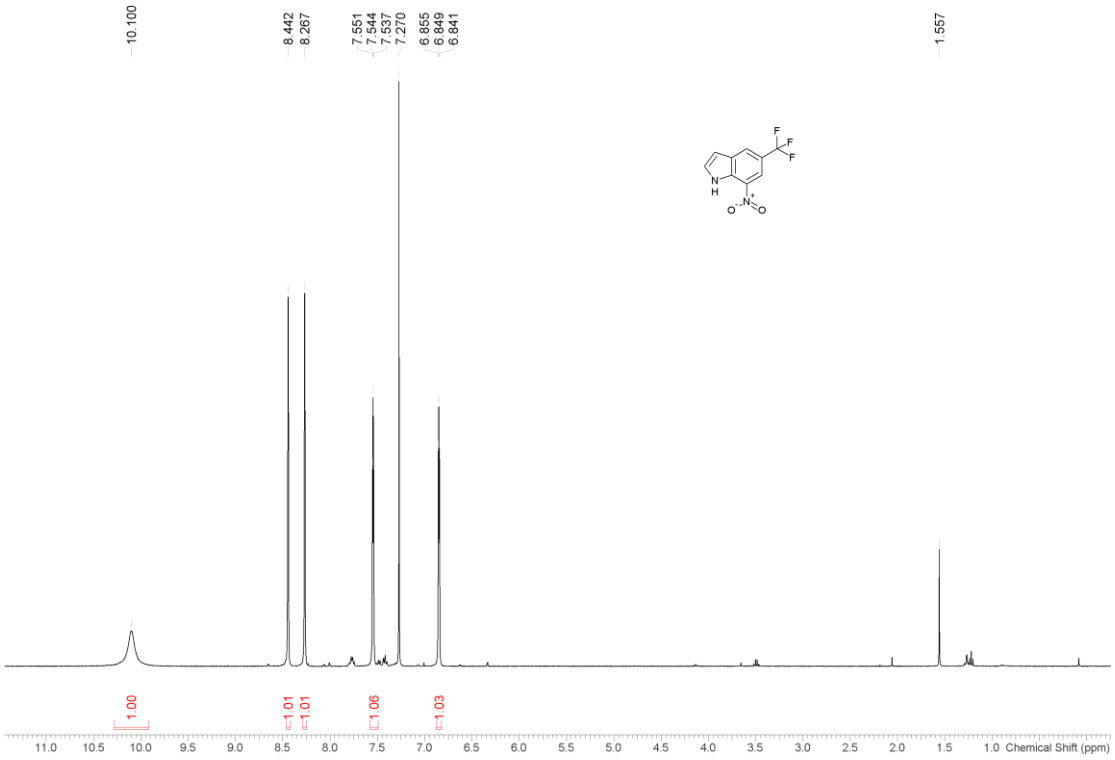

Figure S27. ^{1}H NMR (400 MHz) spectrum of compound **7b** in $CDCl_3$ at 298 K.

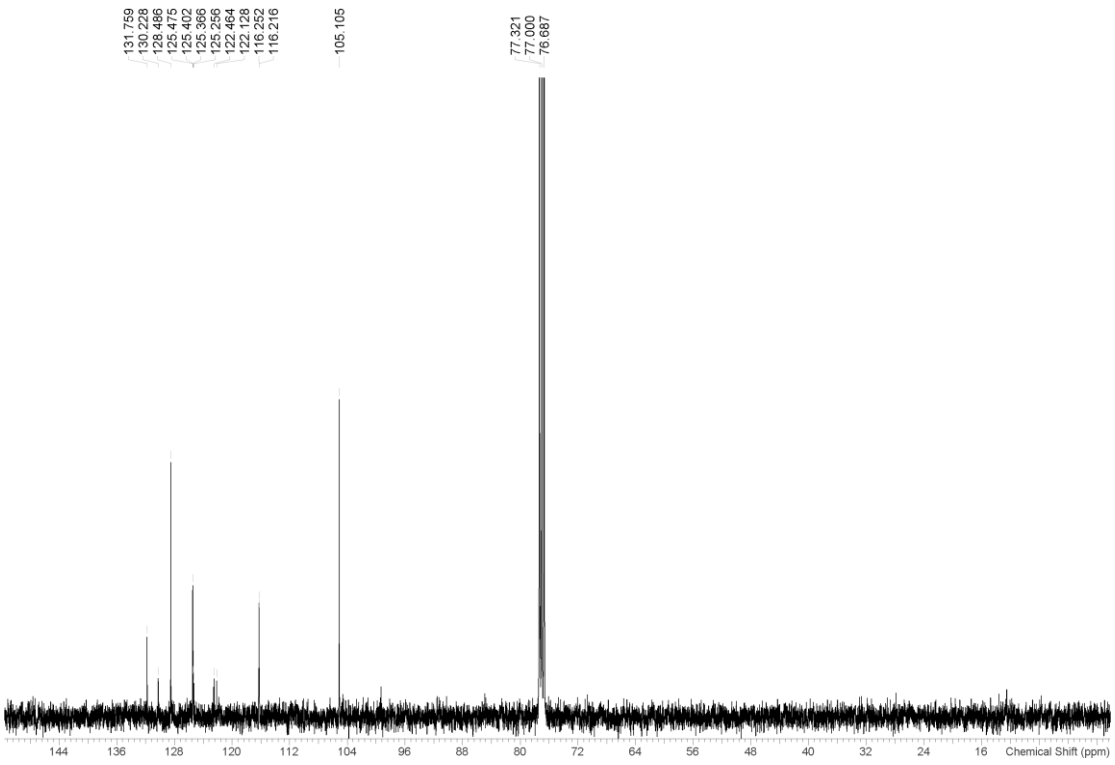

Figure S28. ^{13}C NMR (100 MHz) spectrum of compound **7b** in $CDCl_3$ at 298 K.

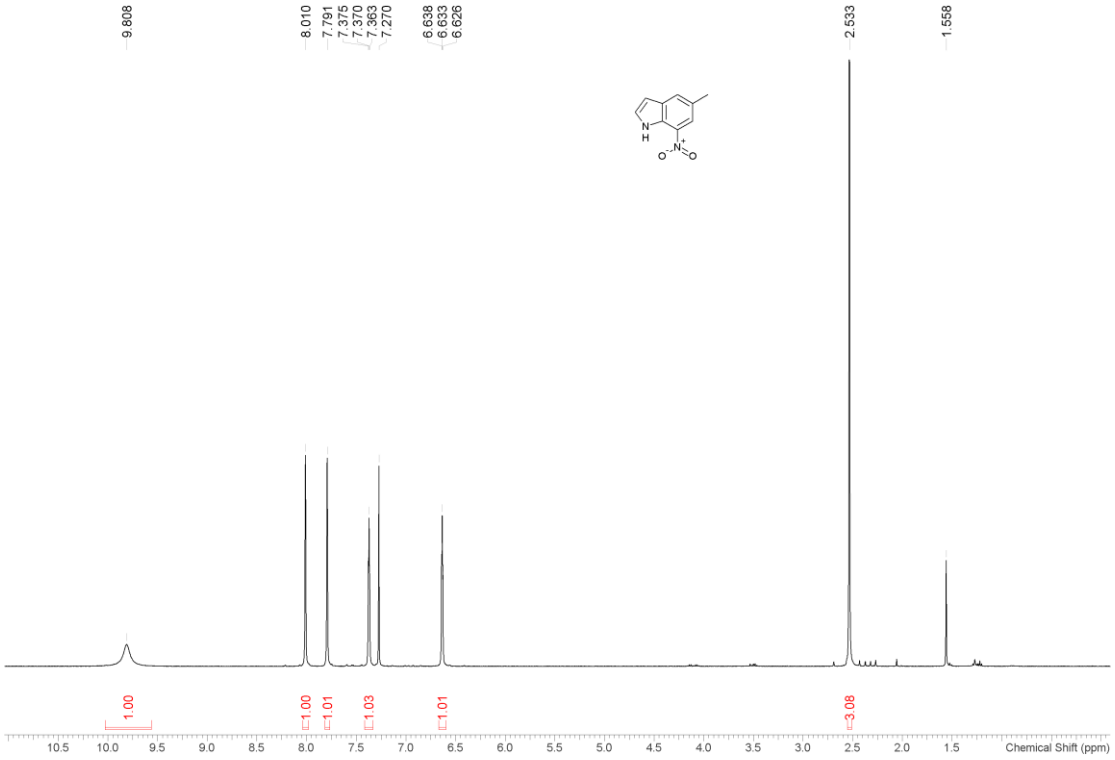

Figure S29. ^{1}H NMR (400 MHz) spectrum of compound **7c** in $CDCl_3$ at 298 K.

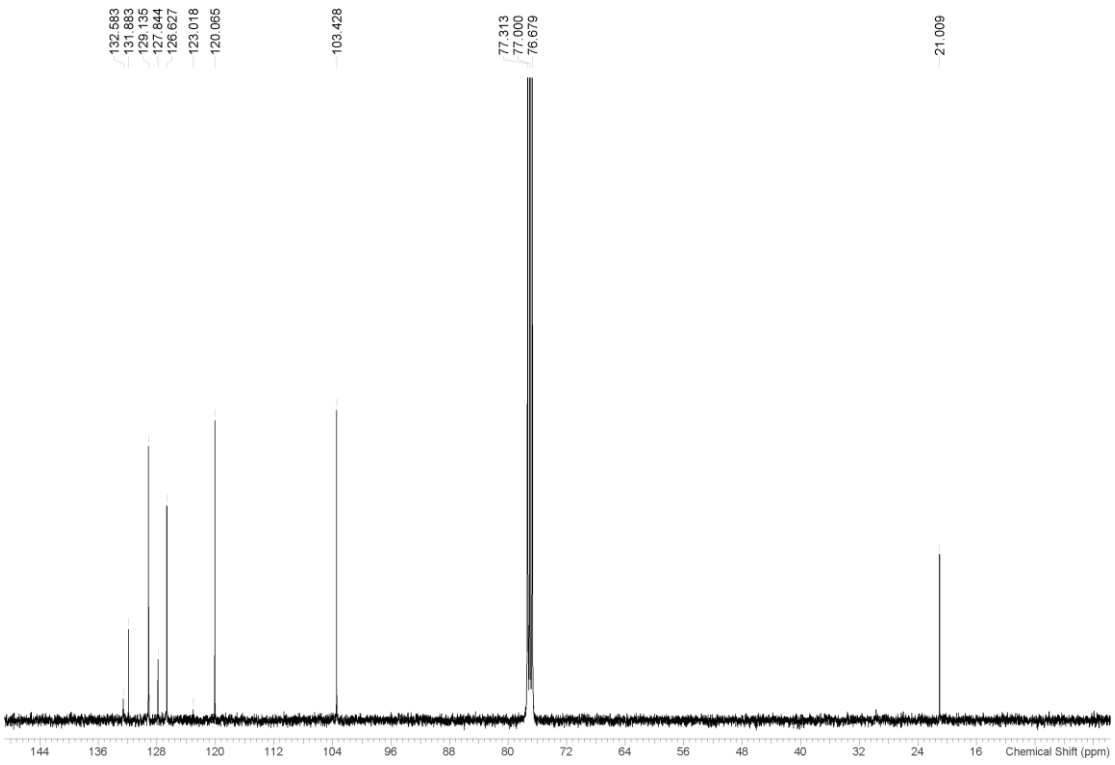

Figure S30. ^{13}C NMR (100 MHz) spectrum of compound **7c** in $CDCl_3$ at 298 K.

Figure S31. ^{1}H NMR (400 MHz) spectrum of compound **7d** in $CDCl_3$ at 298 K.

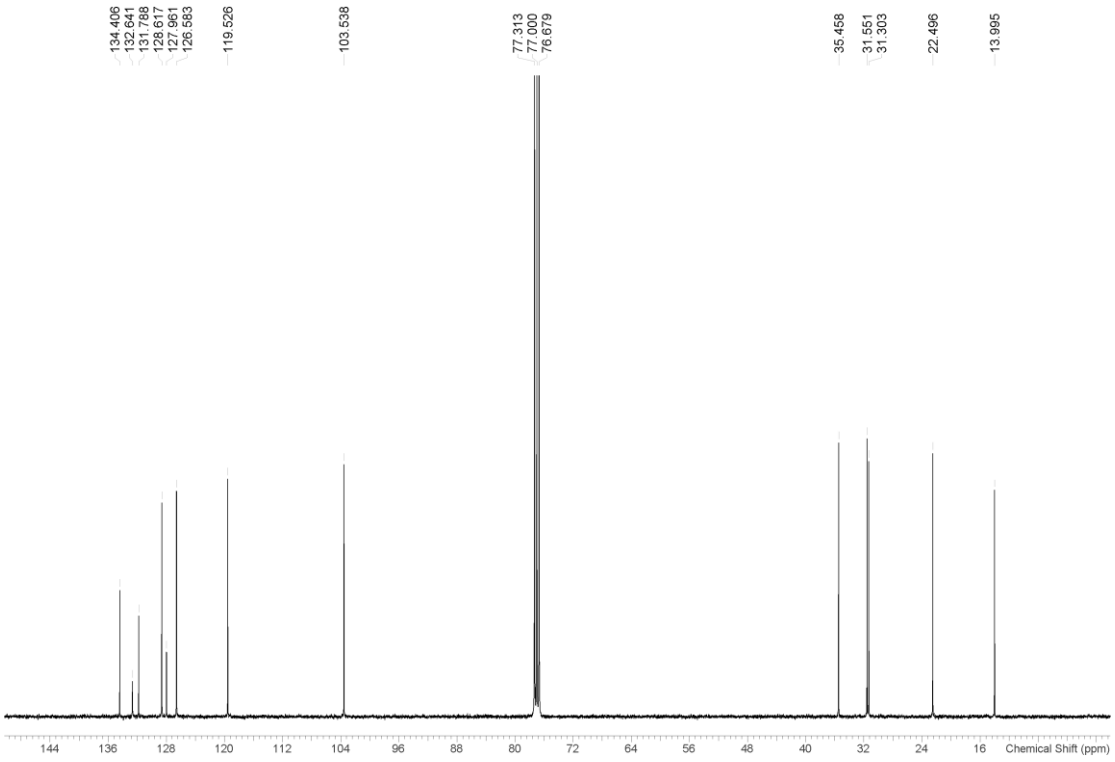

Figure S32. ^{13}C NMR (100 MHz) spectrum of compound **7d** in $CDCl_3$ at 298 K.

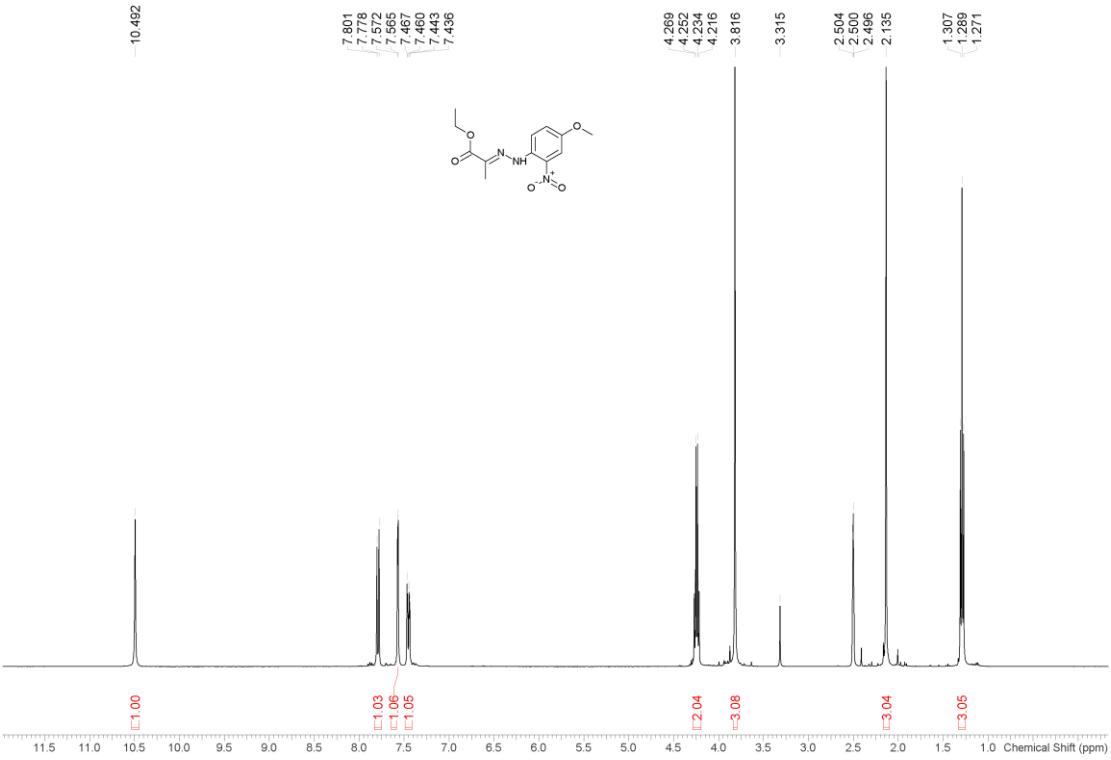

Figure S33. ^{1}H NMR (400 MHz) spectrum of compound **8** in DMSO-d_6 at 298 K.

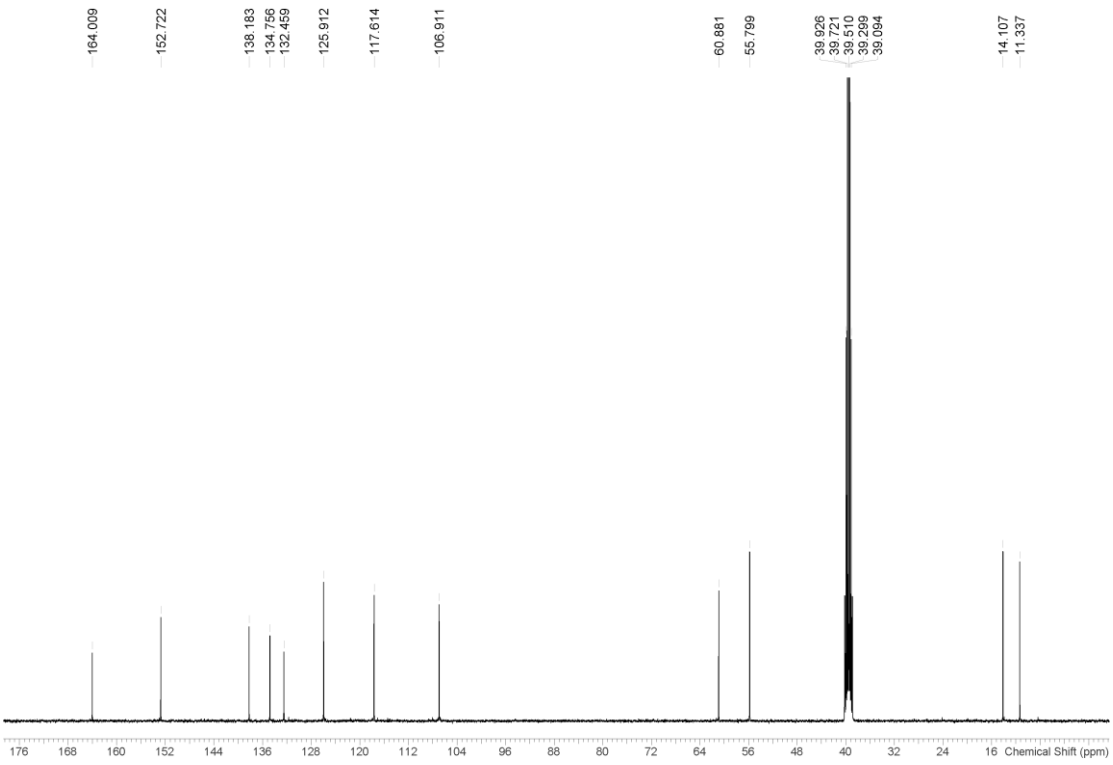

Figure S34. ^{13}C NMR (100 MHz) spectrum of compound **8** in DMSO-d_6 at 298 K.

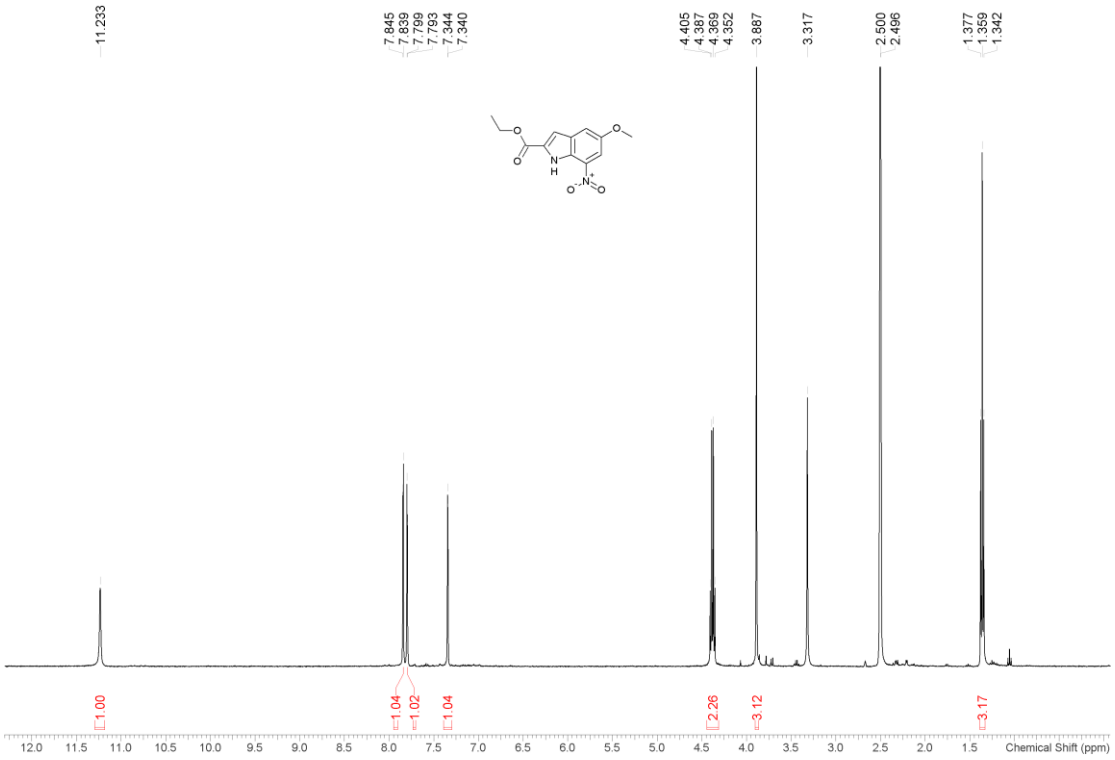

Figure S35. ^{1}H NMR (400 MHz) spectrum of compound **9** in DMSO-d_6 at 298 K.

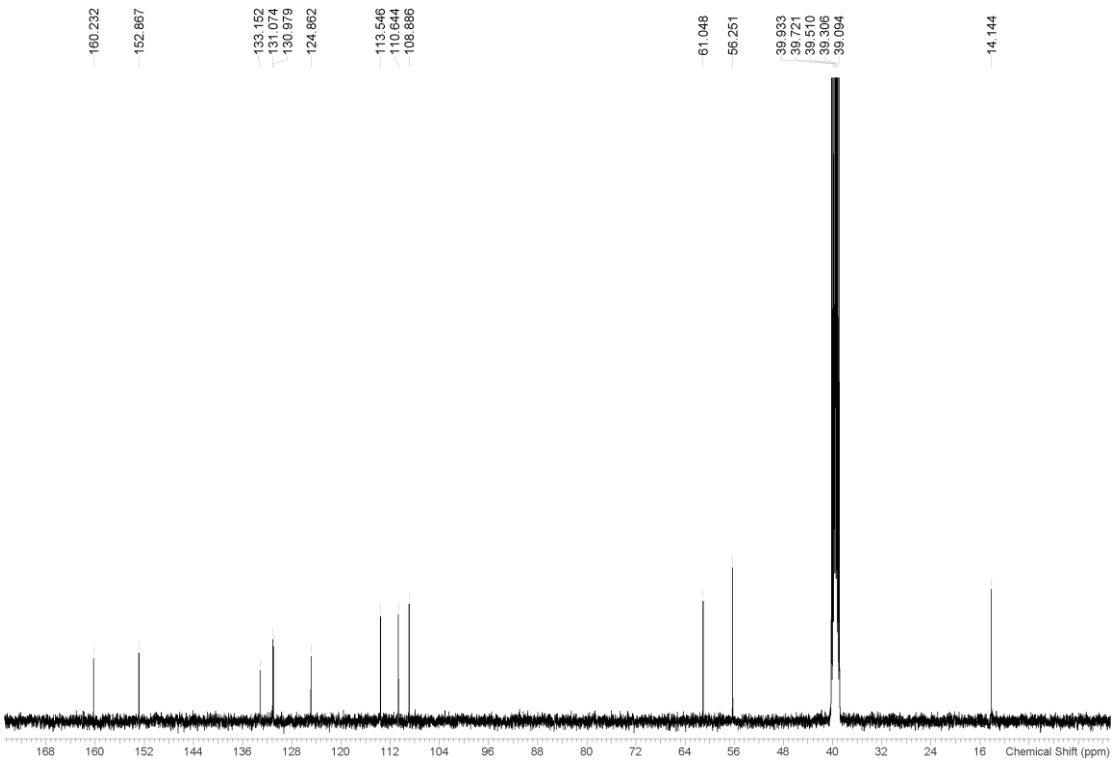

Figure S36. ^{13}C NMR (100 MHz) spectrum of compound **9** in DMSO-d_6 at 298 K.

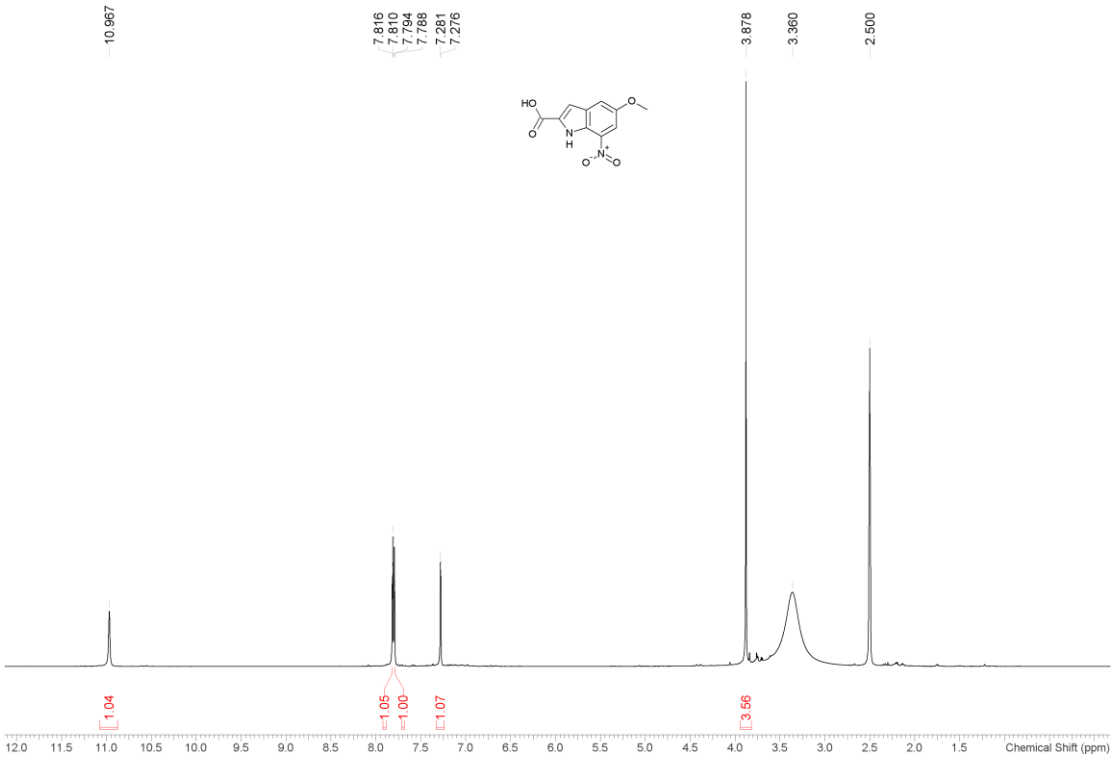

Figure S37. ^{1}H NMR (400 MHz) spectrum of compound **10** in DMSO-d_6 at 298 K.

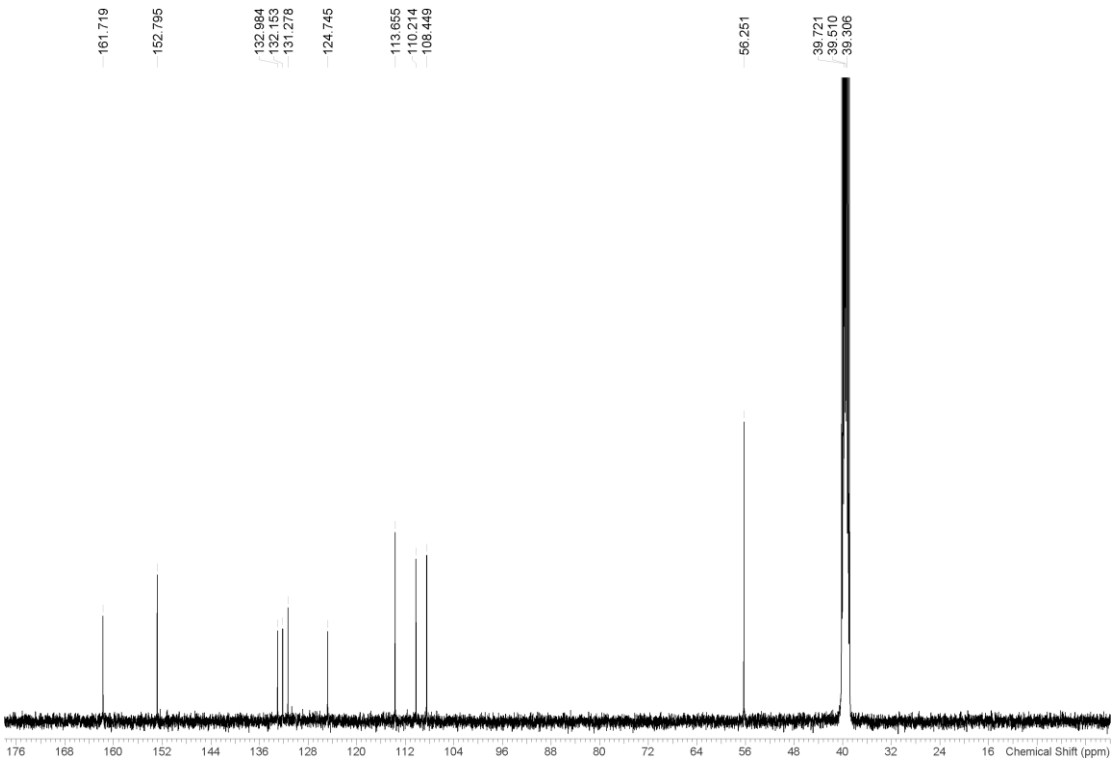

Figure S38. ^{13}C NMR (100 MHz) spectrum of compound **10** in DMSO-d_6 at 298 K.

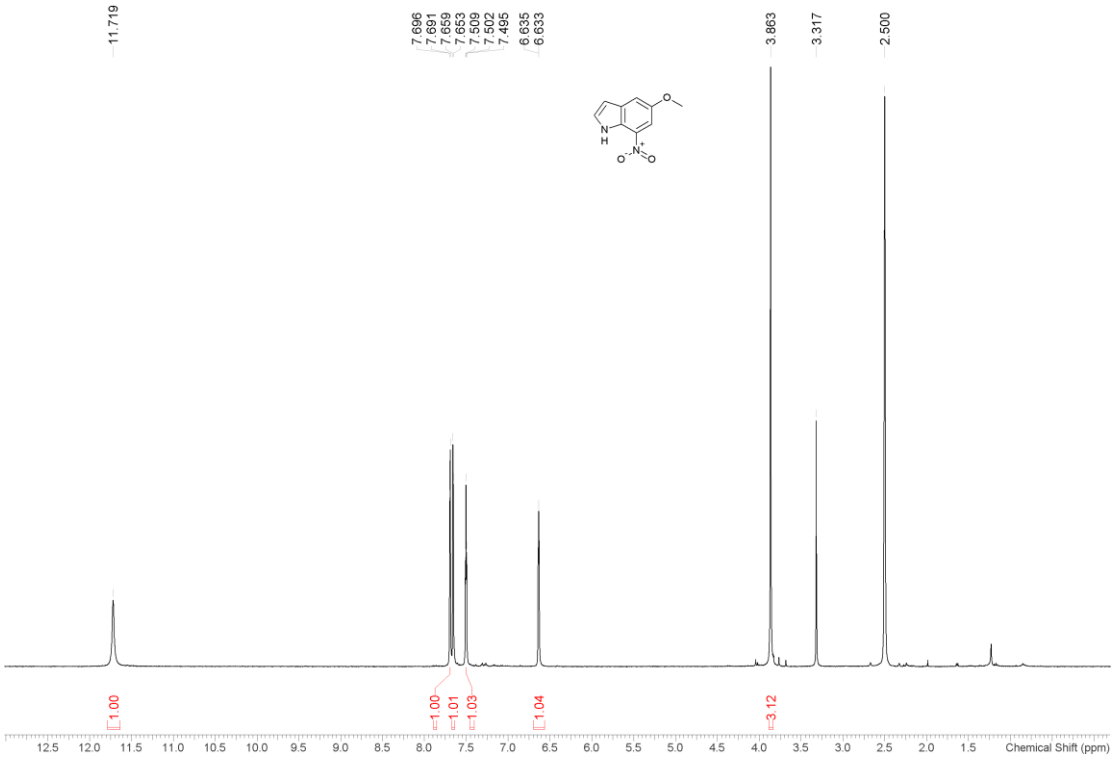

Figure S39. ^{1}H NMR (400 MHz) spectrum of compound **11** in DMSO-d_6 at 298 K.

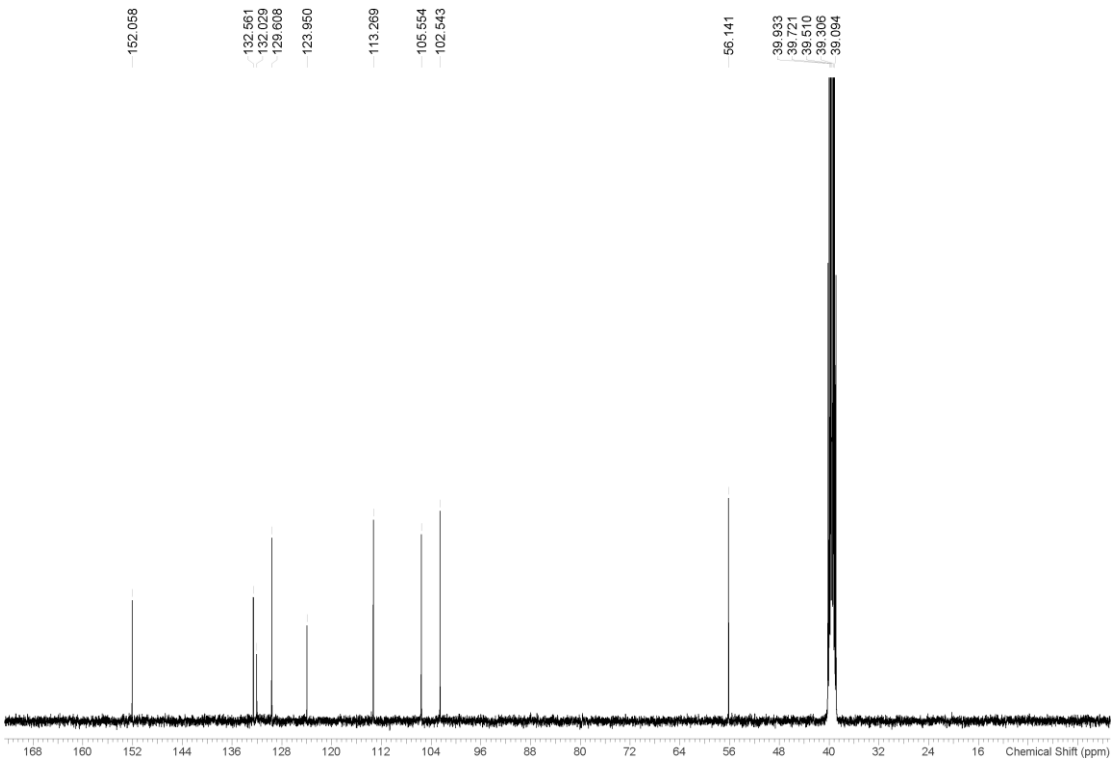

Figure S40. ^{13}C NMR (100 MHz) spectrum of compound **11** in DMSO-d_6 at 298 K.

3. X-ray crystallographic structure and data for complex [1a+HCl]

The X-ray diffraction data was collected on a Rigaku AFC12 goniometer equipped with an enhanced sensitivity (HG) Saturn724+ detector mounted at the window of an FR-E+ Superbright MoKα (λ=0.71073 Å) rotating anode generator with HF Varimax optics, using the CrystalClear-SM Expert 3.1 b27 (Rigaku, 2013) software. Data set was collected at 100 K using an Oxford Cryostream low temperature device. Cell refinement and data reduction was carried out using CrystalClear-SM Expert 3.1 b27 (Rigaku, 2013); olex2.solve (Bourhis et al., 2015) was used to solve structure and SHELXL (Sheldrick, 2008) used to refine structure. All non-hydrogen atoms were refined with anisotropic displacement parameters. Non-hydrogen atoms were anisotropically refined and the hydrogen atoms were placed on calculated positions and refined using a riding model with isotropic displacement parameters based on the equivalent isotropic displacement parameters (U_{eq}) of the parent atom. The fundamental crystal data and experimental parameters for the structure determinations are summarized below. Crystallographic data (excluding structure factors) for the structures in this paper have been deposited with the Cambridge Crystallographic Data Centre as supplementary publication no. CCDC 1441636.

Formula: $C_{15}H_{16}N_3$,$CHCl_3$,Cl; M (g mol^{-1}): 393.13; crystal dimensions (mm^3): 0.21 × 0.02 × 0.01; T (K): 100(2); crystal system: triclinic; space group: *P*-1; a, b, c (Å): 12.586(6), 13.271(7), 13.663(6); α, β, γ (deg): 115.299(7), 95.881(4), 111.985(2); V (Å^3): 1817.0(15); Z: 4; ρ_{calc} (g cm^{-3}): 1.437; μ (mm^{-1}): 0.65; *F*(000): 808; λ (Å): 0.71073 (Mo Kα); θ_{max} (deg): 27.5; measured reflections: 16543; independent reflections: 8306; observed reflections with $I > 2\sigma(I)$: 5703; parameters refined: 416; R_{int}: 0.043; GooF: 1.093; $wR(F^2)$: 0.186; R_1: 0.079.

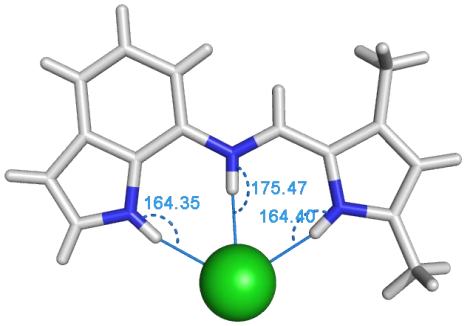

Figure S41. Angles of the hydrogen bonds in [**1a**+HCl].

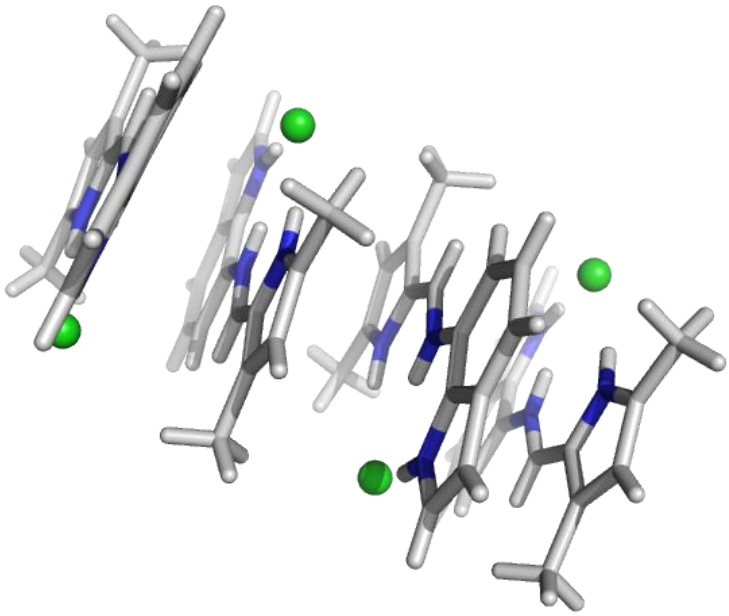

Figure S42. Packing of [**1a**+HCl] in solid state.

4. ^{1}H NMR binding studies

^{1}H NMR titrations were performed by addition of aliquots of the putative anionic guest as the tetra-*n*-butylammonium or tetraethylammonium salt (20 mM), in a solution of the receptor (5 mM) in DMSO-d_6/0.5% H_2O, to a 5 mM solution of the receptor (0.5 mL) with or without 1 equivalent of HPF_6.

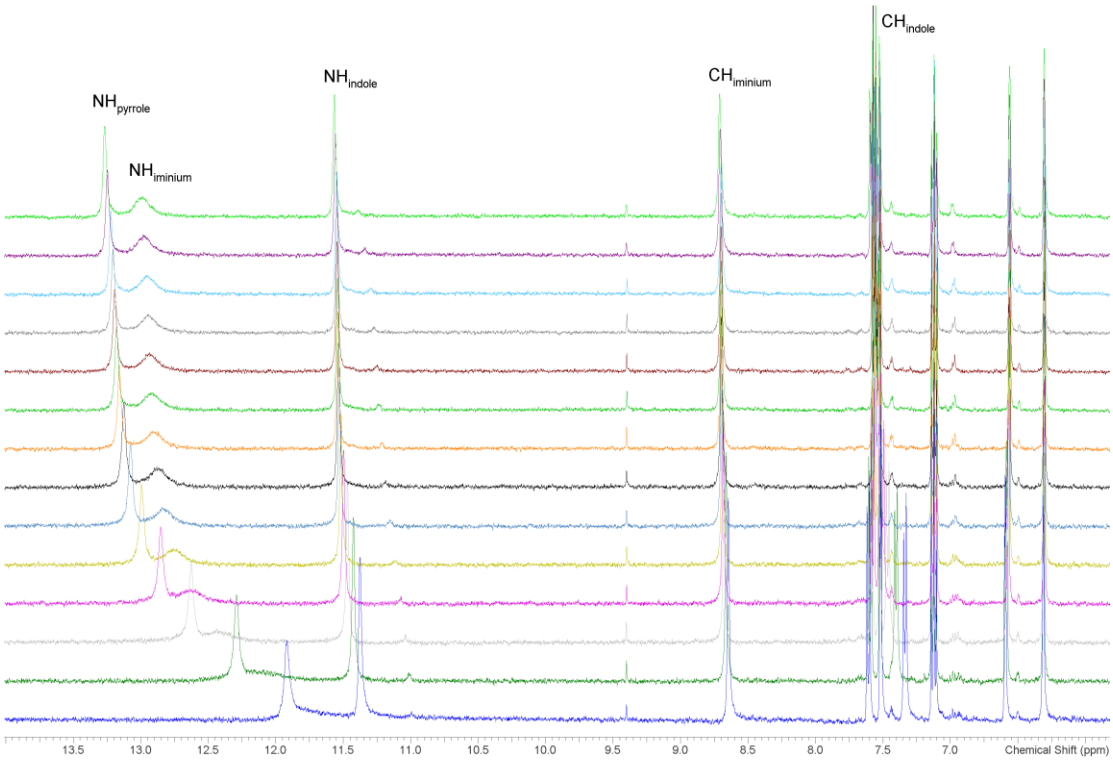

Figure S43. ^{1}H NMR titration of **1a** and 1 equiv of HPF_6 with increasing equivalents tetra-*n*-butylammonium chloride. Small peaks appeared due to slow decomposition of the receptor over time.

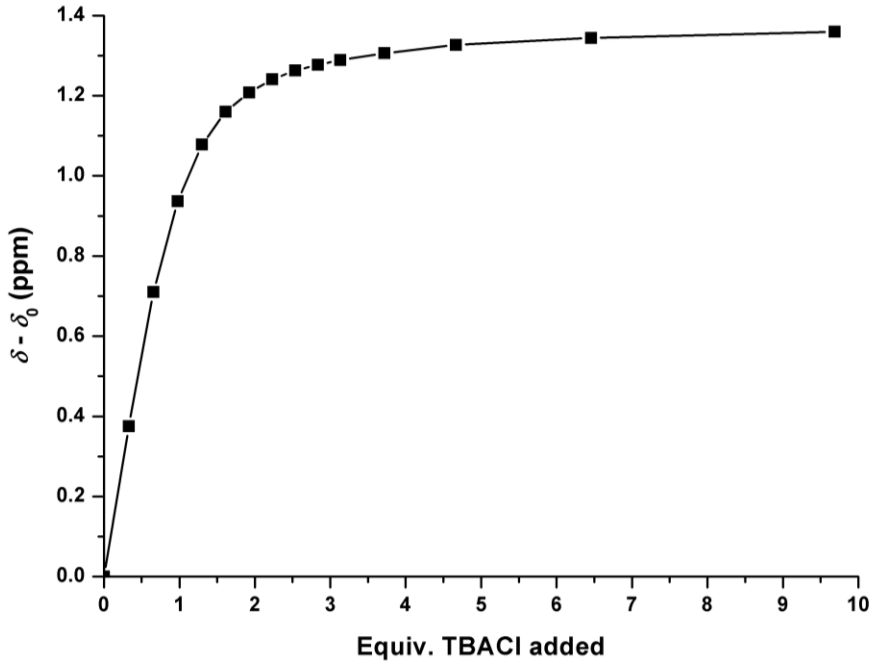

Figure S44. ^{1}H NMR titration of **1a** with increasing equivalents tetra-*n*-butylammonium chloride.

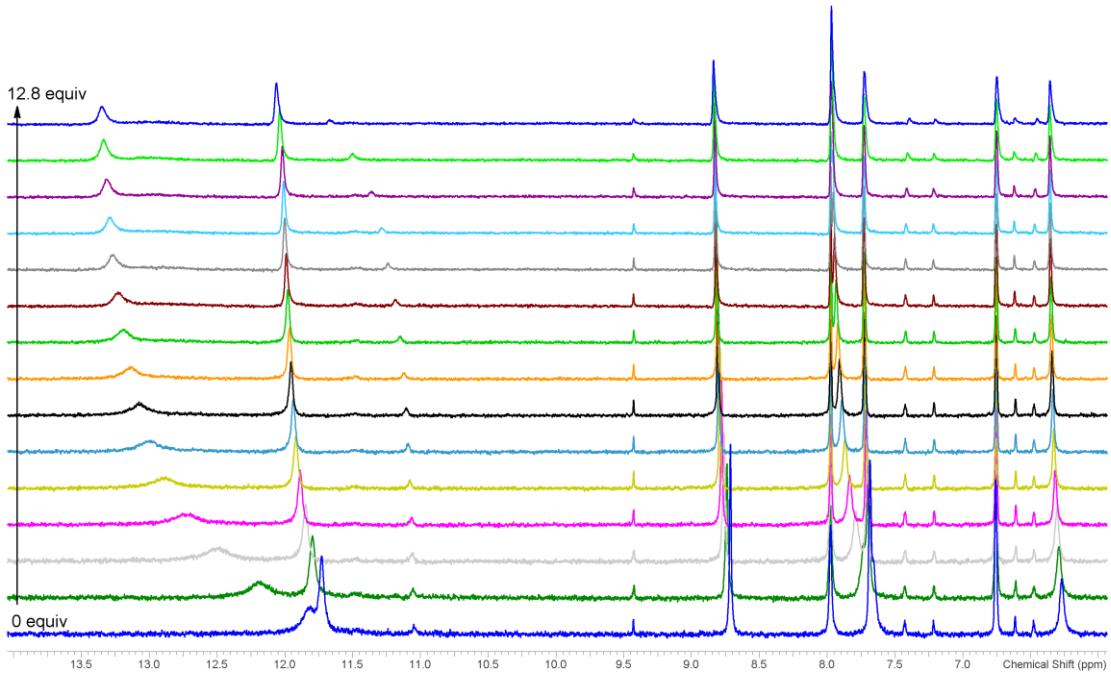

Figure S45. ^{1}H NMR titration of **1b** and 1 equiv of HPF_6 with increasing equivalents tetra-*n*-butylammonium chloride. Small peaks appeared due to slow decomposition of the receptor over time.

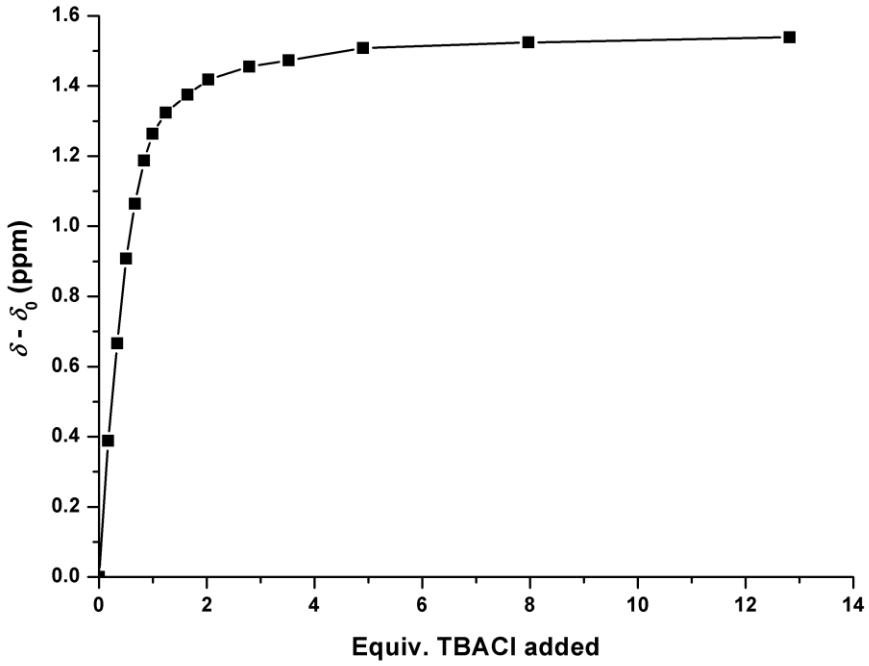

Figure S46. ^{1}H NMR titration of **1b** and 1 equiv of HPF_6 with increasing equivalents tetra-*n*-butylammonium chloride.

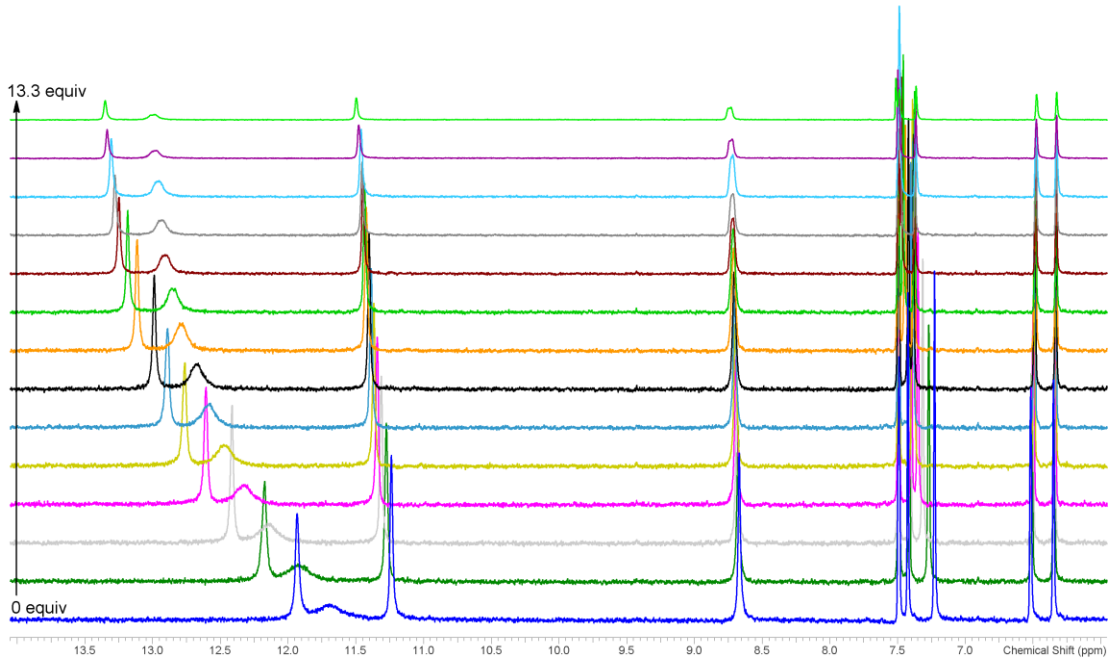

Figure S47. ^{1}H NMR titration of **1c** and 1 equiv of HPF_6 with increasing equivalents tetra-*n*-butylammonium chloride.

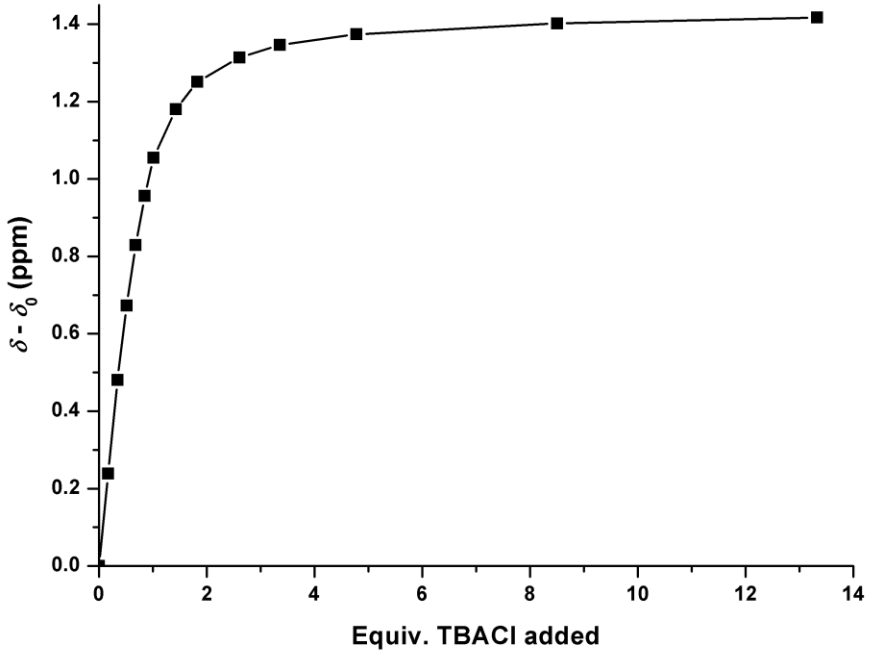

Figure S48. ^{1}H NMR titration of **1c** and 1 equiv of HPF_6 with increasing equivalents tetra-*n*-butylammonium chloride.

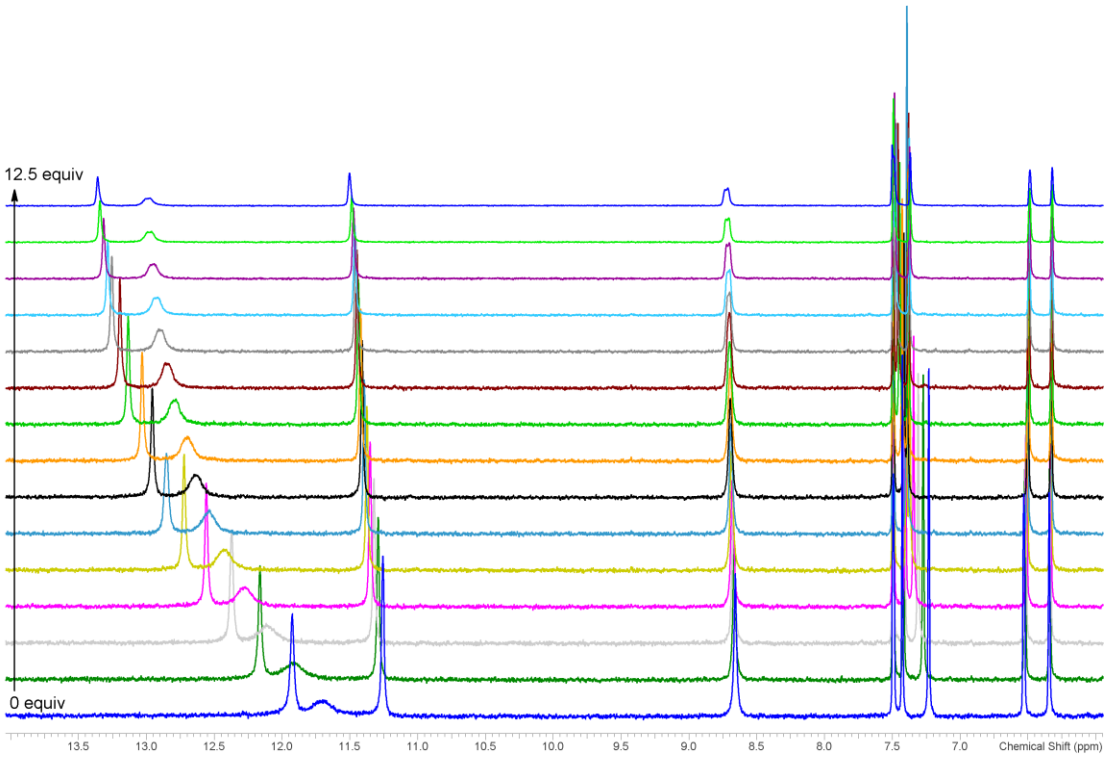

Figure S49. ^{1}H NMR titration of **1d** and 1 equiv of HPF_6 with increasing equivalents tetra-*n*-butylammonium chloride.

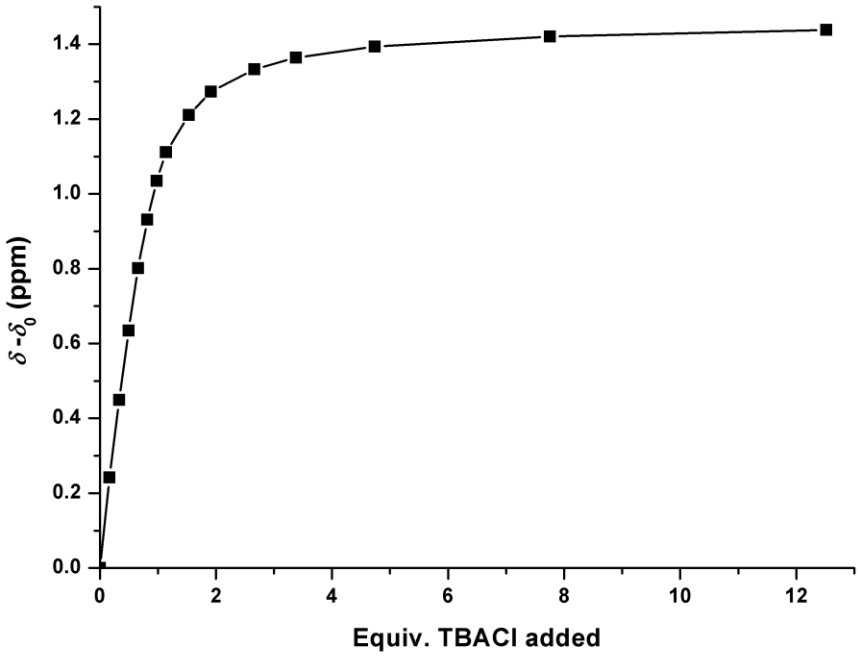

Figure S50. ^{1}H NMR titration of **1d** and 1 equiv of HPF_6 with increasing equivalents tetra-*n*-butylammonium chloride.

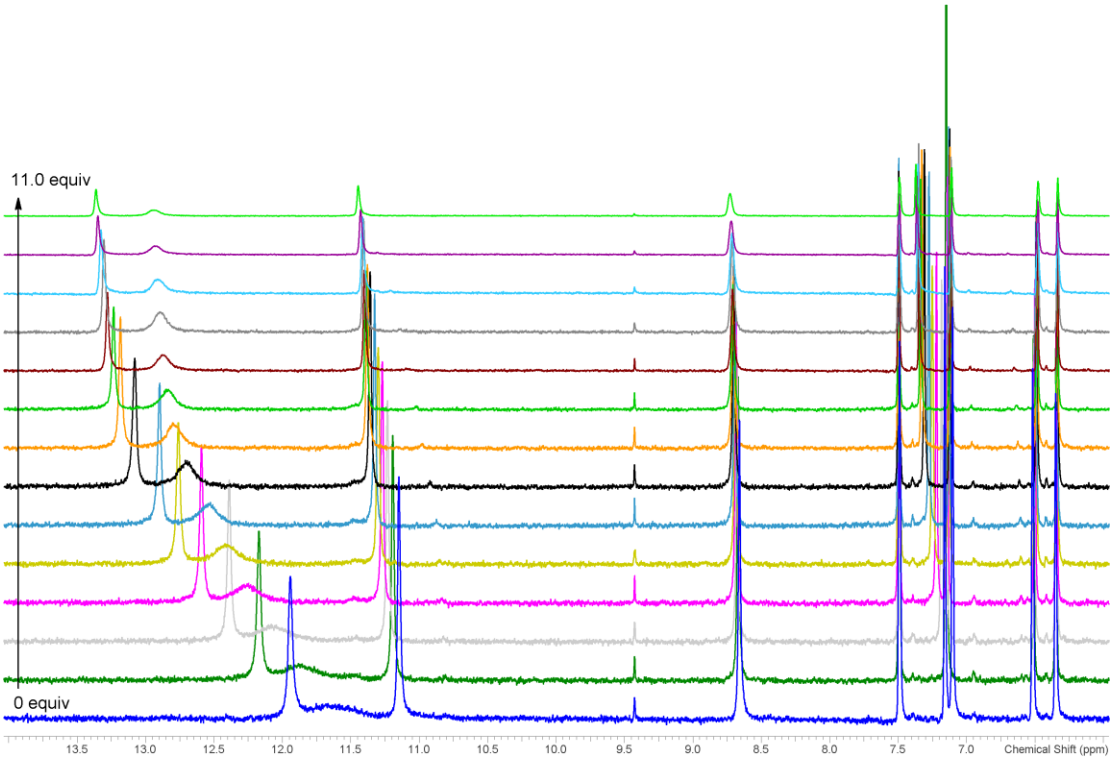

Figure S51. ^{1}H NMR titration of **1e** and 1 equiv of HPF_6 with increasing equivalents tetra-*n*-butylammonium chloride. A small peak appeared due to slow decomposition of the receptor over time.

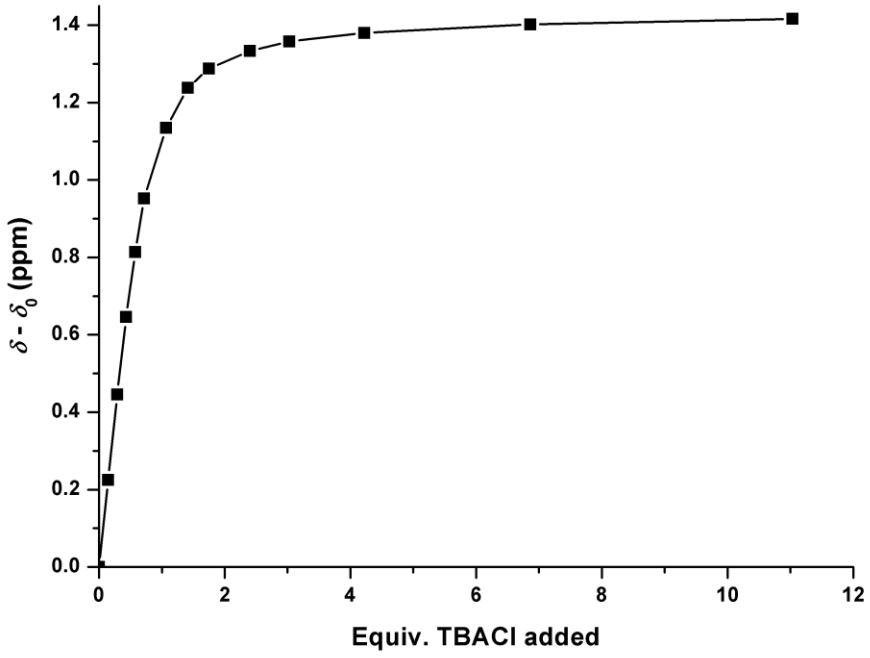

Figure S52. ^{1}H NMR titration of **1e** and 1 equiv of HPF_6 with increasing equivalents tetra-*n*-butylammonium chloride.

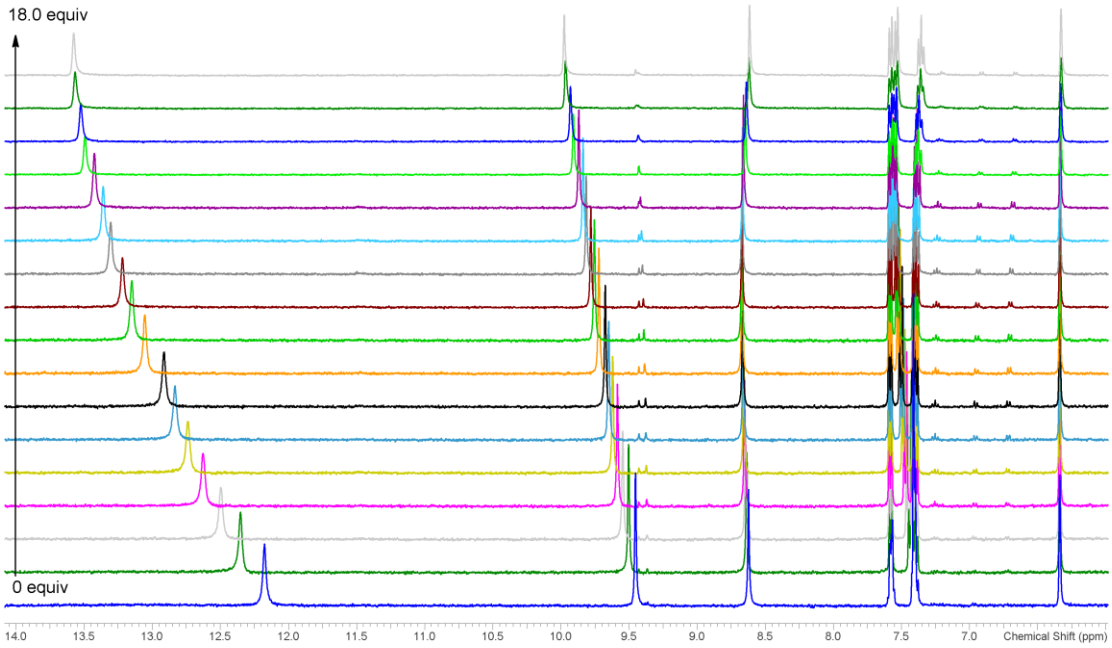

Figure S53. ^{1}H NMR titration of **2** and 1 equiv of HPF_6 with increasing equivalents tetra-*n*-butylammonium chloride. Small peaks appeared due to slow decomposition of the receptor over time.

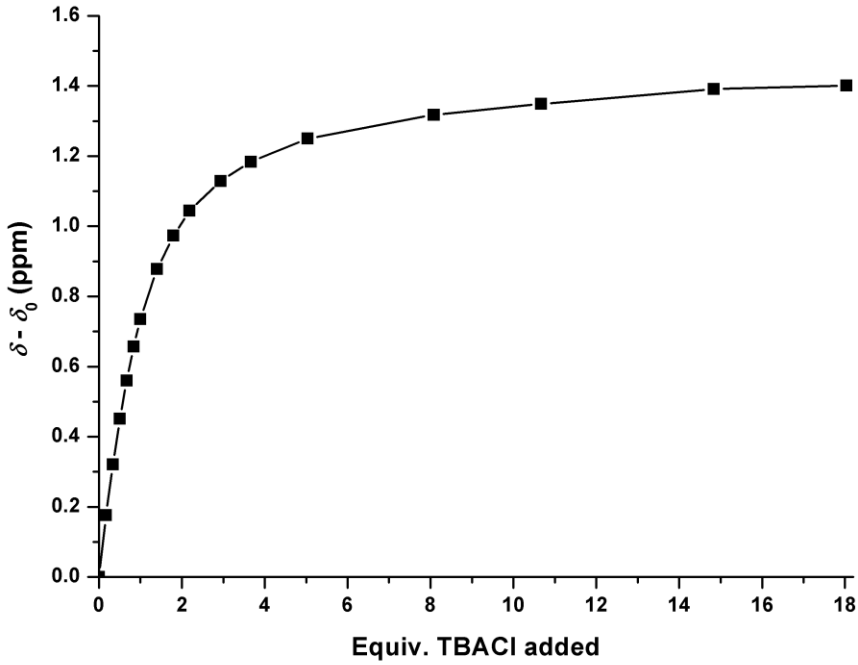

Figure S54. ^{1}H NMR titration of **2** and 1 equiv of HPF_6 with increasing equivalents tetra-*n*-butylammonium chloride.

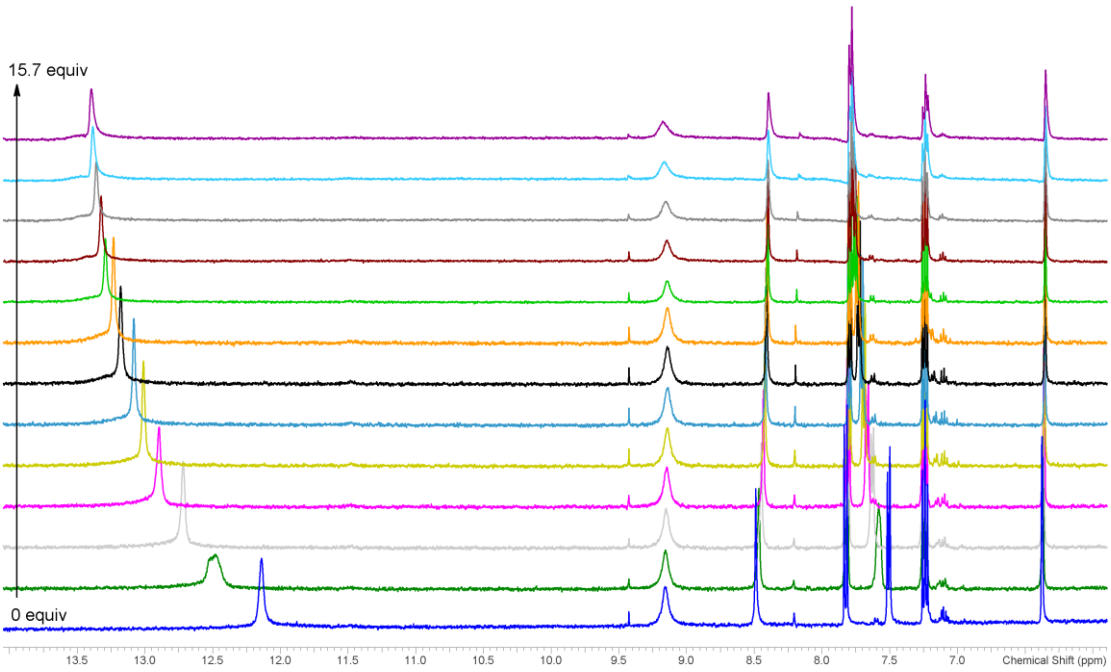

Figure S55. ^{1}H NMR titration of **3** and 1 equiv of HPF_6 with increasing equivalents tetra-*n*-butylammonium chloride. Small peaks appeared due to slow decomposition of the receptor over time.

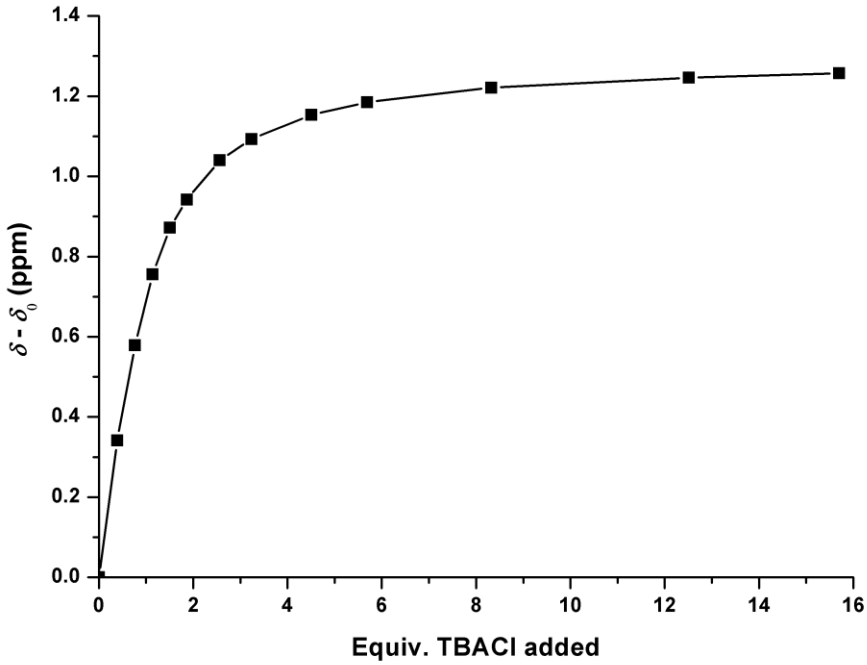

Figure S56. ^{1}H NMR titration of **3** and 1 equiv of HPF_6 with increasing equivalents tetra-*n*-butylammonium chloride.

5. Anion transport studies

POPC (1-palmitoyl-2-oleoyl-*sn*-glycero-3-phosphocholine) was supplied by Genzyme and was stored at –20 °C as a solution in chloroform (1 g POPC in 35 mL chloroform). Octaethylene glycol monododecyl ether was used as detergent and was supplied bi TCI. Chloride concentrations during transport experiments were determined using an Accumet chloride selective electrode.

5.1 Vesicle preparation

A lipid film of POPC was formed from a chloroform solution under reduced pressure and dried under vacuum for at least 4 hours. The lipid film was rehydrated by vortexing with a metal chloride (MCl) salt solution (489 mM MCl, 5 mM phosphate buffer at pH 7.2). The lipid suspension was then subjected to nine freeze-thaw cycles, where the suspension was alternatingly allowed to freeze in a liquid nitrogen bath, followed by thawing in a water bath. The lipid suspension was allowed to age for 30 min at room temperature and was subsequently extruded 25 times through a 200 nm polycarbonate membrane. The resulting unilamellar vesicles were dialyzed against the external medium for 18 h to remove unencapsulated MCl salts. The vesicle suspension was then diluted to a concentration of 1 mM using the external solution.

5.2 Chloride/nitrate transport assay

Unilamellar POPC (with 0 % or 30 % cholesterol) vesicles containing NaCl, prepared as described above, were suspended in the external medium consisting of a 489 mM $NaNO_3$ solution buffered to pH 7.2 with sodium phosphate salts (5 mM buffer). The lipid concentration per sample was 1 mM. A DMSO solution of the carrier molecule was added to start the experiment and the chloride efflux was monitored using a chloride sensitive electrode. At 5 min, the vesicles were lysed with 50 µl of octaethylene glycol monododecyl ether (0.232 mM in 7:1 water:DMSO v/v) and a total chloride reading was taken at 7 min. The initial value was set at 0 % chloride efflux and the final chloride reading (at 7 minutes) was set as 100 % chloride efflux. All other data points were calibrated to these points.

5.3 Chloride/sulfate transport assay

Unilamellar POPC/Chol (7:3) vesicles containing 450 mM NaCl solution buffered to pH 7.2 with 20 mM sodium phosphate salts, prepared as described above, were suspended in the external medium consisting of a 162 mM Na_2SO_4 solution buffered to pH 7.2 with sodium phosphate salts (20 mM buffer). The lipid concentration per sample was 1 mM. A DMSO solution of the carrier molecule was added to start the experiment and chloride efflux was monitored using a chloride sensitive electrode. At 5 min, the vesicles were lysed with 50 µl of octaethylene glycol monododecyl ether (0.232 mM in 7:1 H_2O:DMSO v/v) and a total chloride reading was taken at 7 min. The initial value was set at 0 % chloride efflux and the final chloride reading was set as 100 % chloride efflux. All other data points were calibrated to these points.

5.4 Chloride/bicarbonate transport assay

Unilamellar POPC vesicles containing 450 mM NaCl solution buffered to pH 7.2 with 20 mM sodium phosphate salts, prepared as described above, were suspended in the external medium consisting of a 162 mM Na2SO4 solution buffered to pH 7.2 with sodium phosphate salts (20 mM buffer). The lipid concentration per sample was 1 mM. A DMSO solution of the carrier molecule was added to start the experiment and chloride efflux was monitored using a chloride sensitive electrode. At 2 min, a $NaHCO_3$ solution (1 M in 162 mM Na_2SO_4 buffered to pH 7.2 with 20 mM sodium phosphate salts) was added so that the outer solution contained 40 mM $NaHCO_3$. At 7 min, the vesicles were lysed with 50 µl of octaethylene glycol monododecyl ether (0.232 mM in 7:1 water:DMSO v/v) and a total chloride reading was

taken at 9 min. The initial value was set at 0 % chloride efflux and the final chloride reading was set as 100 % chloride efflux. All other data points were calibrated to these points.

5.5 HPTS (8-hydroxypyrene-1,3,6-trisulphonic acid) assays (H^+/Cl^- co-transport)

A lipid film of POPC was formed from a chloroform solution under reduced pressure and dried under vacuum for at least 4 hours. The lipid film was rehydrated by vortexing with a NaCl (489 mM NaCl buffered to pH 7.2 with 5 mM phosphate) and HPTS solution (1 mM; addition of HPTS to the NaCl solution causes a drop to pH 6.0). The lipid suspension was then subjected to nine freeze-thaw cycles and allowed to age for 30 min at room temperature before extruding 25 times through a 200 nm polycarbonate membrane. The unincorporated HPTS was removed by size exclusion chromatography on a Sephadex G-25 column using a sodium sulfate solution as eluent (162 mM Na_2SO_4, 5 mM phosphate buffer at pH 7.2).
Unilamellar POPC vesicles containing NaCl, prepared as described above, were suspended in a sodium sulfate solution buffered to pH 7.2 with sodium phosphate salts. The lipid concentration per sample was 1 mM. A DMSO solution of the carrier molecule (10 mM) was added to start the experiment. The fluoresence of intravesicular HPTS was monitored by excitation at both 403 nm and 460 nm and recording the emission at 510 nm using an Agilent Cary Eclipse Fluorescence Spectrophotometer. After 240 s the vesicles were lysed with 30 µl of octaethylene glycol monododecyl ether (0.232 mM in 7:1 H_2O:DMSO v/v).

5.6 Hill plots

During Hill plots the chloride/nitrate transport assays are performed as described above for various concentrations of carrier. The chloride efflux (%) 270 sec after the addition of carrier is plotted as a function of the carrier concentration. Data points can then be fitted to the Hill equation using Origin 8.1:

$$y = V_{\max}\frac{x^n}{k + x^n} = 100\%\frac{x^n}{EC_{50} + x^n}$$

where y is the chloride efflux at 270 sec (%) and x is the carrier concentration (mol% carrier to lipid). Vmax, k and n are the parameters to be fitted. Vmax is the maximum efflux possible (often fixed to 100%, as this is physically the maximum chloride efflux possible), n is the Hill coefficient and k is the carrier concentration needed to reach $V_{max}/2$ (when V_{max} is fixed to 100%, k equals EC_{50}). From the Hill plot it is therefore possible to directly obtain $EC_{50,270\ sec}$ values, defined as the carrier concentration (mol% carrier to lipid) needed to obtain 50% chloride efflux after 270 sec.

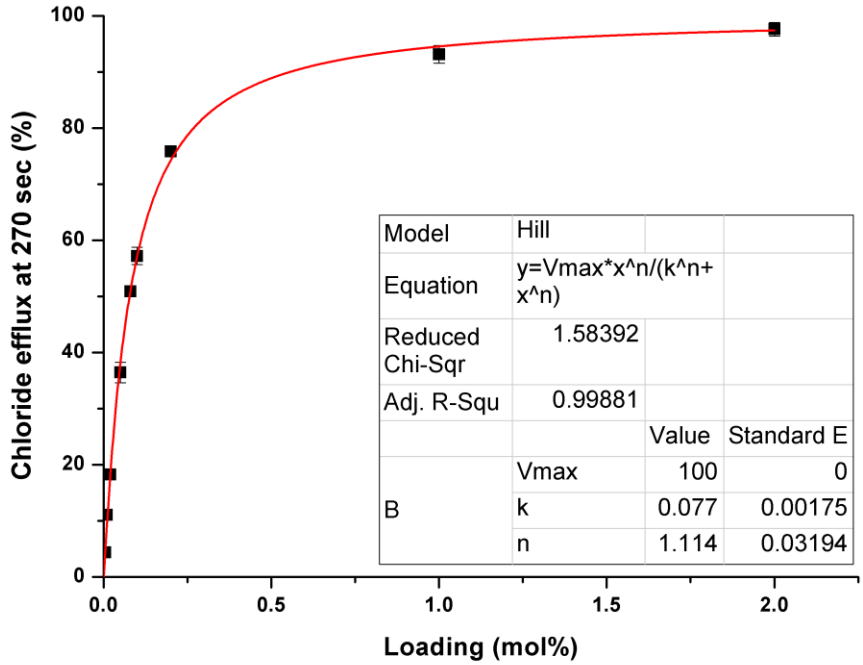

Figure S57. Hill plot for chloride release mediated by receptor **1a** from unilamellar POPC/Chol (7:3) vesicles loaded with 489 mM NaCl buffered to pH 7.2 with 5 mM sodium phosphate salts. The vesicles were dispersed in 489 mM $NaNO_3$ buffered to pH 7.2 with 5 mM sodium phosphate salts.

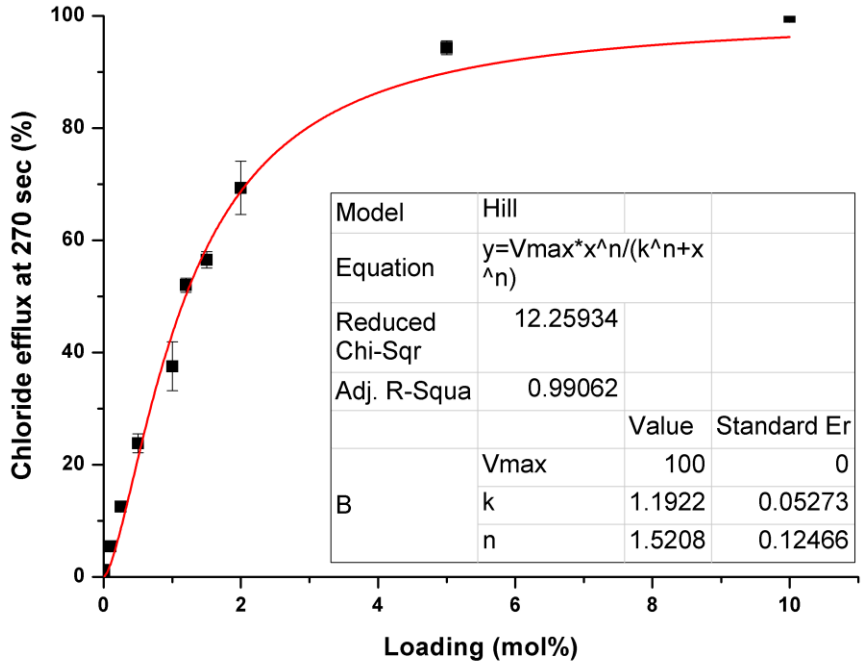

Figure S58. Hill plot for chloride release mediated by receptor **1b** from unilamellar POPC/Chol (7:3) vesicles loaded with 489 mM NaCl buffered to pH 7.2 with 5 mM sodium phosphate salts. The vesicles were dispersed in 489 mM $NaNO_3$ buffered to pH 7.2 with 5 mM sodium phosphate salts.

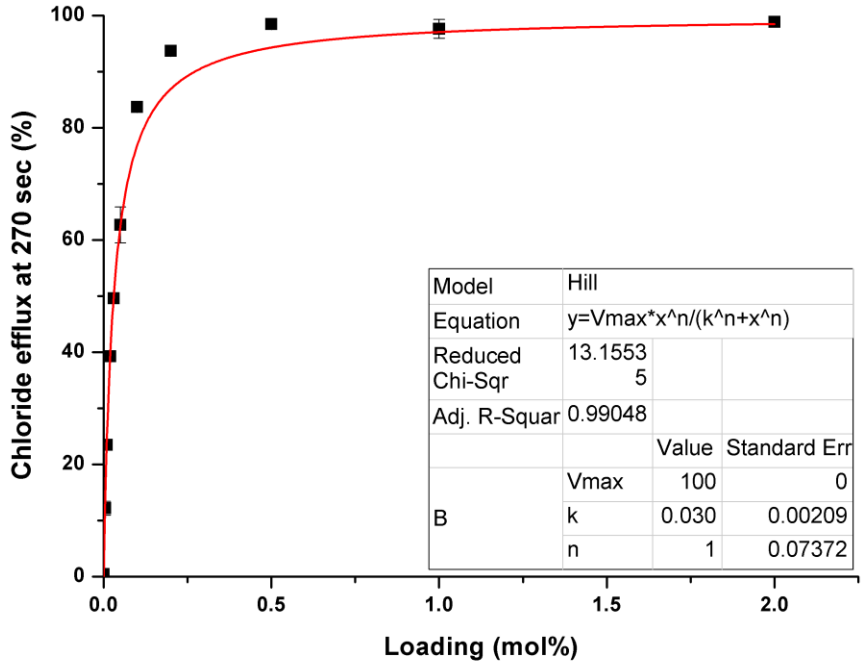

Figure S59. Hill plot for chloride release mediated by receptor **1c** from unilamellar POPC/Chol (7:3) vesicles loaded with 489 mM NaCl buffered to pH 7.2 with 5 mM sodium phosphate salts. The vesicles were dispersed in 489 mM $NaNO_3$ buffered to pH 7.2 with 5 mM sodium phosphate salts.

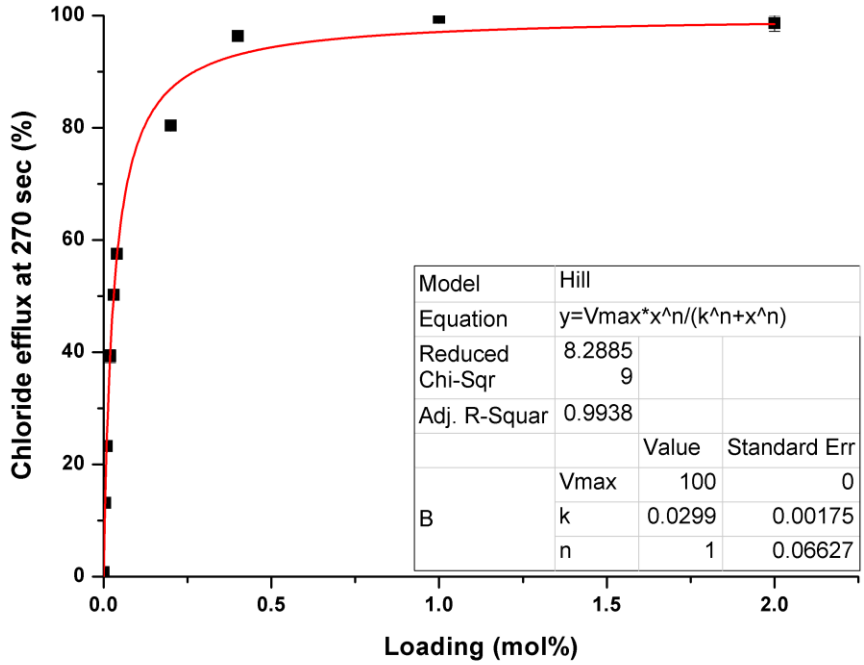

Figure S60. Hill plot for chloride release mediated by receptor **1d** from unilamellar POPC/Chol (7:3) vesicles loaded with 489 mM NaCl buffered to pH 7.2 with 5 mM sodium phosphate salts. The vesicles were dispersed in 489 mM $NaNO_3$ buffered to pH 7.2 with 5 mM sodium phosphate salts.

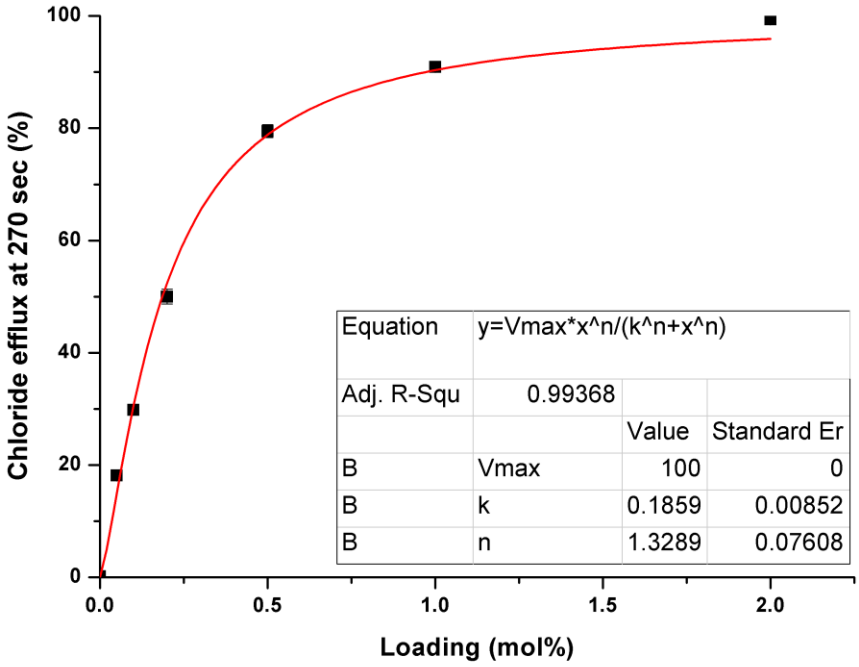

Figure S61. Hill plot for chloride release mediated by receptor **1e** from unilamellar POPC/Chol (7:3) vesicles loaded with 489 mM NaCl buffered to pH 7.2 with 5 mM sodium phosphate salts. The vesicles were dispersed in 489 mM $NaNO_3$ buffered to pH 7.2 with 5 mM sodium phosphate salts.

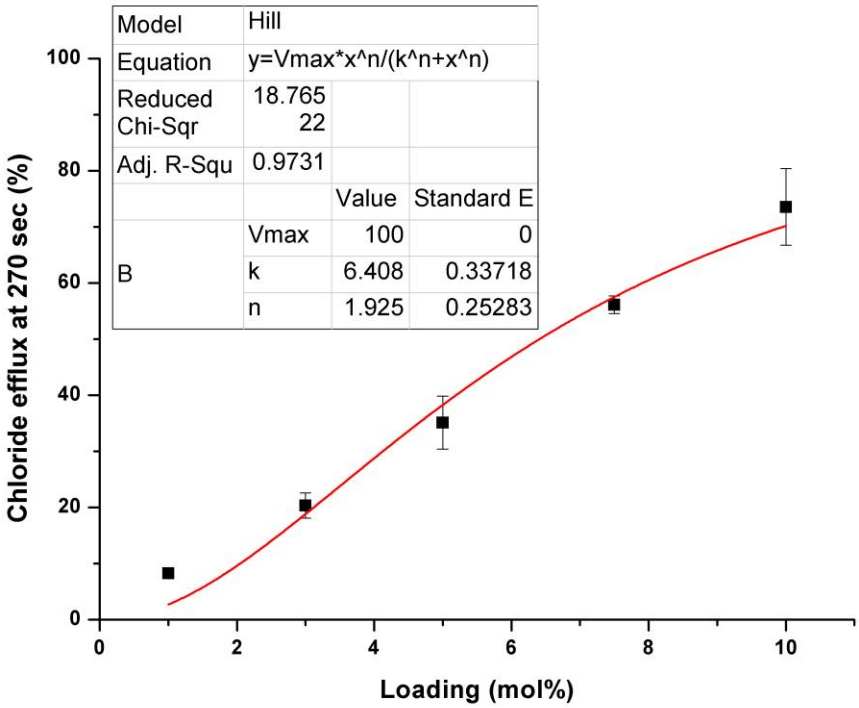

Figure S62. Hill plot for chloride release mediated by receptor **2** from unilamellar POPC/Chol (7:3) vesicles loaded with 489 mM NaCl buffered to pH 7.2 with 5 mM sodium phosphate salts. The vesicles were dispersed in 489 mM $NaNO_3$ buffered to pH 7.2 with 5 mM sodium phosphate salts.

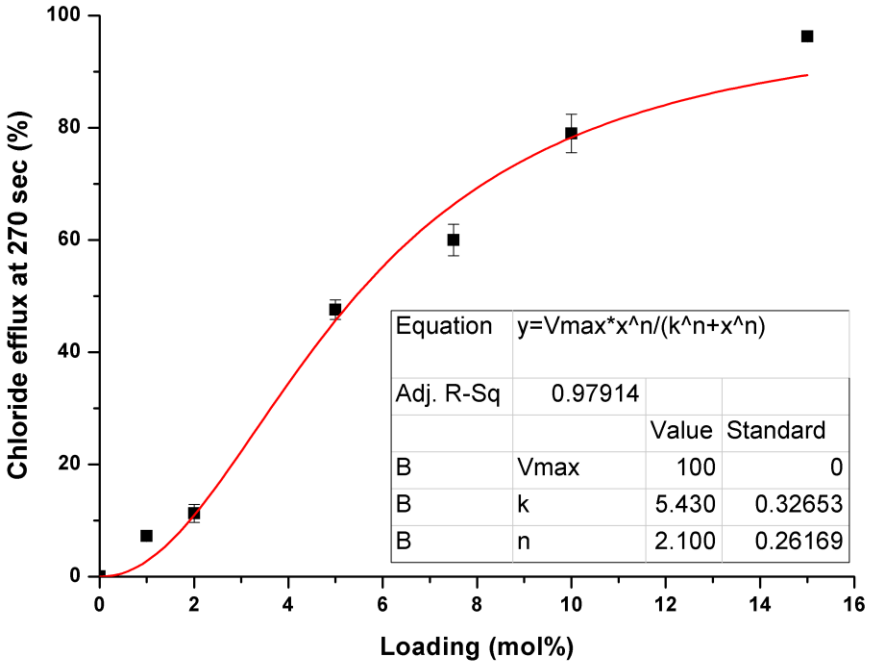

Figure S63. Hill plot for chloride release mediated by receptor **3** from unilamellar POPC/Chol (7:3) vesicles loaded with 489 mM NaCl buffered to pH 7.2 with 5 mM sodium phosphate salts. The vesicles were dispersed in 489 mM $NaNO_3$ buffered to pH 7.2 with 5 mM sodium phosphate salts.

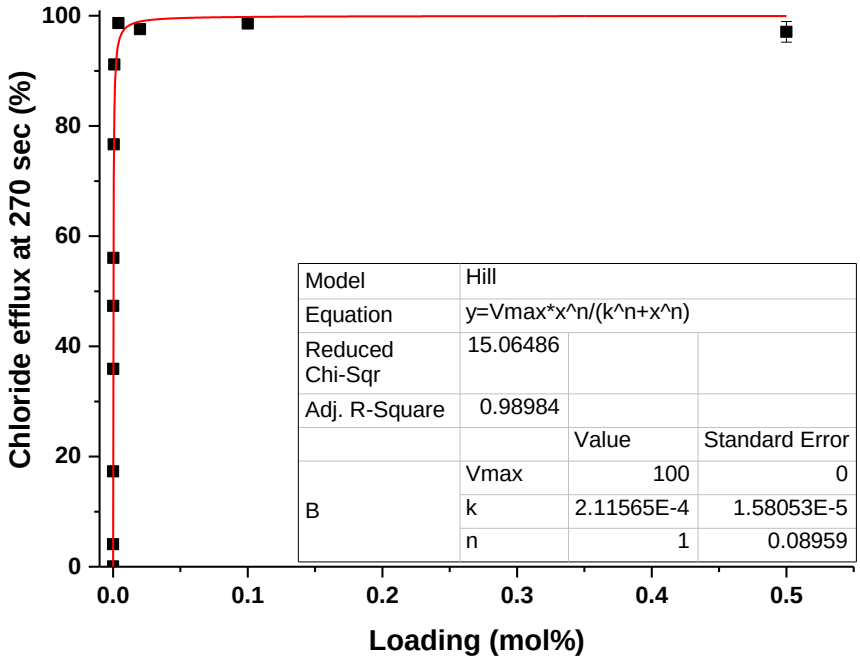

Figure S64. Hill plot for chloride release mediated by receptor **prodigiosin** from unilamellar POPC/Chol (7:3) vesicles loaded with 489 mM NaCl buffered to pH 7.2 with 5 mM sodium phosphate salts. The vesicles were dispersed in 489 mM $NaNO_3$ buffered to pH 7.2 with 5 mM sodium phosphate salts.

5.7 pH variation studies

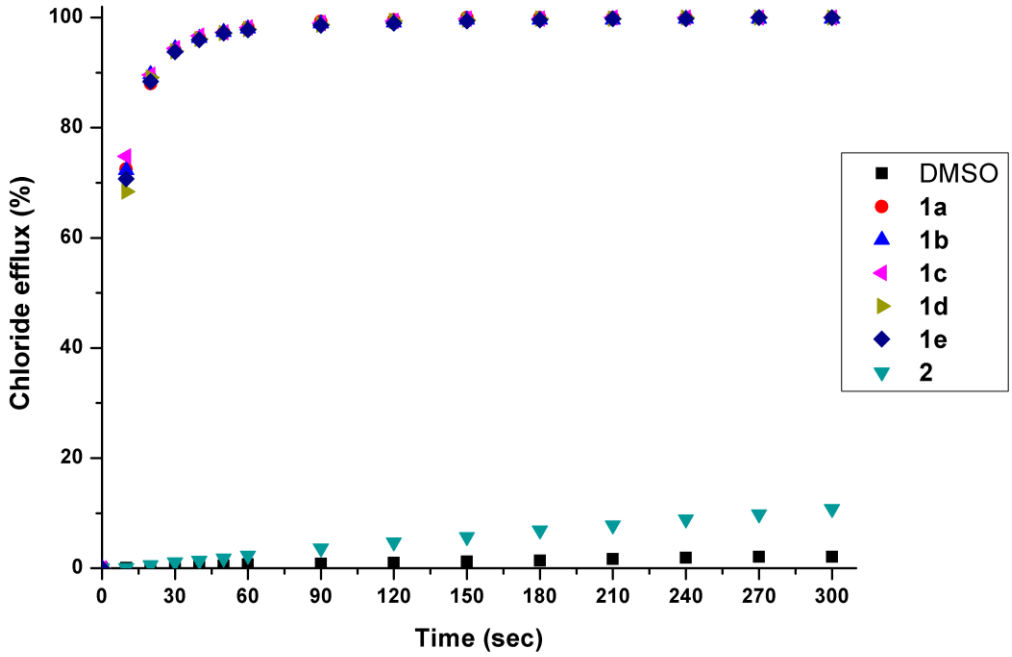

Figure S65. Chloride efflux promoted by receptor **1a–e, 2** (1 mol% carrier to lipid) from unilamellar POPC/Chol (7:3) vesicles loaded with 489 mM NaCl buffered to pH 4.0 with 5 mM citric acid. The vesicles were dispersed in 489 mM $NaNO_3$ buffered to pH 4.0 with 5 mM citric acid.

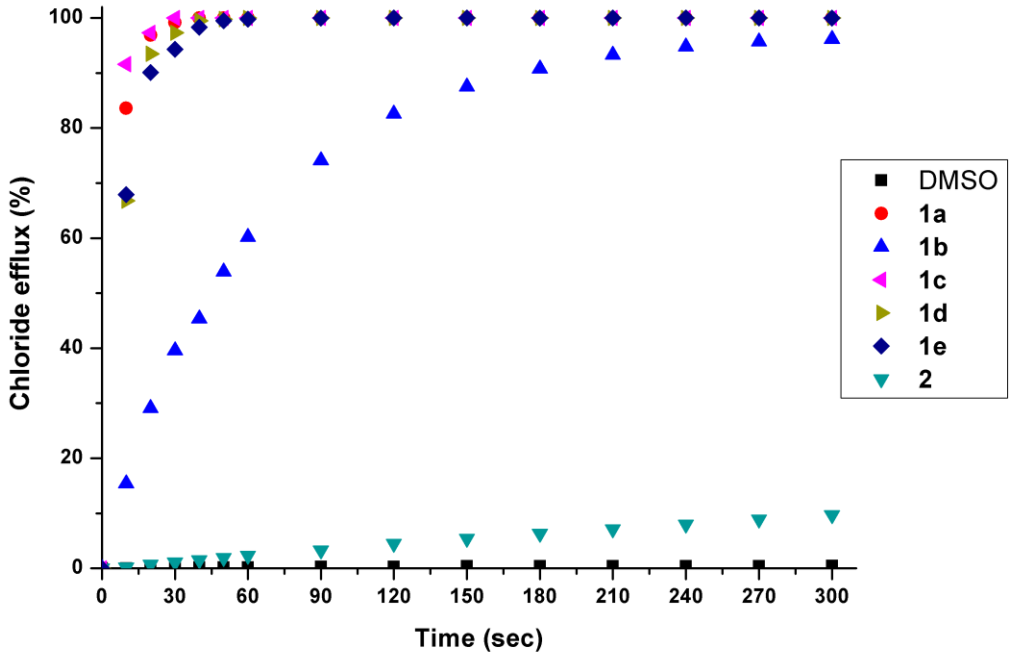

Figure S66. Chloride efflux promoted by receptor **1a–e, 2** (1 mol% carrier to lipid) from unilamellar POPC/Chol (7:3) vesicles loaded with 489 mM NaCl buffered to pH 6.2 with 5 mM piperazine. The vesicles were dispersed in 489 mM $NaNO_3$ buffered to pH 6.2 with 5 mM piperazine.

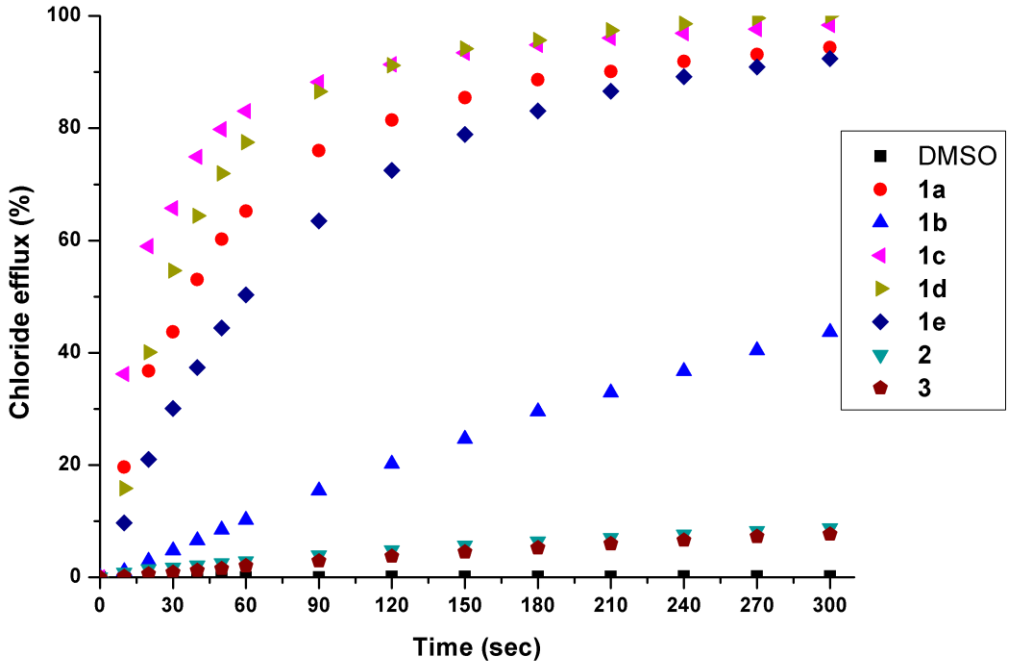

Figure S67. Chloride efflux promoted by receptor **1a–e, 2, 3** (1 mol% carrier to lipid) from unilamellar POPC/Chol (7:3) vesicles loaded with 489 mM NaCl buffered to pH 7.2 with 5 mM sodium phosphate salts. The vesicles were dispersed in 489 mM $NaNO_3$ buffered to pH 7.2 with 5 mM sodium phosphate salts.

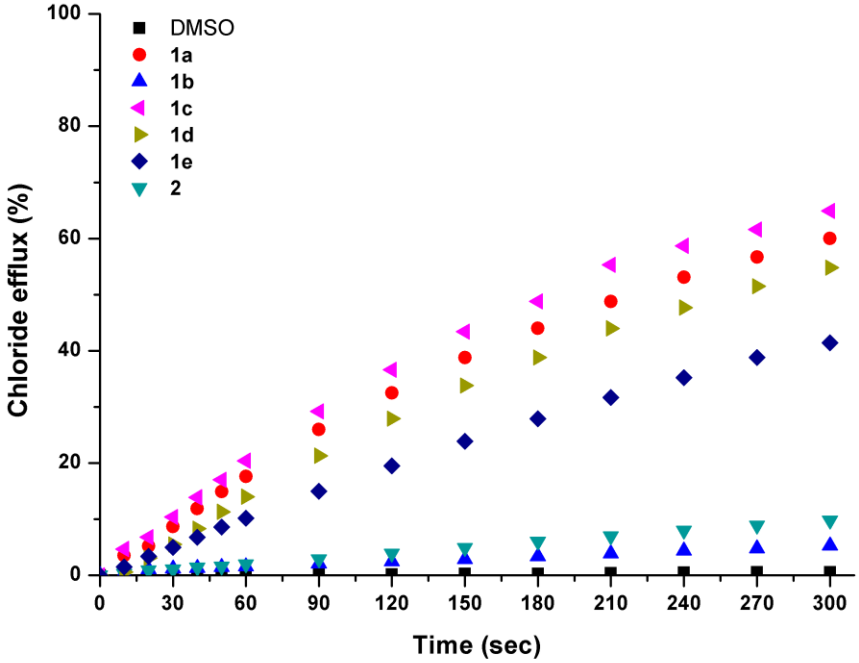

Figure S68. Chloride efflux promoted by receptor **1a–e, 2** (1 mol% carrier to lipid) from unilamellar POPC/Chol (7:3) vesicles loaded with 489 mM NaCl buffered to pH 8.2 with 5 mM sodium phosphate salts. The vesicles were dispersed in 489 mM $NaNO_3$ buffered to pH 8.2 with 5 mM sodium phosphate salts.

5.8 Transport mechanistic studies

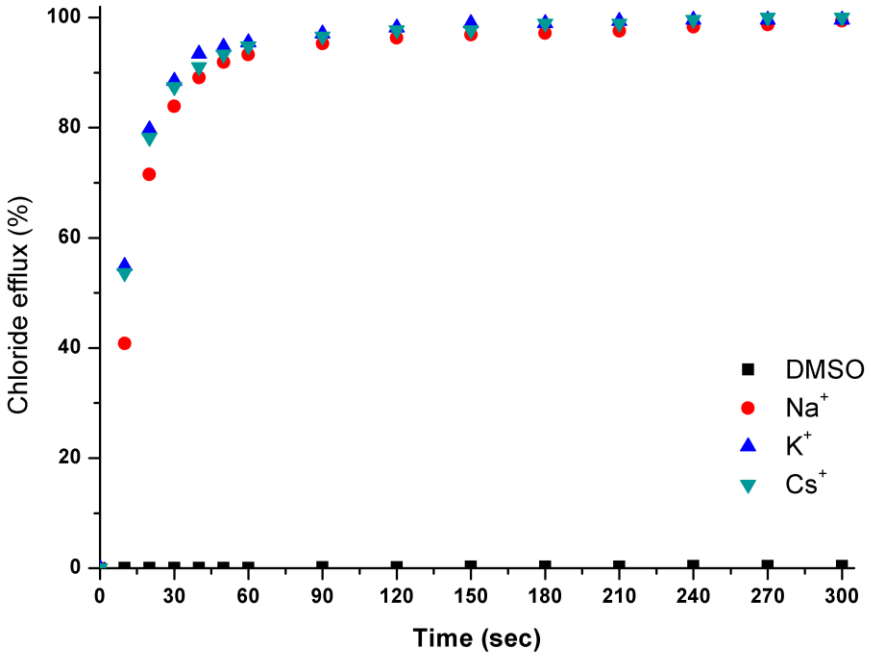

Figure S69. Chloride efflux promoted by receptor **1a** (2 mol% carrier to lipid) from unilamellar POPC vesicles loaded with 489 mM MCl (M = Na, K, Cs) buffered to pH 7.2 with 5 mM phosphate salts. The vesicles were dispersed in 489 mM $NaNO_3$ buffered to pH 7.2 with 5 mM phosphate salts.

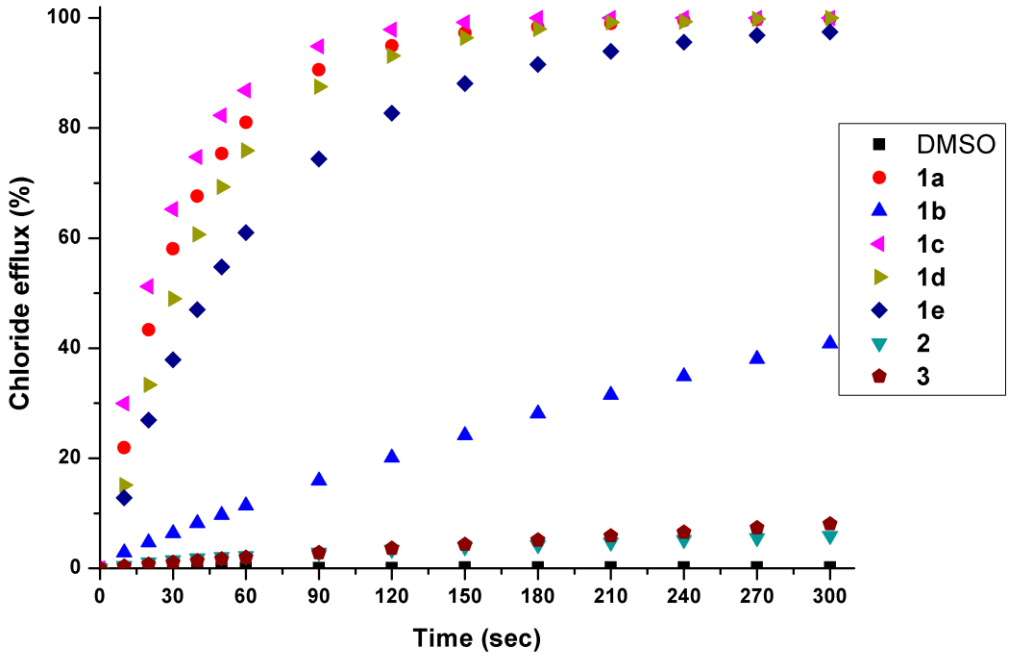

Figure S70. Chloride efflux promoted by receptor **1a–e, 2, 3** (1 mol% carrier to lipid) from unilamellar POPC vesicles loaded with 489 mM NaCl buffered to pH 7.2 with 5 mM sodium phosphate salts. The vesicles were dispersed in 489 mM $NaNO_3$ buffered to pH 7.2 with 5 mM sodium phosphate salts.

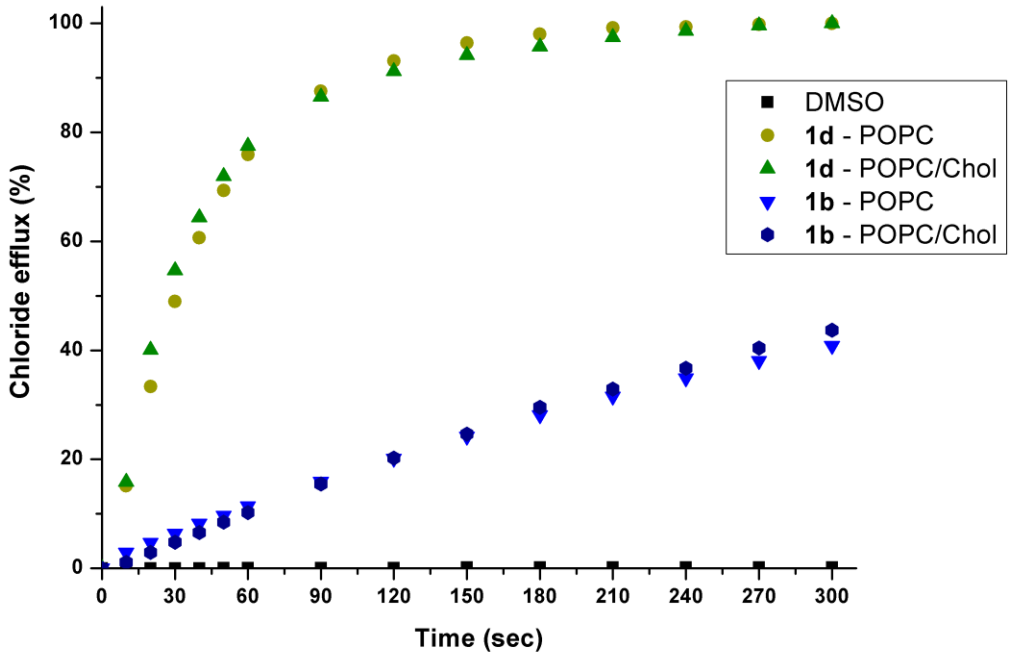

Figure S71. Chloride efflux promoted by receptor **1b** and **1d** (1 mol% carrier to lipid) from unilamellar POPC or POPC/cholesterol vesicles loaded with 489 mM NaCl buffered to pH 7.2 with 5 mM sodium phosphate salts. The vesicles were dispersed in 489 mM $NaNO_3$ buffered to pH 7.2 with 5 mM sodium phosphate salts.

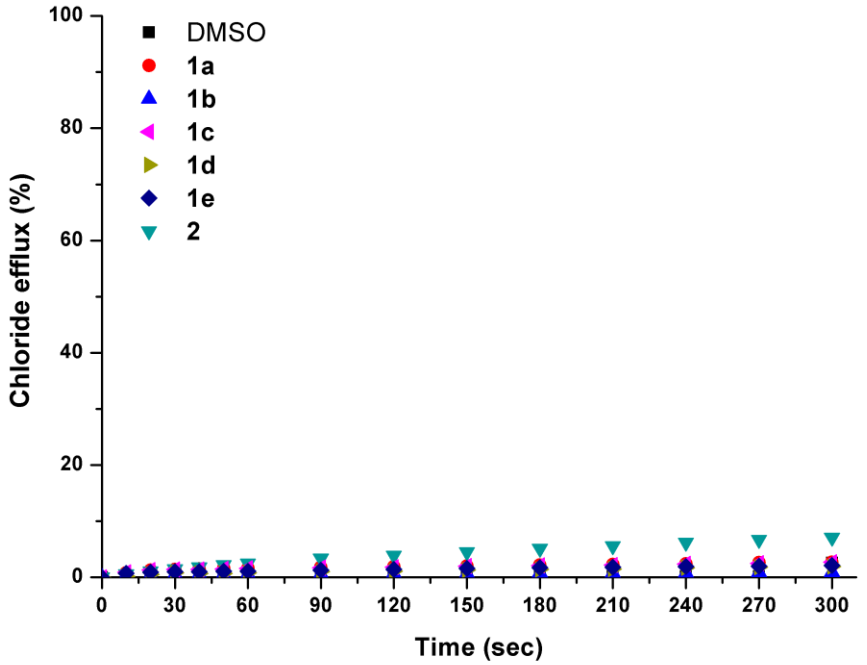

Figure S72. Chloride efflux promoted by receptor **1a–e, 2** (1 mol% carrier to lipid) from unilamellar POPC/Chol (7:3) vesicles loaded with 489 mM NaCl buffered to pH 7.2 with 20 mM sodium phosphate salts. The vesicles were dispersed in 167 mM Na_2SO_4 buffered to pH 7.2 with 20 mM sodium phosphate salts.

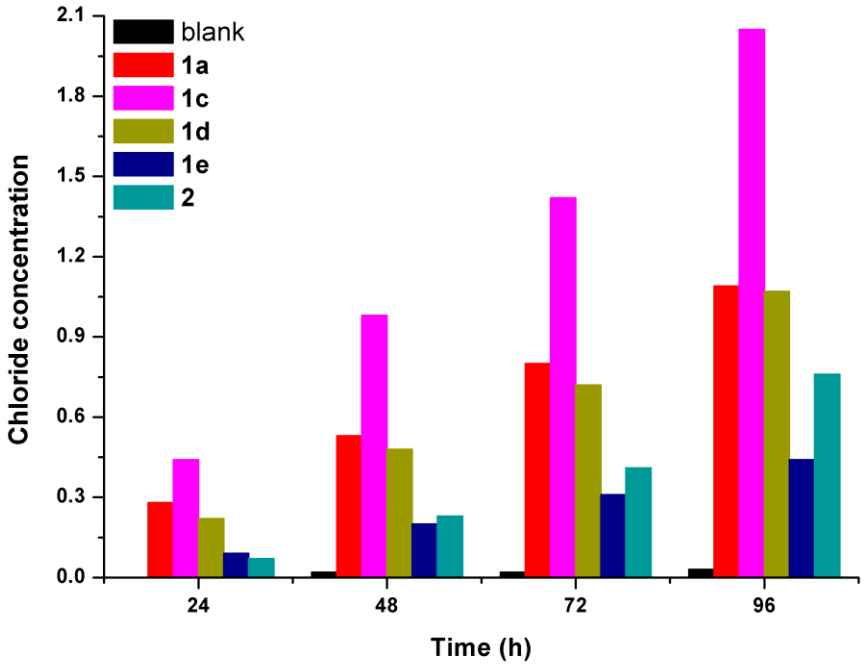

Figure S73. U-Tube experiment. Chloride transport facilitated by receptor **1a, 1c–e, 2** (1 mM in chloroform between two aqueous phases (489 mM NaCl and 489 mM $NaNO_3$, buffered to pH 7.2 with 5 mM sodium phosphate salts.

6. Hydrolysis stability studies

A spectrophotometric procedure was used to determine the hydrolysis rate for perenosin **1a** at pH 4.0 and at pH 7.2 (in solution and included in bilayer membrane). The UV-vis spectra were recorded on a Shimadzu UV-1800 UV-vissable spectrophotometer recorded at 20 °C with baseline correction using standard 10 mm quartz glass cells. A fixed amount of 12 µL of a DMSO stock solution (5 mM) was added to 3 mL buffer solution (5 mM sodium phosphate salt) solution keeping the ionic strength constant with 0.1 M NaCl.

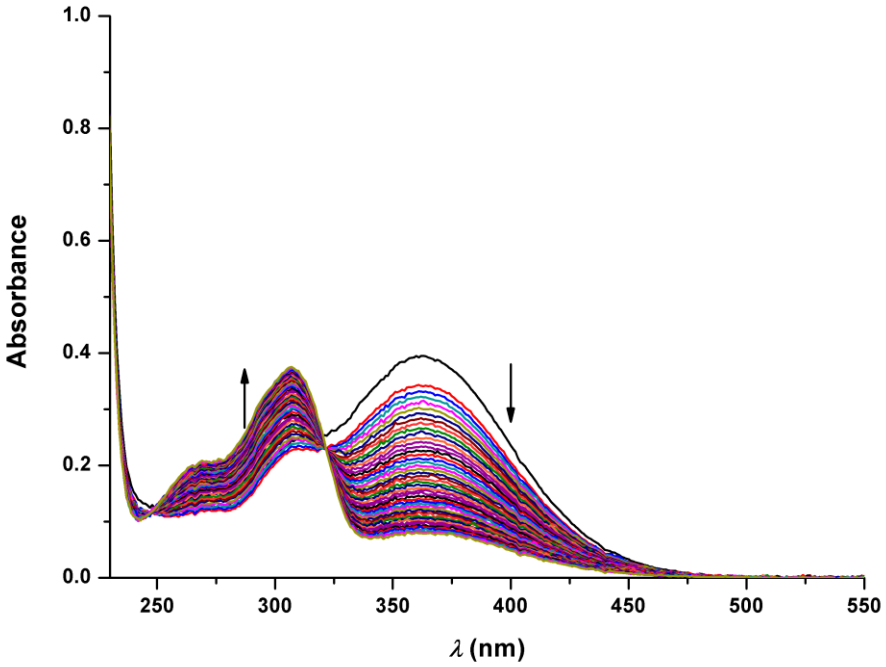

Figure S74. UV-vis absorbance spectra for the hydrolysis of **1a** in phosphate buffer (50 mM; 0.1 M NaCl) at pH 7.2 at 20 °C as a function of time (0.0 to 23.5 h, with 0.5 h increments).

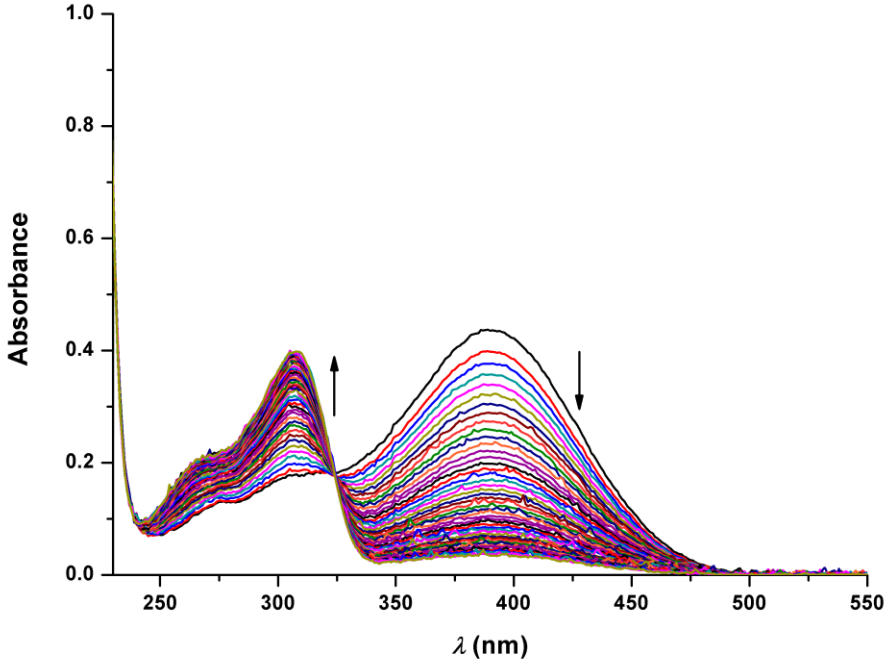

Figure S75. UV-vis absorbance spectra for the hydrolysis of **1a** in citric acid buffer (50 mM; 0.1 M NaCl) at pH 4.0 at 20 °C as a function of time (0.0 to 23.5 h, with 0.5 h increments).

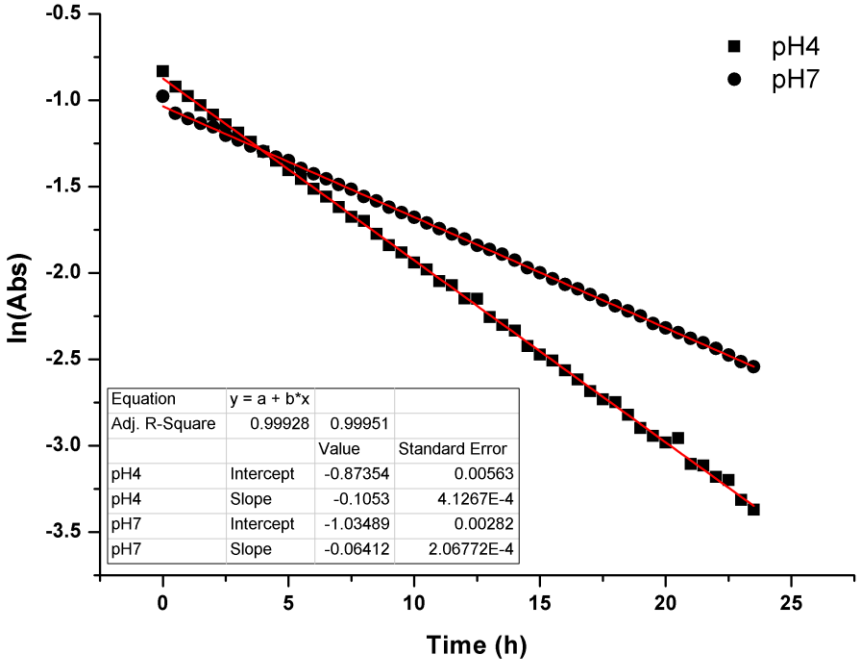

Figure S76. Plot of ln(Abs) versus time for the rate of hydrolysis of **1a** in citric acid buffer (50 mM; 0.1 M NaCl) at pH 4.0 and phosphate buffer (50 mM; 0.1 M NaCl) at pH 7.2, at 20 °C.

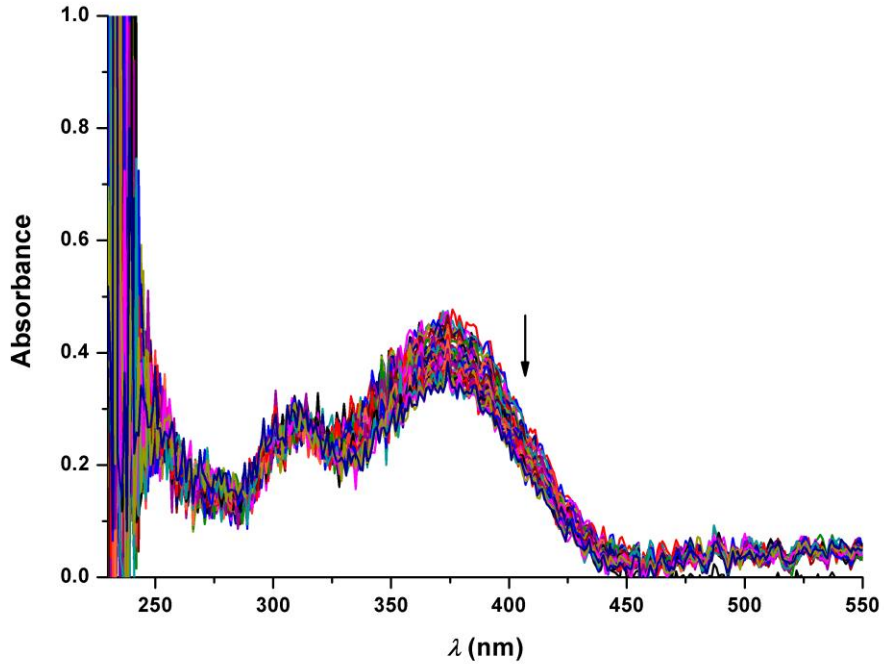

Figure S77. UV-vis absorbance spectra for the hydrolysis of **1a** in POPC/Chol (7:3) vesicles in phosphate buffer (50mM; 0.1 M NaCl) at pH 7.2 at 20 °C as a function of time (0.0 to 23.5 h, with 0.5 h increments).

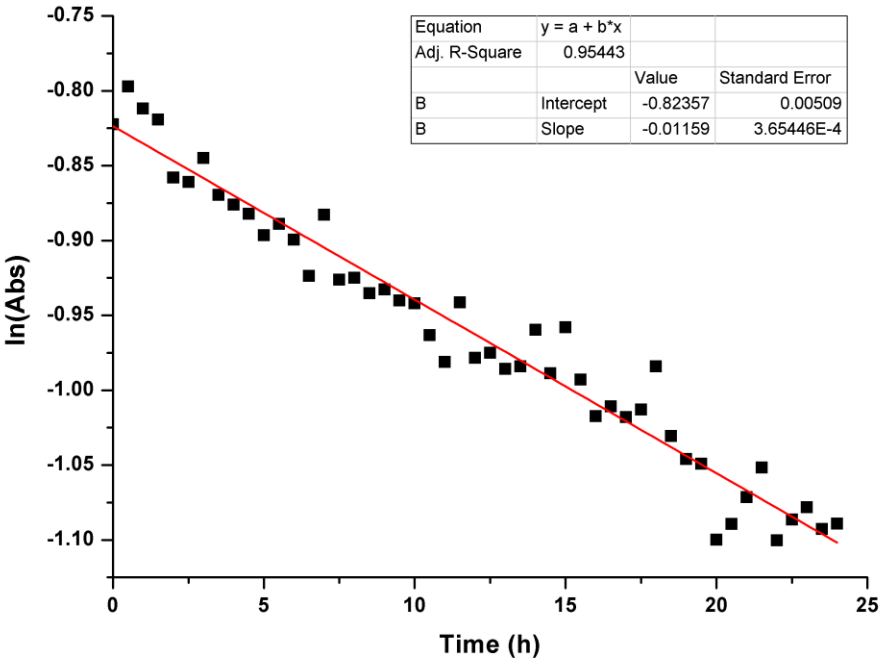

Figure S78. Plot of ln(Abs) versus time for the rate of hydrolysis of **1a** in POPC/Chol (7:3) vesicles in phosphate buffer (50mM; 0.1 M NaCl) at pH 7.2 at 20 °C.

7. pK_a determination

A spectrophotometric procedure was used to determine the apparent pK_a values for perenosins **1a**–**e**, **2**. The UV-vis spectra were recorded on a Shimadzu UV-1800 UV-vissable spectrophotometer recorded at 20 °C with baseline correction using standard 10 mm quartz glass cells. A fixed amount of 12 μL of a DMSO stock solution (5 mM) was added to 3 mL buffer solution (5 mM sodium phosphate salt) solution keeping the ionic strength constant with 0.1 M NaCl.

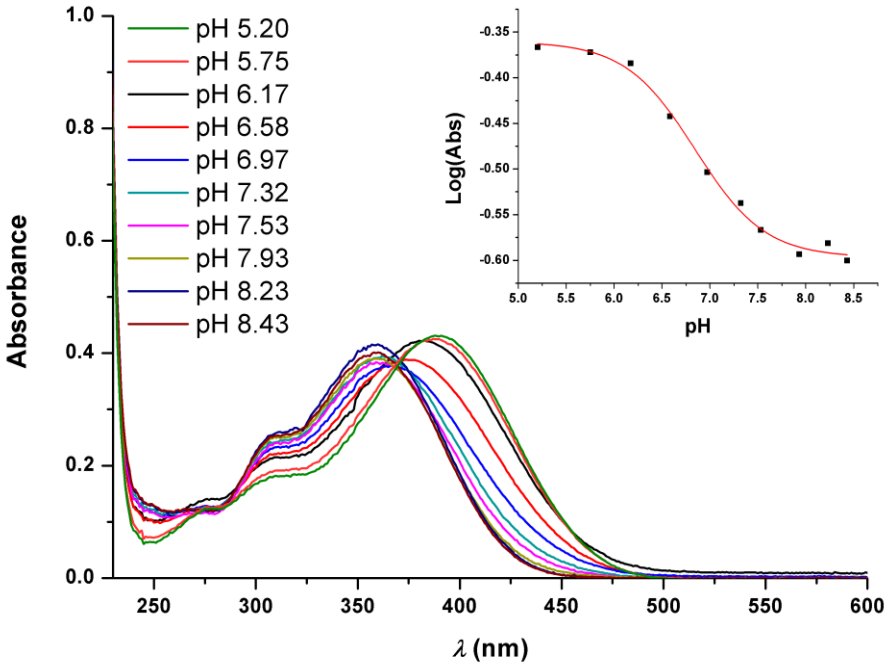

Figure S79. UV-vis absorbance spectra for **1a** as a function of pH in phosphate buffer (0.1 M NaCl) at 20 °C. Inset: Log(Abs) versus pH (at 390 nm).

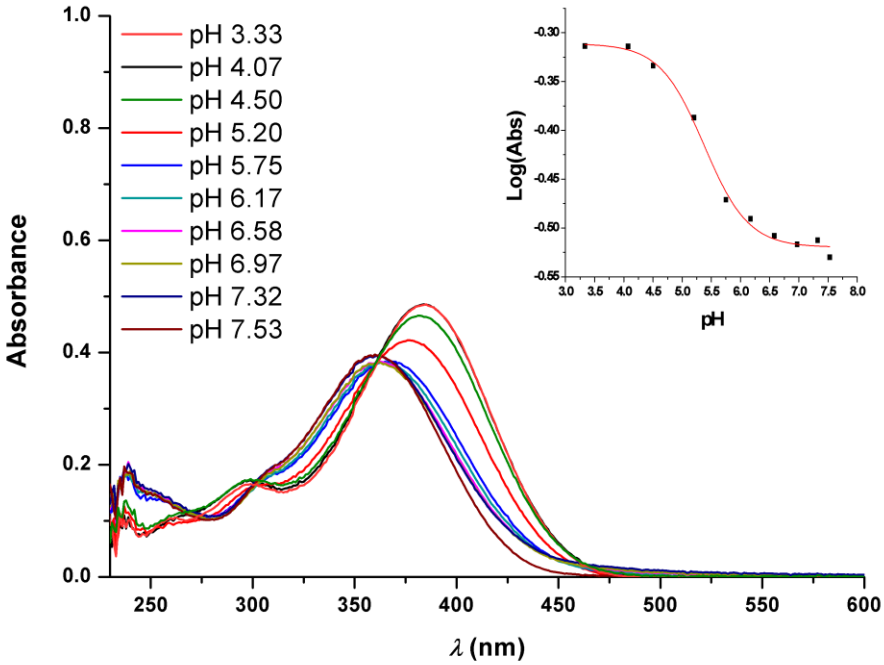

Figure S80. UV-vis absorbance spectra for **1b** as a function of pH in phosphate buffer (0.1 M NaCl):DMSO (2.80:0.20 mL) at 20 °C. Inset: Log(Abs) versus pH (at 385nm).

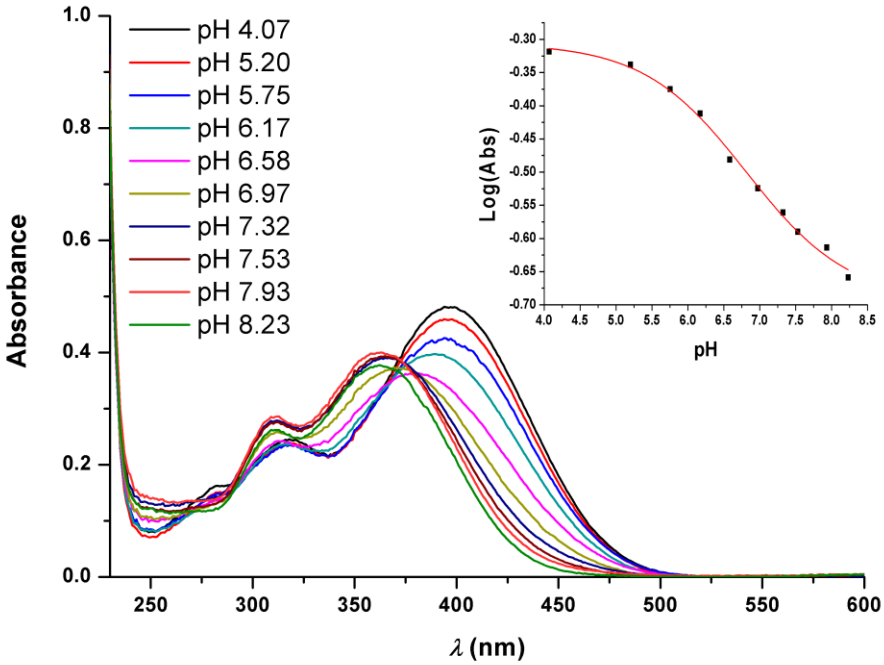

Figure S81. UV-vis absorbance spectra for **1c** as a function of pH in phosphate buffer (0.1 M NaCl) at 20 °C. Inset: Log(Abs) versus pH (at 398 nm).

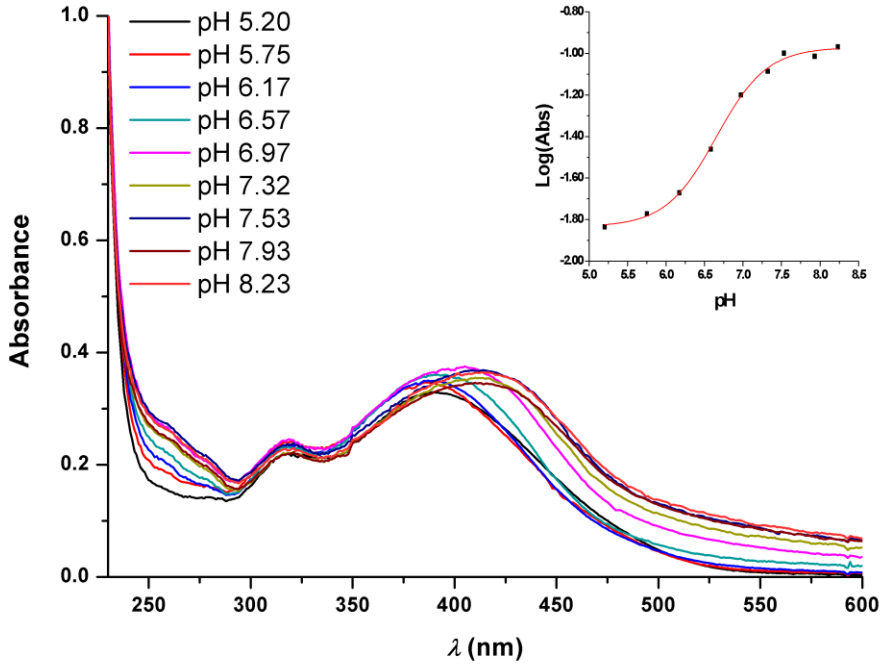

Figure S82. UV-vis absorbance spectra for **1d** as a function of pH in phosphate buffer (0.1 M NaCl) at 20 °C. Inset: Log(Abs) versus pH (at 531 nm). Due to low the poor solubility of the compound in this medium this set of data has to be approach with care.

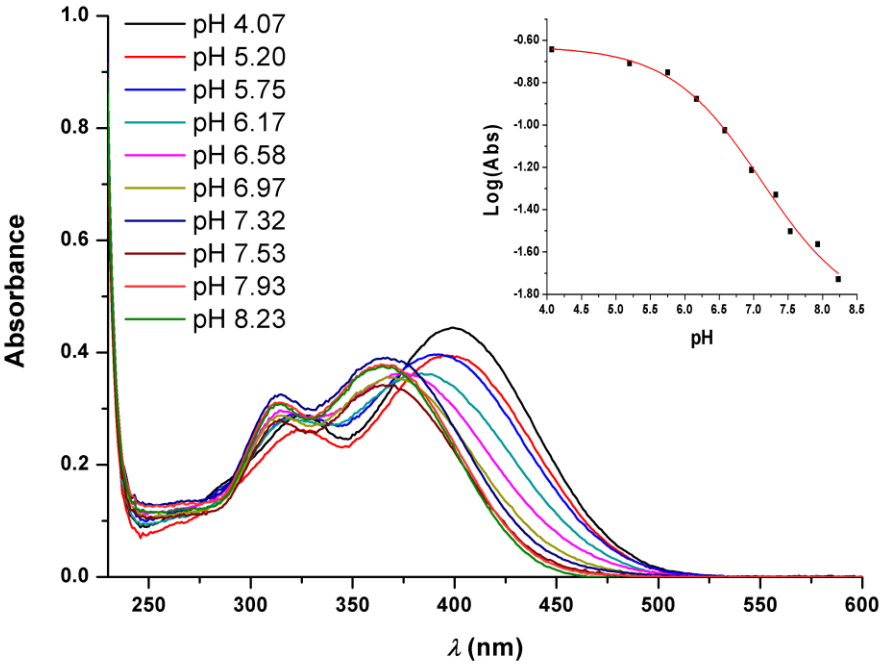

Figure S83. UV-vis absorbance spectra for **1e** as a function of pH in phosphate buffer (0.1 M NaCl) at 20 °C. Inset: Log(Abs) versus pH (at 445 nm).

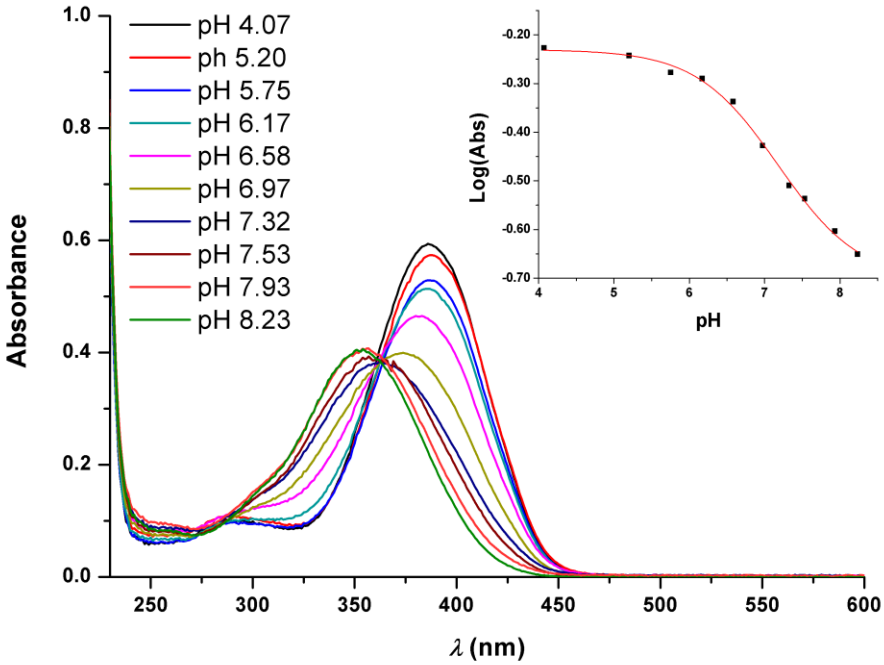

Figure S84. UV-vis absorbance spectra for **2** as a function of pH in phosphate buffer (0.1 M NaCl) at 20 °C. Inset: Log(Abs) versus pH (at 386 nm).

8. In vitro assays

Cell culture, cell treatments, transfection and cell counting
All cell culture reagents were purchased from Life Technologies unless otherwise stated. Cell lines were sourced from the American Type Culture Collection (ATCC) and not grown continually for more than 3 months. All cells were cultured at 37°C in a humidified 5% CO_2 atmosphere.

Cell viability assays
MCF-7 (human breast adenocarcinoma) cells, MDA-MB-231 (metastatic human breast adenocarcinoma) cells and MCF-10A (human mammary normal epithelial) cells were seeded in triplicate at 8000 cells per well, 10,000 cells per well and 10,000 cells per well, respectively, on 96-well plates 16 hours prior to dosing with the test compounds in 200 µl of fresh medium; final concentration of solvent DMSO in each well was 0.5% v/v. MTT-based cell proliferation assays were performed 24 hours post-dosing, as follows: MTT (Sigma) was prepared in sterile PBS and added to cells to a final concentration of 1 mM (10% v/v). Cells were then incubated for 4 hours at 37 ^{o}C until intracellular punctate purple precipitates were clearly visible under the microscope. An equal volume of DMSO was then added and the cells incubated for 10 minutes in the dark at room temperature with agitation to dissolve the insoluble formazan particles. Absorbance was measured at 570 nm on a microplate reader (Tecan Infinite M200 Pro). Each experiment was repeated three times. All values are expressed as the mean ± SEM.

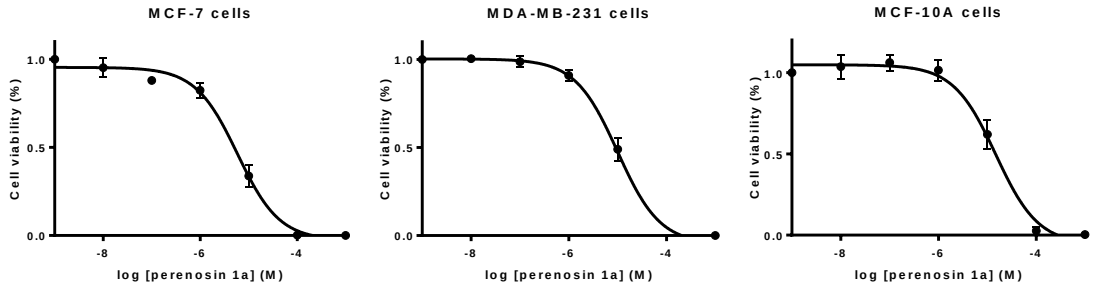

Figure S85. Dose-dependence of cytotoxicity on MCF-7, MDA-MB-231 and MCF-10A cells induced by **1a** after 24 h.

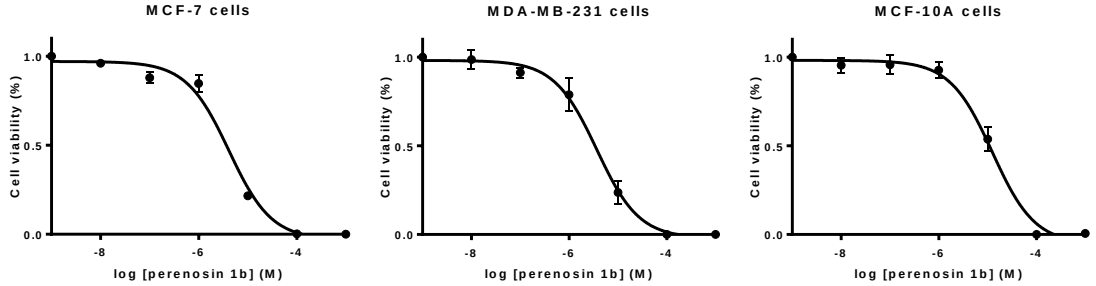

Figure S86. Dose-dependence of cytotoxicity on MCF-7, MDA-MB-231 and MCF-10A cells induced by **1b** after 24 h.

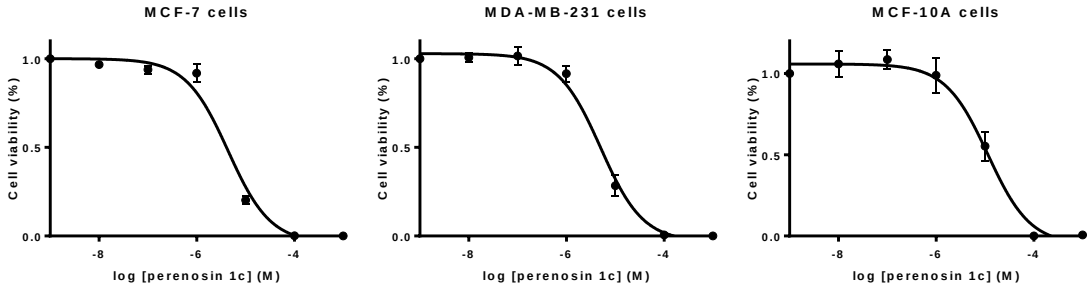

Figure S87. Dose-dependence of cytotoxicity on MCF-7, MDA-MB-231 and MCF-10A cells induced by **1c** after 24 h.

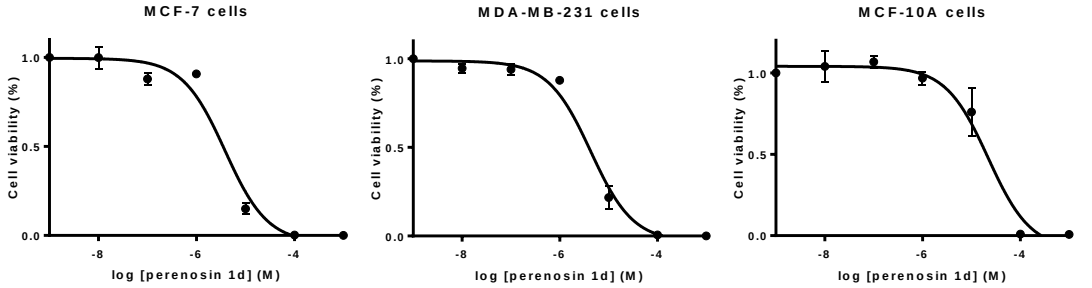

Figure S88. Dose-dependence of cytotoxicity on MCF-7, MDA-MB-231 and MCF-10A cells induced by **1d** after 24 h.

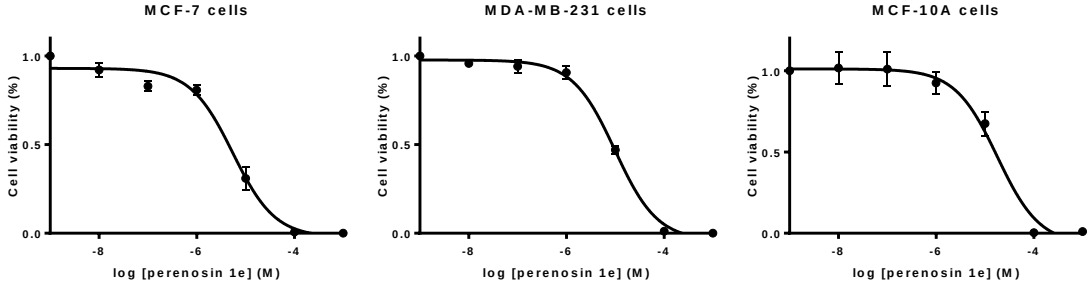

Figure S89. Dose-dependence of cytotoxicity on MCF-7, MDA-MB-231 and MCF-10A cells induced by **1e** after 24 h.

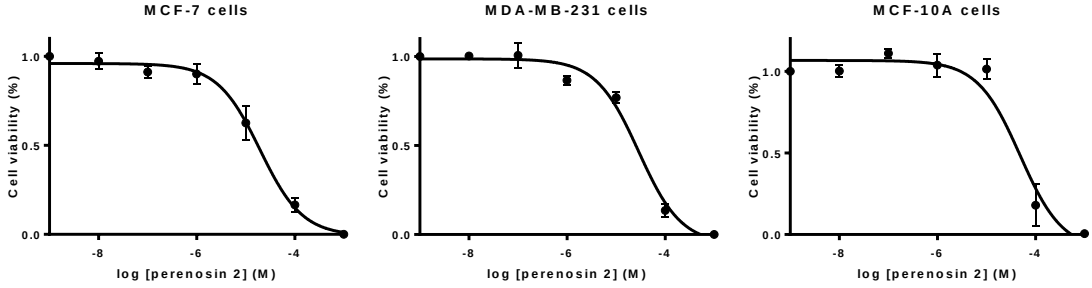

Figure S90. Dose-dependence of cytotoxicity on MCF-7, MDA-MB-231 and MCF-10A cells induced by **2** after 24 h.